Dendrochronological Reconstruction of Precipitation Trends to 1591 AD in the Sooke Watershed, Vancouver Island, British Columbia

by

Lauren Kirsten Farmer
BA, Geography, Concordia University, 2016

A Thesis Submitted in Partial Fulfillment
of the Requirements for the Degree of

MASTER OF SCIENCE

in the Department of Geography

We acknowledge with respect the Lekwungen peoples on whose traditional territory the university stands and the Songhees, Esquimalt and W̱SÁNEĆ peoples whose historical relationships with the land continue to this day.

Dendrohydrological Reconstruction of Precipitation Trends to 1591 AD in the Sooke Watershed, Vancouver Island, British Columbia

by

Lauren Kirsten Farmer
BA, Geography, Concordia University, 2016

Supervisory Committee

Dr. Dan J. Smith, Supervisor
Department of Geography

Dr. Johannes Feddema, Departmental Member
Departmental of Geography

Dr. Tobi Gardner, Outside Member
Capital Regional District

Dr. Elizabeth Campbell, Outside Member
Pacific Forestry Centre; Canadian Forest Service

Abstract

By 2050, mean annual temperature on Vancouver Island, British Columbia is expected to rise by 1.5°C and summer precipitation is expected to decrease 14% below pre-industrial levels. The purpose of this thesis was to extend the Sooke Watershed precipitation record by developing proxy records from annual Douglas-fir tree rings, with the goal of being able to provide information about the pre-historical range of precipitation variation that could assist future water management decisions. Robust dendrohydrological relationships were established to extend the instrumental record of precipitation back to the year 1591.

To provide geographic context for the hydrologic history of the Sooke Watershed, I examined Douglas-fir climate-radial growth relationships across western Canada to three monthly climate variables: precipitation, average air temperature, and Hargreaves Climatic Moisture Deficit (CMD). Ten study sites were chosen to represent a gradient of climate conditions where Douglas-fir grows in Alberta and British Columbia. In order to explore how growth sensitivities varied over time, long- and short-term climate-growth relationships at these study sites were analyzed and compared to those established for the Sooke Watershed. A short-term analysis of the radial growth of Douglas-fir trees in the Sooke Watershed revealed the presence of a negative climate-growth relationship to the June and July temperature of the growing year starting in 1990. Further, the radial growth of Douglas-fir trees at all sample sites was moisture limited, whereby they exhibited strong positive growing season correlations to precipitation and negative correlations to CMD. Lastly, lagged negative effects of August and September precipitation and CMD were present and related to the annual radial growth increments. These results signify

that: the rise in air temperature in recent decades is limiting the radial growth of Douglas-fir trees in the Sooke Watershed; annual variation in ring-width increments is regulated by the amount of precipitation that falls near the end of the prior growing season; and, moisture availability in the spring of the current year of growth plays an important role in determining the annual increment of radial growth. Collectively, the results suggest that the radial growth of Douglas-fir trees within the Sooke Watershed are sensitive to interannual climate fluctuations and future growth is likely to be altered by changes in temperature and precipitation regimes.

These climate-growth relationships justified the development of a May-June-July precipitation reconstruction for the Sooke Watershed. Using a novel detrending method, an Ensemble Empirical Mode Decomposition, I created a model that explained 28% of the May-June-July precipitation variability. Results from the dendrohydrological analyses extend the understanding of the water supply area May-June-July precipitation record to 1591. The reconstruction revealed four major summer drought episodes that exceeded severity during the instrumental record severity: 1594-1596, 1662-1665, 1796-1797, and 1898-1899. Four extreme summer pluvial episodes were also observed from 1646-1647, 1689-1690, 1793-1794, and 1920-1921. The findings of the research provide information about historical summer precipitation trends within the Sooke Watershed – the primary water supply area to Greater Victoria. Notably, the research places summer drought and pluvial events recorded within the instrumental record into a much longer context, permitting an understanding of natural frequency and duration of hydrological events in the Sooke Watershed.

Table of Contents

List of Tables

List of Figures

Acknowledgements

Grad school has certainly been a humbling journey and an exercise in persistence. The experience has taught me how to be undaunted by failure and how to stay motivated through many long days of solitary, hard work. The direction of my thesis changed multiple times throughout this journey in an effort to create a thesis that I felt I could be proud of. I am satisfied now.

Grad school has also given me countless formative and unique experiences. Most notable are my summers spent in the remote glacier backcountry of the Coast Mountains. We hopped in helicopters, jumped glacier crevasses without ropes, fought off grizzly bears, and excavated cabins built by the Mundays. That's not far from an exaggeration. We did some science too. Although my thesis did not end up with a glaciological focus, I feel extremely grateful to have learned about that environment from Dan's plethora of knowledge. Thank you, Dan, for showing me landscapes that few people will ever see, for your constant calming presence, and for dealing with my never-ending ideas.

Another incredible experience was my trip to Taiwan, which was made possible through an NSERC scholarship and through my extremely supportive host supervisor Dr. Biing T. Guan at the National Taiwan University. Dr. Guan made it his absolute duty to ensure I was learning as much as I could when I wasn't suffering from dengue fever or the flu. I feel privileged to have seen this part of the world and to have worked with academics on a global scale. To this day, I am astonished by the generosity of the Taiwanese people.

I am beyond grateful for the amazing team of powerful female scientists at the Pacific Forestry Centre; Elizabeth, Lara, Jessie, and Jenny. Also to Gurp for providing

me with maps. Although it was often challenging to work while enrolled in grad school, this experience allowed me to branch off from my thesis topic and to learn from researchers in different fields. Thank you especially to Elizabeth Campbell for your constant support, for challenging me, and for having faith in my ability to develop new skills. You greatly improved the caliber of this research - a contribution for which I am immensely grateful.

Thank you to Joel and Tobi at the CRD for your enthusiasm, edits, data, and funding. Thank you to Johan for the countless, dedicated hours in the Environmental Modelling class and for teaching me how to create a water budget model. I always appreciated your novel ideas. Thank you to Bethany Coulthard for sitting through numerous distressed phone calls with me. This reconstruction would not have been possible without your guidance. Thank you to David Atkinson for your expertise and for introducing me to pumpkin scones. Thank you to Ben for the many walks on campus, to Anna and Tavi for the laughs shared on glaciers, and to all the UVTRL and UVic students that have made my time on campus more enjoyable: Alessia, Lee, Bryan, Jill.

Most of all, thank you to my Montreal and Victoria friends and family for keeping me sane with countless adventures, phone calls, love, and support. Maybe now you'll understand what I've been doing the last few years.

Chapter 1: Introduction

1.1. Introduction

The world's climate is changing due to human-induced increases in atmospheric greenhouse gases. Global temperatures are projected to increase by 1.5°C above pre-industrial levels between 2030 and 2052 (IPCC 2018) if greenhouse gases continue at the current rate, with climate models predicting distinct regional consequences (Barnett et al. 2005; Huntington 2006). These regional climate outcomes include localized increases in the mean annual temperature and significant precipitation extremes (IPCC 2018). As the climate warms, it is expected that average future climates may resemble those occurring during extreme drought years of the past (Van Loon and Laaha 2015). These changes are expected to introduce major ecological impacts in forest ecosystems, with cascading economic and social implications that include detrimental effects to urban water supplies (Jarrett 2008).

The Province of British Columbia (BC), although water-rich, is not immune to water scarcity. Periods of drought on Vancouver Island are increasing in duration and intensity (Coulthard et al. 2016; Simms and Brandes 2016). In BC, a four level drought classification is used to explain the severity and appropriate level of response to drought codnitions. In 2015, severe drought conditions occurred across much of the province, and in June 2016, southern Vancouver Island experienced a Level 4 drought – a declaration that had never been applied in June before (Simms and Brandes 2016). This classification indicated that water supply was insufficient to meet socio-oeconomic and ecosystem needs.

The Sooke Lake Reservoir and Watershed on southern Vancouver Island, hereafter referred to as the Sooke Watershed, provides the majority of the drinking water required by communities in the Greater Victoria area (Capital Region District 2007). Despite being in a regional climate characterized by wet winters (Kolisnek 2005), the watershed is particularly vulnerable to drought in the summer due to its small size and shallow soils. Since 1916, four drought periods (1928-1930, 1940-1942, 1991-1995, 2001-2003) were severe enough to warrant implementation of a drought management action plan (Capital Regional District 2001; Kolisnek 2005) and prompted expansion of reservoir storage by 70% in 2002.

1.2 Research Rationale

Population growth and climate change are expected to put pressure on the GVWSA water resources in the future. Population growth has long been tied to the amount of water used in metropolitan centres. From a 2011 base, the region's average annual population is expected to grow by approximately 1% by 2038, leading to an increased demand on a limited supply of water (Capital Regional District 2018a). In addition to population growth, the Greater Victoria Capital Regional District's water resources are expected to undergo pressure from a changing climate. Models project that the watershed will likely experience more extreme events, including longer and more intense summer droughts that will increase the risk of fire in the watershed and higher precipitation totals that may lead to winter and spring flooding.

The CRD manages 98% of the lands providing source water to reservoirs in the Sooke Watershed (Capital Regional District 2004). CRD water managers have set

stewardship goals within their management policies and strategies that prioritize the maintenance of a healthy, sustainable, water supply (Capital Regional District 1999). The CRD's 2018 Climate Action Annual Report (Capital Regional District 2018) focused on the need to take action on climate change and on the requirement to protecting valuable resources like water, in order to provide for a more resilient future. Additional strategies were outlined by the Resource Planning Section of Watershed Protection (Capital Regional District 2018). These strategies describe sources of information that would help watershed managers better understand the potential effects of climate change on the GVWSA, including the need to review how the latest climate change projections for the Sooke Watershed are within historical range of variation.

The current understanding of water supplies in the Greater Victoria region are based exclusively on instrumental records of variability recorded during the 20th century. In the case of the Sooke Watershed, the instrumental record of precipitation extends to 1914 and the streamflow records are of shorter duration and only extend back to 1995. Collectively these instrumental records describe only a portion of the historic range in hydrological variability that the CRD is likely to experience in the future, meaning that extreme events and worst-case scenario drought conditions are likely underestimated. While there is a high level of uncertainty associated with the future, paleoclimatic data has played a major role in convincing hydrologists and water resource planners that instrumental records rarely describe the degree of historical variability necessary for strategic water resource planning (Meko and Woodhouse 2011).

A key motivation for this research was to extend the understanding of Sooke Watershed's historical precipitation record back centuries by developing proxy records

from annual tree rings. Dendrohydrology, a subfield of dendrochronology, the analysis of annual tree ring patterns, is one of the few avenues available for developing long-term precipitation reconstructions with annual and/or seasonal resolution (Meko and Woodhouse 2011). The resulting proxy records of precipitation variability have been widely incorporated over the past 30 years into a variety of water conservation and hazard management schemes, as well as into numerous climate change adaptation and mitigation strategies (e.g., Earle 1993). The research results presented in the thesis will provide a better understanding of the Watershed's vulnerability to climate change and is intended to assist with future water management decisions to safeguard the long-term water supply in the Sooke Watershed.

1.3 Research Objectives

The objectives of my research were to:

1. Develop climate-radial growth relationships for Douglas-fir in several stands located within the Sooke Watershed.
2. Compare Douglas-fir climate-radial growth relationships to those elsewhere in western Canada.
3. Develop pre-instrumental proxy records of precipitation variability in the Sooke Watershed.
4. Examine the temporal patterns of drought and precipitation in the Sooke Watershed, and document their linkages to major atmospheric and oceanic climatic teleconnections.

1.4 Structure of the Thesis

This thesis is organized into five chapters. Following this introductory chapter, Chapter 2 provides an overview of the study area and a review of climate variability in

the instrumental record. Chapter 3 examines the relationships between climate and radial growth of Douglas-fir located in the watershed. The findings of this analysis were compared to climate-growth relationship established within stands of Douglas-fir trees located at sites across southern Alberta and BC, to establish the basis for a modeled precipitation reconstruction for the Sooke Watershed. Chapter 4 describes how the May-June-July precipitation reconstruction was developed from a master chronology of tree ring-widths and describes those findings within the context of recent precipitation extremes, that is, periods of drier- and wetter-than average precipitation conditions. The conclusions of the thesis are presented in Chapter 5, along with potential future areas of research.

Chapter 2 : Study Area

2.1 Study Area

The Greater Victoria Water Supply Area (GVWSA) is comprised of 20,549 hectares (ha) of protected drinking water catchment lands. The Sooke Lake Watershed and Reservoir, hereafter referred to as the Sooke Watershed, is the primary supply source (Figure 2.1). The adjacent Goldstream Watershed and Reservoir system provides a secondary water supply source, and the Leech Watershed is identified as a future water supply area (Capital Regional District 2017a) (Figure 2.1).

The Sooke Watershed is located in the inner coastal region of Vancouver Island, BC, approximately 40 km north of the City of Victoria (Lat 48º30’50”N. Long 123º42’1”W; Figure 2.1). The watershed catchment area contains eighteen creeks or streams with total sub-basin areas greater than 3 ha in size (Figure 2.1). The natural catchment area for the Sooke Wateshed covers 6,720 hectares. A portion of the water in Council Lake Watershed is diverted through a pipeline and channel to enter the south basin of Sooke Lake Reservoir (Capital Regional District Water Department 1999). The reservoir is 8.3 km long with a maximum width of 1.6 km, a maximum depth of 75 m, and a total volume of 160.3 million cubic meters, of which 92.7 million cubic meters is useable for water supply (Capital Regional District 2015).

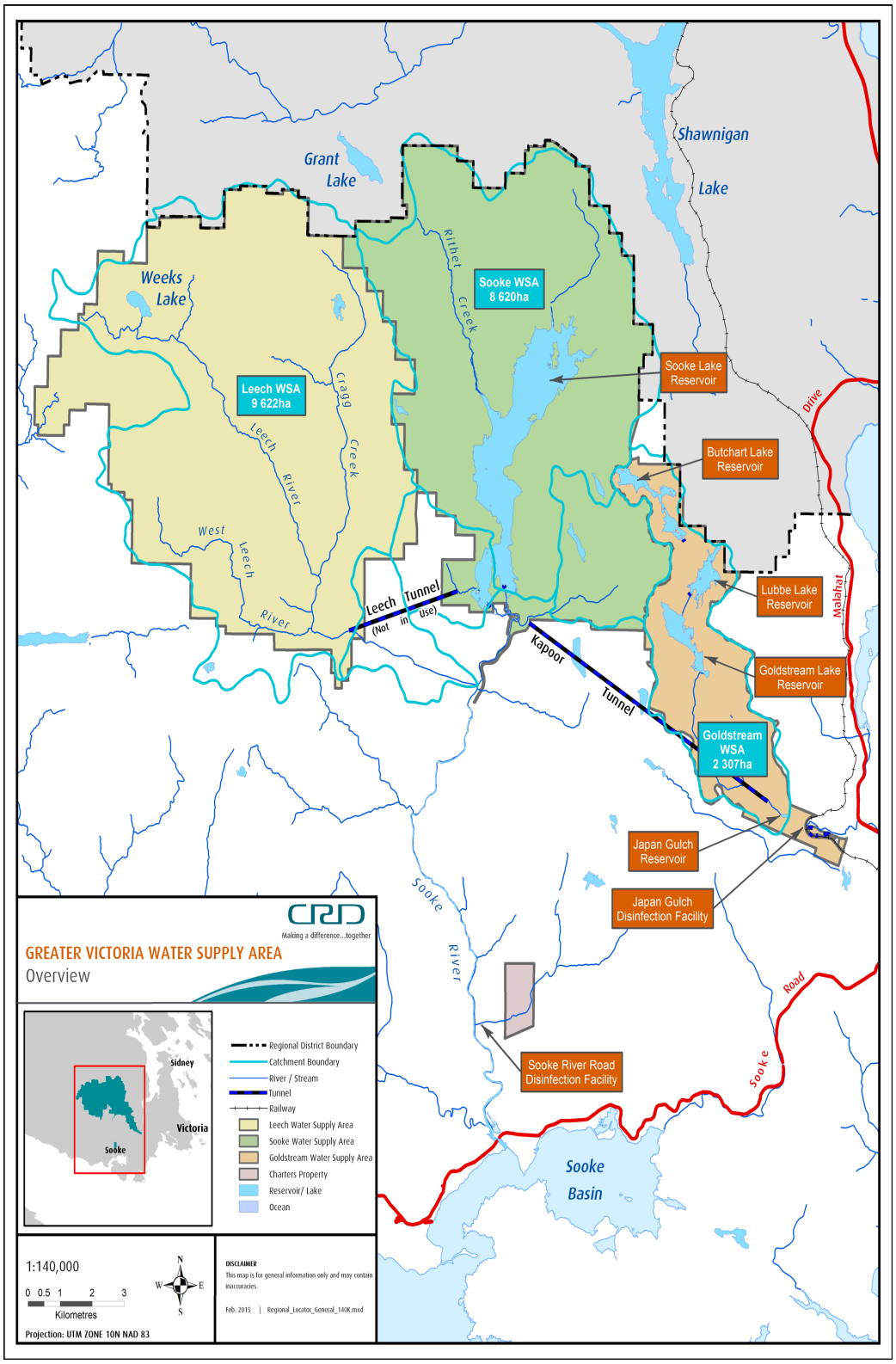

Figure 2.1: GVWSA principal watersheds, reservoirs, rivers, creeks (source: Mike Burrell, Capital Regional District, personal communication)

The GVWSA is located in the Nanaimo Lowland physiographic region (Capital Regional District 1999). Most of the GVWSA consists of gently rolling, low-relief hills and ridges, with a maximum elevation of 941 m asl at Survey Mountain in the Leech Watershed and slopes that rise to 600 m asl on the southeast basin boundary. The northeast portions of the Sooke and Goldstream watersheds consist of well-rounded and hummocky hills with minor bluffs and cliffs.

Surficial deposits in the GVWSA are largely the result of glaciation. During the Fraser Glaciation, glaciers originating on the BC mainland crossed the Strait of Georgia and covered Vancouver Island approximately 19,000 to 18,000 years ago (Alley and Chatwin 1979). The GVWSA landscape was significantly changed by this event through the scouring and removal of surficial sediments in some places, and the deposition of till in others. Fluvioglacial remnants were deposited by meltwater rivers during the deglaciation stages in some locations (Greater Victoria Water District 1994). Deglaciation led to deposition of sands and gravels in lateral channels on the side and below the retreating glacier, which led to the raised kame terraces bordering present day creeks and rivers. The surface expression of these glacial and proglacial deposits reflect the shape of the underlying bedrock (Howes and Kenk 1988) and, where deposits are thin (i.e., morainal veneers), there tend to be rock exposures. Since deglaciation 12,000 to 11,000 years ago, there has been only limited geomorphic activity related to land sliding and gully erosion within the Sooke Watershed (Capital Regional District 1999).

The main pedogenic process on well-drained sites in the GVWSA is podzolization (Greater Victoria Water District 1994). On well-drained, steep upper slopes, soils are classified as Podzols and have a distinct reddish-brown colour in the

upper 75 cm of the soil profile. At lower slope positions, leaching due to percolating water is less intense. Elsewhere in the GVWSA less acidic soils are generally Brunisolic, and are characterized by lighter colours and higher base saturations (Jungen 1985).

Forests characterized by coniferous species are the dominant vegetation in the GVWSA. They are characterized primarily by coniferous tree species. Dominant conifer species include Douglas-fir (*Pseudotsuga menziesii* var. *mensiesii*) and western red cedar (*Thuja plicata*), with a minor constituent of western hemlock (*Tsuga heterophylla*) and western white pine (*Pinus monticola*), lodgepole pine (*Pinus contorta*), and grand fir (*Abies grandis*) (Capital Regional District 1999). Deciduous dominated forests make up a small component of the GVWSA; red alder (*Alnus rubra*), big leaf maple (*Acer macrophyllum*) are in moist draws and riparian sites while arbutus (*Arbutus menziesii*), and Garry oak (Capital Regional District 1999) are typically on dry, rocky outcrops. The forest understory is dominated by salal (*Gaultheria shallon*), Oregon-grape (*Mahonia aquifolium*), and various mosses (Jungen 1985; Capital Regional District 1999).

Mature forests dominated by Douglas-fir trees greater than 140 years old presently cover approximately 20% of the Sooke Watershed (Capital Regional District 1991). Prior to 1911, mature Douglas-fir forests were extensive in the watershed (Smiley et al. 2016). Between 1911 and 1915, deforestation occurred resulting from reservoir inundation. Fires, logging activity and clear-cutting between 1920 to 1940 reduced the extent of very old Douglas-fir stands in the watershed (Smiley et al. 2016). Forest harvesting ceased in the mid-1990s as a result of public and legal opposition. Overall, since 1911, 2430 ha of forest has been logged and replanted, and 640 ha deforested for construction of water reservoirs and associated infrastructure. Currently, the forests of the

Watershed are dominated by coastal Douglas-fir with stands over 300 years old. The youngest stands were planted after logging near the turn of the century, while the old-growth stands regenerated following natural disturbances that occurred more than 200 years ago (Capital Regional District 1991).

2.2 Climate

The climate of the study area is influenced by the Pacific Ocean and surrounding mountain ranges. Proximity to the Pacific Ocean means that the region has a maritime climate. However, the Pacific Ocean and mid-latitude location also brings storms and onshore winds related to the westerlies (low-pressure systems) (Bryson and Hare 1974; Werner 2007). The Vancouver Island and Olympic Mountains form a barrier to Pacific Ocean air masses and causes strong rain shadow within the GVWSA (Capital Regional District Water Department 1999a; Jarrett 2008). Westerly winds move moist air masses eastward from the Pacific Ocean over the slopes of the Sooke Watershed and, combined with the elevation differences in the watershed, result in spatially variable precipitation (Fairburn 2001; Jarrett 2008).

The study area has distinct dry and wet seasons. The region receives, on average, about 1500 mm of precipitation a year, more than 80% of which falls as rain between October and March in the Sooke Watershed (Meidinger and Pojar 1991; Capital Regional District Water Department 1999a; Werner 2007). At the highest elevations of the watershed, snow falls occasionally from December to February and contributes no more than 6% of the annual precipitation (Capital Regional District Water Department 1999a; Zhu and Mazumder 2008). Maximum average annual temperatures occur during July and

August and average monthly precipitation is less than 30 mm in July and August, often resulting in late growing-season droughts because of high rates of evapotranspiration (Werner 2007). The winter season is associated with prevalent low-pressure systems (cyclonic) (Werner 2007) and prevailing winds predominantly from the southeast (Tuller 1979; Whitfield and Stahl 2010). Summer months are dominated by a high-pressure system (anticyclonic) (Bryson and Hare 1974) that brings warmer temperatures (Werner 2007). The summer season is also characterized by northwest winds (Tuller 1979), with the Vancouver Island Ranges modifying easterly moving moisture-laden air masses originating in the Pacific Ocean. Atmospheric rivers (AR) also trigger extreme precipitation events in BC (Radić et al. 2015). These warm 'conveyor belts' of extra tropical cyclones act as a high-speed transportation vessel for concentrated water vapour in the atmosphere (Steinschneider et al. 2018) that collides with the western cordilleran flank of Pacific North America to significantly enhance winter precipitation events, which leads to flooding and rapid mass movement events (Radić et al. 2015).

2.3 Ocean-Atmospheric Teleconnections

Large-scale ocean-atmospheric phenomena, or teleconnections, influence the climate of the GVWSA. The most influential atmospheric and sea-surface climate modes are presumed to be described by the El Niño-Southern Oscillation (ENSO), the Pacific Decadal Oscillation (PDO), the Pacific-North American Oscillation (PNA), and the northern and southern hemisphere annular modes (Mantua et al. 1997; Shabbar et al. 1997; Cayan et al. 1999; Bonsal et al. 2001; Stahl et al. 2006; Werner 2007). ENSO and the PDO modify precipitation amounts and temperature in the Pacific Northwest by

strengthening and changing the position of the Aleutian Low and North Pacific high-pressure systems and the westerly winds that deliver water vapor to the continental interior in late fall and winter (Steinman et al. 2014).

ENSO events persist for 6 to 18 months and have two phases. In the Pacific Northwest, the ENSO influence on climate is strongest from October to March (Mantua et al. 1997). Winters following the onset of an El Niño event in BC are generally warmer and drier than normal (Shabbar and Khandekar 1996; Stahl et al. 2006; Shabbar et al. 1997; Pike et al. 2010). The negative wet phase of ENSO, known as La Niña, occurs when the Aleutian Low weakens or shifts to a more westerly position and promotes a more northerly storm track (Trenberth 1997; Dettinger et al. 1998; Pike et al. 2010). La Niña winters are generally cooler and wetter than average, and are associated with higher streamflow events in rain-dominated watersheds (Fleming et al. 2007) .

The PDO operates on decadal timescales and persists for 20 to 30 years due to periodic shifts between two dominant patterns of sea surface temperatures in the North Pacific Ocean. The warm (positive) phase of the PDO is characterized by unusually high sea surface temperature along the west coast of North America, caused by a deepening of the Aleutian Low and enhanced high-pressure ridge over the Canadian Rocky Mountains that displaces the polar jet stream northward and inhibits the outflow of cold arctic air (Mantua et al. 1997). The PDO cold (negative) phase, where the jet stream is displaced southward, results in more frequent arctic outflow events and hence lower temperatures. Positive PDO phases are associated with positive winter temperature anomalies and with negative precipitation anomalies in the mountains and interior, which also reduce the snowpack (Pike et al. 2010).

The Pacific-North American (PNA) is a mode of low-frequency that results in alternating pressure patterns in the Northern Hemisphere, between the west coast of North America and eastern Pacific/southeastern USA (Latif and Barnett 1994; Yu and Zwiers 2007; Mood 2019; NOAA 2019). The PNA frequently plays a pivotal role in winter temperature regimes in western North America, as it creates strong pressure gradients off the BC coast. Negative phases of the PNA are characterized by a weak Aleutian low, westerly airflows, and a northward shift of Pacific storm tracks (Yu and Zwiers 2007). Positive PNA phases are associated with southerly airflows across western North America, a high-pressure system over the southern North American cordillera, and a southward shift of the Pacific storm track (Wise et al. 2015; Mood 2019).

2.4 Weather Station Records and Observed Climate Trends in the GVWSA

To gain an understanding of historical climatic trends in the GVWSA, preliminary analyses of precipitation and air temperature data from 1914 to 2016 and 1919 to 2016, respectively, were undertaken from records archived by the Capital Regional District (Tobi Gardner, *personal communication*). Daily precipitation and air temperature records in the GVWSA were first collected at the Sooke Dam meteorological station (Lat 48°31'04" N, Long 123°42'00"W longitude, 183 m asl; Figure 2.1) in 1914. Minimum and maximum temperatures were measured from 1919 to 1966, while total rain, snow, and precipitation was measured daily using a manual gauge starting in 1903 (Werner 2007). Between 1966 and 1995, air temperature was not measured, and daily maximum and minimum temperatures were transposed into the Sooke Dam record from Shawinigan Lake (Lat 48°38’49”N, Long 123°37’37”W, 159 m asl, Figure 2.1), the closest

Atmospheric Environment Services (AES) station recording air temperature data (Capital Regional District 1999a). In 1970, the Sooke Dam precipitation gauge was moved to a tower mounted on top of the water intake platform. From 1970 to the early 1980s, the climatological data was collected at the north end of the reservoir, after which data collection continued at the dam site. In the 1990s, multiple meteorological stations were installed in the Sooke Watershed, increasing the spatial coverage of precipitation and temperature measurements, and adding instruments to monitor more climate variables such as wind speed, wind direction, humidity, and radiation (Werner 2007). Meta-data for measurements made before the 1990s is limited and little is known about when the gauges were read and where they were located (Werner 2007; Jarrett 2008).

The mean annual air temperature at the Sooke Dam meteorological station ranged from 6.5°C (1950) to 11.1°C (2015) between 1914 to 2016, averaging 8.8 ± 5.9 °C (Figure 2.2). While the warmest month is July with an average temperature of 16.5 ± 1.4, the coldest month is January with an average temperature of 2.0 ± 2.1 °C (Figure 2.3). Average annual temperatures increased from 1919-1948 to1987-2016 by 1.3 °C (Figure 2.3). The annual precipitation at the Sooke Dam meteorological station has ranged from 799 mm in 1985 to 2556 mm in 1967 (Figure 2.2), with an average annual precipitation of 1641 mm ± 324 mm. Precipitation is typically greatest during December, representing 18% of total annual rainfall, (294 ± 119 mm) and July is typically the driest month with rainfall totals averaging 23 ± 19 mm and representing 1% of annual rainfall (Figure 2.2).

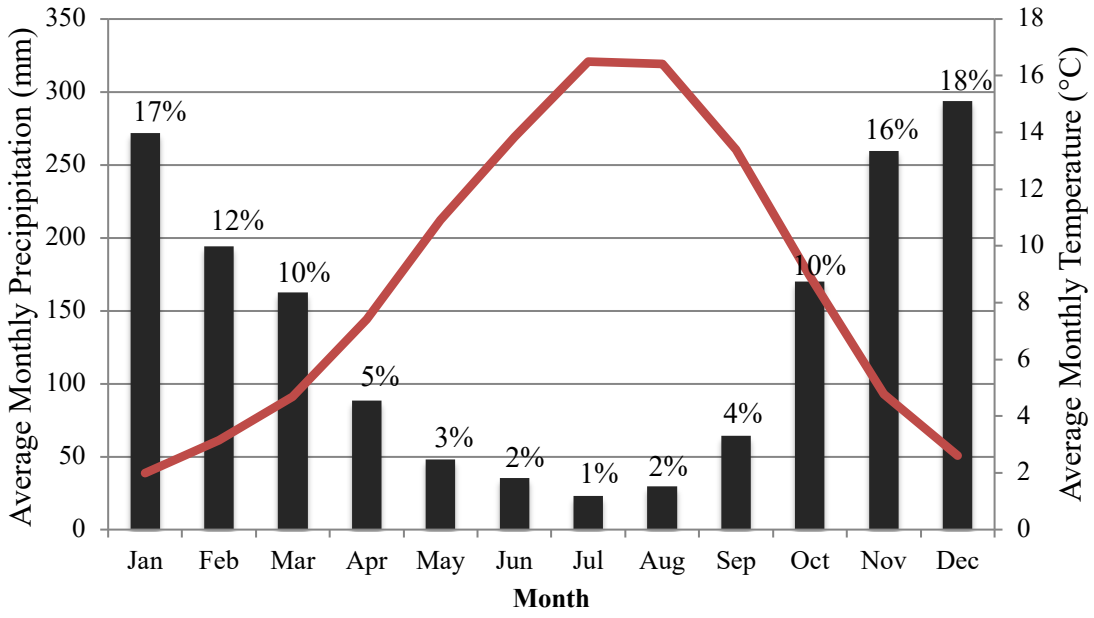

Figure 2.2: A climograph of the monthly percent distribution of total precipitation and monthly average temperature from 1919 to 2016 at the Sooke Dam meteorological station. The bars demonstrate the average monthly total precipitation (mm) and the red line represents the average monthly temperature.

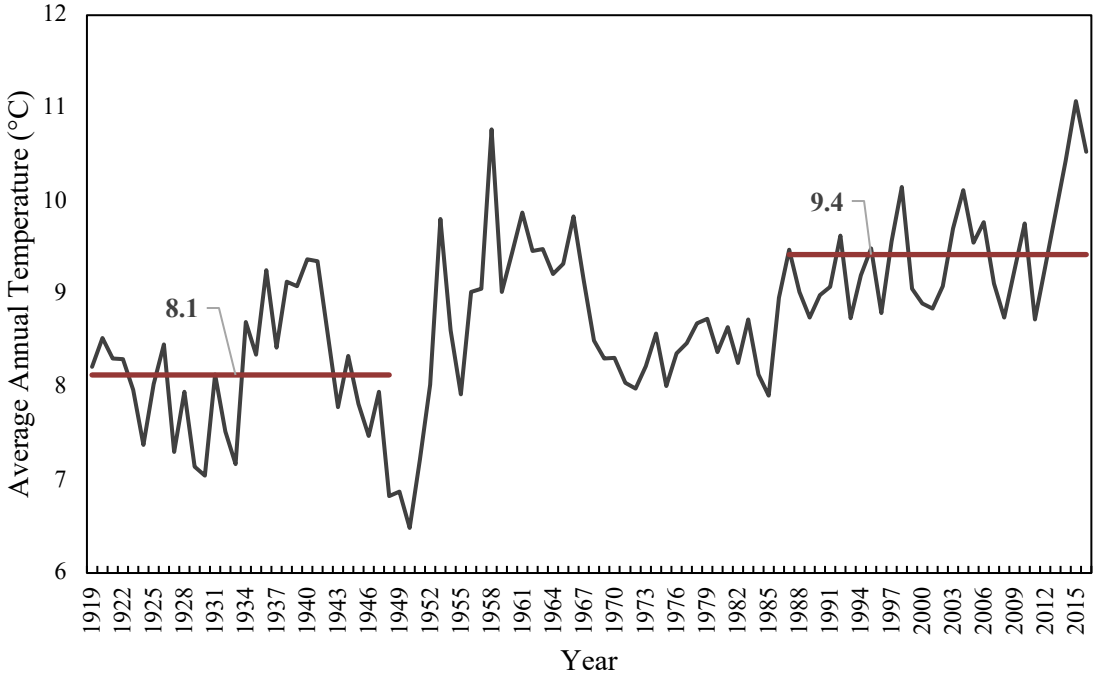

Figure 2.3: Average annual temperature of Sooke Dam meteorological station data from 1919 to 2016. First and last 30-year averages in red.

2.4 Summary

This chapter identified the location of the Sooke Watershed and described its essential characteristics and general features. An in-depth description of the Sooke Watershed is necessary for developing climate-growth relationships in Chapter 3, as it provides details of the possible interactions that drive forest growth aside from climate. The description of climate data and teleconnections contextualizes the understanding of precipitation patterns in the May-June-July reconstruction of Chapter 4. The study area description provides context to the research presented in the following chapters by providing the biogeographic and hydroclimatic setting in which the results are placed.

Chapter 3 : Characterizing Douglas-fir radial growth responses to annual temperature and precipitation fluctuations

3.1 Introduction

The distribution of tree species and forest productivity are strongly linked to climate (Aber et al. 2001; Parmesan 2006; McKenney et al. 2007). Global mean annual temperature is expected to increase 1.5°C since its pre-industrial state by 2030 to 2052 (IPCC 2018). Such changes in temperature, and changes to precipitation regimes, are likely to alter tree growth and forest productivity, as well as the species composition of local forests (Parmesan 2006). Understanding and quantifying how trees have responded to recent climate variations provides insight that will help to predict future changes in tree growth and forest productivity, which may have substantial ecological impact and socio-economic impacts, particularly for forest resource-dependant communities.

In western North America, several tree species are already exhibiting the potential effects of climate change, either through the direct effect of drought or indirectly by drought-associated health decline (Allen et al. 2010). Douglas-fir (*Pseudotsuga menziesii*) is an ecologically and economically important tree species in western North America forests. With a geographic range extending from northern British Columbia (BC) to central Mexico, the species grows under a wide range of climate, site, and soil conditions (Hermann and Lavendar 1990; Weiskittel et al. 2012; Littke et al. 2018). Douglas-fir has two widely recognized varieties: *menziesii*, the coastal variety, and *glauca*, the interior variety. Douglas-fir trees in the interior parts of its geographic range generally grow under cooler winters and warmer, drier summers than the coastal variety (Coops et al. 2010). Projections about the suitability of future habitat for Douglas-

fir suggest some substantial changes (Rehfeldt et al. 2006; Weiskittel et al. 2012). By 2090, Douglas-fir habitat is expected to shift from coastal areas of North America to the interior, despite a small projected change in terms of area (-4%) (Weiskittel et al. 2012). While Douglas-fir in BC is projected to lose much of its current climatic habitat and gain additional habitat at higher elevations and latitudes (Hamann and Wang 2006; Wang et al. 2012), the extent of Douglas-fir occurring in coastal Oregon and Washington is expected to significantly decrease (Rehfeldt et al. 2006). This habitat loss is expected to be a consequence of climate changes that will result in average temperatures falling outside the physiological limit of Douglas-fir (Coops et al. 2010). Expectations on future productivity are also variable, with decreasing productivity expected in coastal areas, modest increases in productivity expected within interior areas (Weiskittel et al. 2012), and growth reductions projected to decrease in higher elevation populations (Chen et al. 2010).

The study of temporal variations in annual tree ring-widths, also known as dendrochronology (Fritts 1976), is useful for examining the effects of climatic change on forests. Dendrochronology research of Douglas-fir in western Canada has largely focused on: comparing ring-widths climate sensitivity to Ponderosa pine chronologies (Watson and Luckman 2002); comparing northern and southern distributions of the interior variety (Griesbauer and Green 2010); analyzing the variation of climate-growth relationships on southern Vancouver Island (Griesbauer et al. 2019); and comparing climate-growth responses within the interior variety (Griesbauer et al. 2011; Wood and Smith 2015). Other notable studies focused on examining the radial growth response of Douglas-fir to climate variability across the natural geographic range of the species including those of

Little et al. (1999); Case and Pederson (2005); González-Elizondo et al. (2005); Littell and Peterson (2005); Chen et al. (2010); and Lee et al. (2016).

While the radial growth of interior Douglas-fir is limited by low precipitation totals and high growing season temperatures, the radial growth of coastal Douglas-fir tends to be limited by summer 'dryness' and the temperature of the preceding winter (Chen et al. 2010). The interior variety grows more slowly than the coastal variety, both at interior locations and in coastal settings. The radial growth of the coastal variety is further limited by cool growing season temperates (Oliver et al. 1986; McCreary et al. 1990). Generally, the relationship between the radial growth of Douglas-fir growth and climate in the Pacific Northwest has been associated with water availability (Littell et al. 2008; Littke et al. 2018; Griesbauer et al. 2019).

The intent of this chapter was to examine the radial growth-climate relationships of Douglas-fir in southern BC and Alberta. The research extends knowledge from previous research, where information about growth responses among Douglas-fir in the interior parts of its range in Canada is lacking. The approach I took was to first examine how the radial growth of Douglas-fir trees located within the Sooke Watershed changes in response to variations in the annual fluctuations in temperature, precipitation, and the Hargreaves Climatic Moisture Deficit (CMD) since the beginning of the 20th century. I then compared climate-growth relationships in the Sooke Watershed to those in other biogeoclimatic zones of BC, and Alberta. Gaining a better understanding of these climate-growth relationships offered insight into how Douglas-fir forests in western Canada will change in the future. It also provided the background information necessary for the model-based reconstruction of historical precipitation presented in Chapter 4.

3.2 Objectives

The objectives of this chapter were:

1. to develop an understanding of the spatial and temporal variability in radial growth-climate relationships for Douglas-fir in the Sooke Watershed.

2. to compare these Sooke Watershed climate-growth relationships to other Douglas-fir growth-climate relationships in regional climates of western Canada.

3.3 Study sites

Coastal and interior Douglas-fir are widely-distributed across large gradient of climate conditions (Figure 3.2). The characteristics of these regional climates are represented by the Biogeoclimatic Ecosystem Classification (BEC) of BC and the Alberta Natural Regions classification systems (Pojar et al. 1987; Natural Regions Committee 2006). These systems delineate a variety of regional climates within the range of Douglas-fir in BC and Alberta. In this study, I used these ecosystem classification systems to stratify the selection of tree increment core samples so they represented a wide range of regional climates in which Douglas-fir grows in western Canada.

3.3.1 Sooke Watershed study sites

Most of the GVWSA is classified as falling within the very dry, maritime Coastal Western Hemlock biogeoclimatic subzone (CWHxm). CWHxm climates are, in general, characterized by dry summers and prolonged water deficits in the growing season that can last 2 to 3 months. Winters are moist and mild, receive minimal snowfall, and are characterized by a frost free period of about 200 days (Klinka et al. 1979; Capital Regional District Water Department 1999a). Higher elevations in the north as well as western portions of the Sooke Watershed fall within the eastern CWHxm1 variant, which is characterized by a drier climate, higher mean annual temperature, and lower mean

annual precipitation than CWHxm2 (Table 3.3) (Capital Regional District Water Department 1999a). I sampled sites in the Sooke Watershed that were located in both the CWHxm1 and CWHxm2 biogeoclimatic zones.

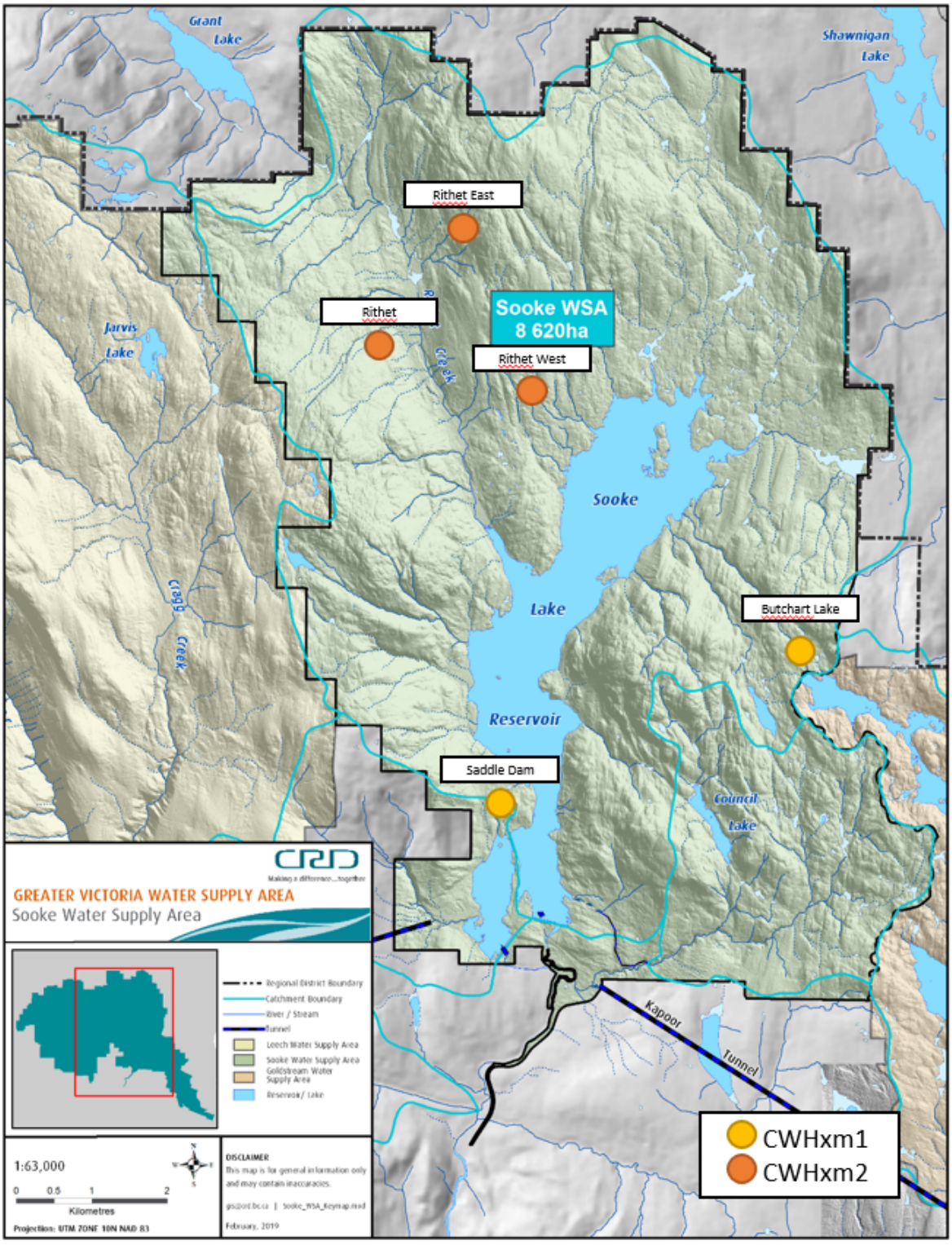

Figure 3.1: Sooke Watershed tree-ring sample sites.

Sampling sites at Butchart Lake, Farmer Saddle Dam, and Saddle Dam were located in CWHxm1 (Figure 3.1). Sites at Rithet, Rithet West, and Rithet East were located in BEC zone CWHxm2. North of the Sooke Watershed, CWHxm1 occurs above 280 m asl on cool aspects and 350 m asl on warm aspects. South of the Sooke Watershed, CWHxm1 occurs above 450 m asl on cool aspects and above 500 m asl on warm aspects. The CWHxm2 ranges from 280 to 700 m asl on cool aspects and from 350 to 800 m asl, on warm aspects north of the Sooke Watershed. South of the Sooke Watershed reservoir, the variant occurs above 450 m asl on cool aspects and above 500 m asl on warm aspects (Pojar and Meidinger 1987).

3.3.1.1 CWHxm1 sampling site characteristics

The Saddle Dam site is located at an east facing, bottom-slope position (239 m asl) on a rocky outcrop with shallow soil along the southwestern edge of the Sooke Reservoir (Figure 3.1). While there was no indication of forest harvesting at the site, fire scars were evident on a number of trees. The forest was comprised of mature and very old trees, had an open canopy, with numerous standing dead trees and fallen decaying logs. Douglas-fir was the dominant canopy tree species; a small number of arbutus (*Arbutus menziesii*) and lodgepole pine (*Pinus contorta*) occurred in the canopy. There was a patchy shrub layer composed largely of salal (*Gaultheria shallon*), scattered amounts of Nootka rose *(Rosa nootkatensis*), western juniper (*Juniperis occidentalis*) and red huckleberry (*Vaccinium parvifolium*) (Jarrett 2008). Most of the ground was covered by a moss layer of Oregon beaked moss (*Kindbergia oregana*).

The Butchart Lake site occurred on an east-facing, upper-slope position (525 m asl) of mesic sites, with deeper soils than the Saddle dame site. Many fallen and partially-

decomposed trunks suggested that wind is an important disturbance at this site. This type of disturbance opens up the canopy and allows growth spurts in the surrounding trees. There was also abundant evidence of forest fires at the site, with charcoal found on most trunks. Salal (*Gaultheria shallon*) and Oregon beaked moss (*Kindbergia oregana*) were the main components of the understory at this site.

3.3.1.2 CWHxm2 site characteristics

The Rithet East site is located at a west-facing, mid-slope position on a slope in the Rithet Creek basin (Figure 3.1). Evidence of historical forest harvesting was present and an overgrown access road cuts through the centre of the site. The soil was very well drained with gravel, stones and cobbles distributed throughout the soil horizon (Jarrett 2008), and was classified as having a dry soil-moisture and medium soil-nutrient regime. The forest at Rithet East is an even-aged Douglas-fir stand with abundant western red cedar growing in the understory. Western white pine (*Pinus monticola*), arbutus and bigleaf maple saplings were observed at the top boundary of the site, as well as an understory consisting of bunchberry (*Cornus canadensis*) and Oregon grape.

The Rithet West site is located on a mid-slope, east-facing position (415 m asl) in the Rithet basin (Figure 3.1). There are several standing dead trees and fallen decaying logs on the lower boundary of the site, above an adjacent spur road. The soil is well drained with a thin humus form, and the site is bordered by a ravine on the southern side. Three tree species dominate the forest canopy; Douglas-fir, western red cedar, and western hemlock. The forest canopy is multi-layered with trees of various sizes and ages. A dense shrub layer is present and comprised entirely of salal. A widespread moss layer of Oregon beaked moss covered the majority of the open ground.

The Rithet site is located on a south-facing, mid-slope position (513 m asl) on the north-west side of the Sooke Watershed and on the west side of Rithet Creek (Figure 3.1). The forest is dominated by Douglas-fir, with occasional western red cedar. There were several fallen trees on the site, with several standing dead trees observed and fallen partially-decayed logs, suggesting possible wind or insect disturbance. A dense salal shrub layer was present across all Rithet sites as well as a widespread Oregon beaked moss layer, and occasional bunchberry *(Cornus canadensis*), which covered the majority of the open ground.

3.3.2 Supplemental study sites

The supplemental study sites included in this research were selected by reviewing tree-ring data obtained from the BC Forests, Lands, Natural Resource Operations and Rural Development (BCFLNRORD) Permanent Sample Plots (PSP) and the Canadian Forest Service National Forest Inventory plots and other research plots. Douglas-fir sites were selected in nine BC BEC zones and one plot was identified in the Alberta foothills (Figure 3.2). These sites represent a wide range of the climate conditions in which Douglas-fir grows in western Canada. Tree-ring samples in zone MSdm1 were chosen to represent Douglas-fir growing at high elevations, samples in zone SBSdw3 were chosen to represent Douglas-fir near the northern limits of its geographic range, and samples from the Canadian Rocky Mountains Natural Region plot (RMNR), were chosen to represent Douglas-fir growing near its eastern geographic limits in the Alberta foothills (Figure 3.2).

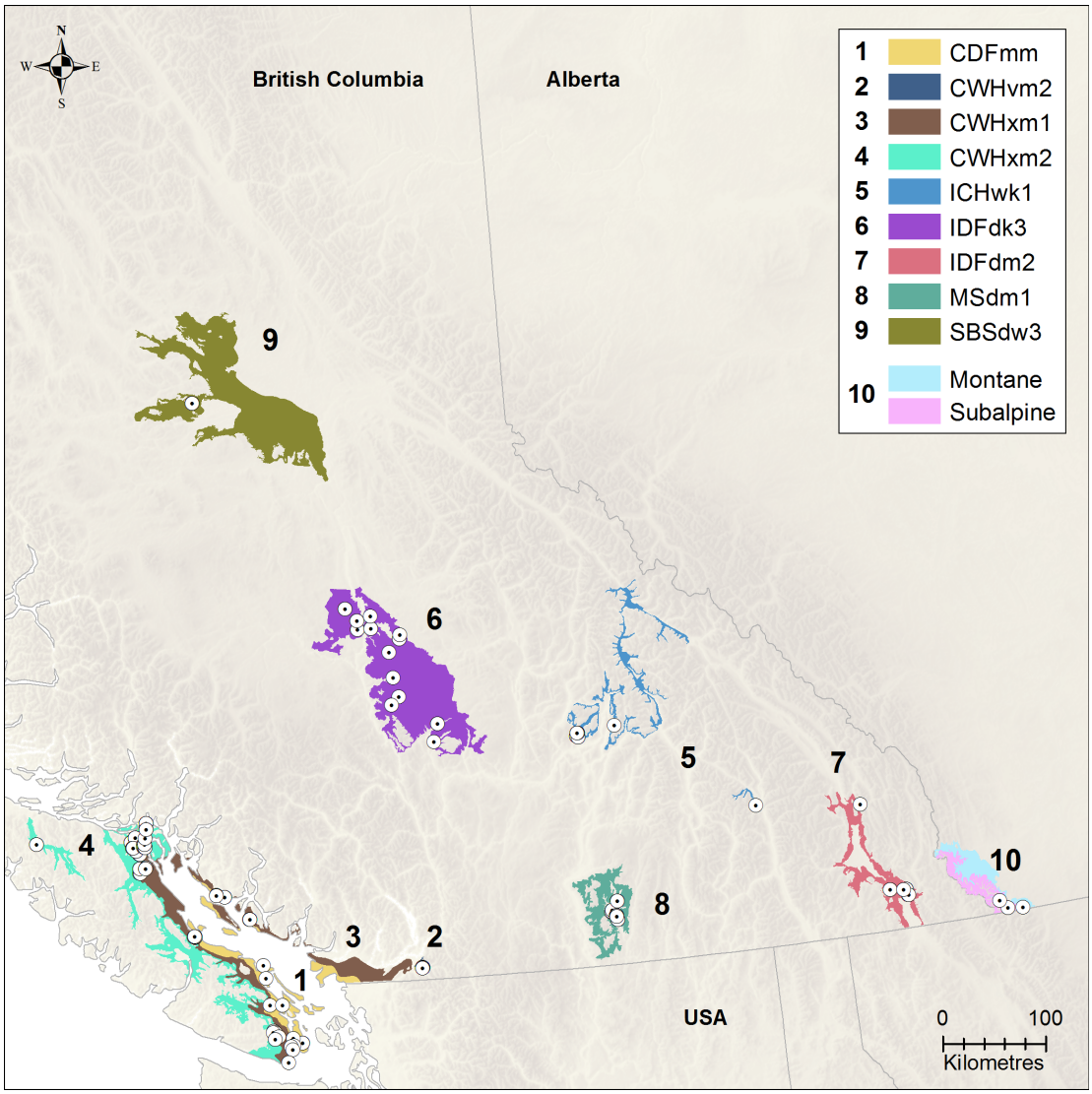

Figure 3.2: Location of plots from which tree-ring data were obtained. Samples were selected over a range of biogeoclimatic zones in BC and AB. Bullseye symbols identify the locations of the plots described in Appendix B. Sites in close proximity are represented by a single bullseye.

3.4 Methods

3.4.1 Tree-ring data

Douglas-fir increment core data from the Sooke Watershed were gathered from a variety of sources: field sampling in 2017 and archived tree ring data collected by Jarrett (2008) in 2006, from permanent sample plots established by the BC Forests, Lands, Natural Resource Operations and Rural Development (FLNRORD), and from tree-ring

data archived at the Canadian Forest Service, Pacific Forestry Centre (PFC). The tree cores collected in 2006 by Jarrett (2008) and in 2017 for this study were sampled using a 5.2 mm increment borer. Approximately 20 trees were sampled per site, with two samples being taken per tree, following standard dendrochronological protocols (Briffa et al. 1992). As many of the tree cores sampled during the FLNRO and PFC surveys were not collected with dendrochronological analysis in mind, the number of trees sampled per site ranged from 1 to 20. Tree-ring data from multiple sites were combined to represent each of the biogeoclimatic zones considered (Figure 3.2).

After air drying the cores collected in 2006 and 2017, they were glued to mounting blocks and sanded to a fine polish to distinguish ring boundaries. Digital images of the cores were processed using a high-resolution scanner. A WinDendro^{TM} image processing measurement system was used to measure the tree-ring widths. Visual cross-dating of the ring-width data was completed following standard cross-dating protocols (Stokes and Smiley 1996).

The ring-width series in each biogeoclimatic zone were used to develop master chronologies for each regional climate (Appendix B). The process of developing a master chronology was undertaken in three steps. First, COFECHA (Dendrochronology Program Library described in Holmes 1983) was used to verify that each ring was assigned the correct date; this software conducts a cross-dating procedure that examines correlations between 50-year segments with 25-year lags at a significance level of 0.01 (Grissino-Mayer 2001). Individual tree-ring series were then detrended with the ARSTAN command in the dplR software (Bunn 2008) using a mean standardization function to remove age-related trends in the time series (Cook and Krusic 2005). Standardized tree-

ring series where then averaged to produce a master chronology for each regional climate. The dplR package was then employed to calculate various descriptive statistics for the master chronology including mean sensitivity and expressed population signal (EPS) of each master chronology. Mean sensitivity provides a measure of interannual growth variation (Cook and Kairuikstis 2013). EPS estimates the strength of the climate signal retained in the annual rings, where an EPS value of 0.80 is suggested as the minimum value for adequately capturing the hypothetical population growth signal in the sample size (Wigley et al. 1984). The top three widest and narrowest years of ring width growth for each chronology were then reported as marker years. The marker years in each chronology were intended to demonstrate that annual growth increments across some biogeoclimatic zones are controlled by similar factors.

3.4.2 Climate data

Data for three climate variables at each site (air temperature, precipitation, and the Hargreaves Climate Moisture Deficit (CMD)) were obtained from ClimateWNA (Wang et al. 2016), which downscales gridded (4 x 4 km) monthly temperature and precipitation data for the reference normal period (1961-1990) from PRISM (Daly et al. 2008) and WorldClim (Hijmans et al. 2005) to scale-free point locations. Latitudinal and longitudinal coordinates for individual plots in each BEC zone were entered to obtain temperature and precipitation data per plot, which was then averaged to create data representing the climate of for samples obtained from that biogeoclimatic zone (Wang et al. 2016) (Table 3.1). CMD is derived from temperature and precipitation data and is the sum of the monthly difference between a Hargreaves reference evaporation (E_{ref}; mm) and precipitation (mm). If E_{ref} is less than precipitation then the monthly CMD is

zero (in this case the precipitation minus E_{ref} is a climatic moisture surplus) (Wang et al. 2012).

Table 3.1: Averaged Climate Data from 1901-2016.

Site	MAT	MWMT	MCMT	MAP	MSP	AHM	SHM	PAS
CDFmm	9.7	17.0	2.8	985.9	152.9	20.6	121.0	107.7
CWHvm2	6.3	15.1	-2.4	1718.3	387.6	9.7	41.7	346.2
CWHxm1	9.1	17.3	1.4	1351.9	208.5	14.7	92.2	149.7
CWHxm2	8.2	16.5	0.6	1750.2	217.0	10.7	81.7	185.8
ICHwk1	4.1	16.0	-8.5	885.4	282.6	17.0	61.9	850.6
IDFdk3	3.6	15.2	-10.3	430.1	206.3	32.3	77.9	949.7
IDFdm2	5.2	17.8	-8.4	497.4	213.3	31.5	90.3	764.3
MSdm1	3.5	15.2	-8.6	590.9	223.8	23.4	74.3	886.2
RMNR	2.7	14.7	-9.7	1082.6	423.4	12.3	38.2	1015.5
SBSdw3	2.3	14.1	-12.5	524.9	232.8	23.9	63.3	1186.8

Note: MAT, mean annual temperature (°C); MWMT, mean warmest month temperature (°C); MCMT, mean coldest month temperature (°C); MAP, mean annual precipitation (mm); MSP, May to September precipitation (mm); AHM, annual heat-moisture index (MAT+10)/(MAP/1000)); SHM, summer heat-moisture index ((MWMT)/(MSP/1000)); PAS, precipitation as snow (mm) between August in previous year and July in current year

3.4.3 Climate-growth relationships

I first undertook an analysis of climate-radial growth relationships on master tree-ring chronologies for biogeoclimatic zones within the Sooke Watershed (i.e., CWHxm1 and CWHxm2). Following this, I completed an analysis of established master chronologies for several other subzones to assess the influence of large-scale climate variables on regional Douglas-fir growth. In both analyses, correlations with prior and current year monthly climatic values were tested. The R package TreeClim (Zang and Biondi 2015) was used to quantify climate-growth relationships.

Correlation and response coefficients were computed between the precipitation, temperature, and CMD variables and the master tree-ring chronology developed for each regional climate. I conducted analyses of climate-growth relationships at two temporal

scales. I developed climate-growth relationships for entire length of the climate data (1901 to 2016) to gain a longer snapshot of the forest response to climate change. However, because tree species responses to climate over large temporal scales are often relatively coherent (Griesbauer et al. 2019), while short-term scales show greater variation in climate response, I also developed growth-climate relationships on a shorter temporal scale analyzing data in 25-year moving intervals. This shorter temporal scale allowed me to explore how growth sensitivities vary over time (Griesbauer and Green 2010; Griesbauer et al. 2019).

Short-term climate-growth relationships were quantified with moving correlation functions (MCFs) to describe the growth response to multiple climatic variables over a moving time window (Biondi 2000; Biondi and Waikul 2004; Carrer and Urbinati 2006). A 25-year moving window was chosen for analysis, offset by 1-year increments (e.g. 1901-1926, 1902-1927…), to provide a fine temporal resolution while ensuring sufficient degrees of freedom. The 25-year moving windows were reported by stating the last year of the 25-year window. For each 25-year time window, the significant response coefficients were entered into a multiple regression model to determine the adjusted coefficient of determination between climate and growth. Climate-growth relationships were deemed stable if correlations did not fluctuate from positive to negative throughout the timeframe. Long-term (1901-2016) climate-growth relationships were also computed using a static correlation with Dcc function in Treeclim. For both long- and short-term windows, a correlation was considered strong if $p < 0.05$. Short-term climate-growth results were intended to provide insight into shifts in climate-growth relationships over

time, whereas long-term analyses were intended to demonstrate the persisting effects of climate on growth regardless of shifting relationships.

Frequency distributions of regression coefficients for the relationship between annual ring-widths and climate variables were used to identify the most influential variables on growth. Influential variables were identified by statistically significant correlations ($p < 0.05$). Specifically, current and prior monthly climate variables were focused on to determine which climate variables explained the greatest effect on tree ring-width (Littell et al. 2008).

3.5 Results

3.5.1 Dendrochronological characteristics of chronologies

The Sooke Watershed CWHxm1 and CWHxm2 standardized chronologies have EPS values exceeding 0.8, indicating that they contain sufficient site signal for climate analysis (Wigley et al. 1984). Chronology mean sensitivity and inter-series correlation (IC) were higher in CWHxm1 than CHWxm2 (Table 3.2). The Sooke Watershed and supplementary chronologies of standardized tree ring-widths varied considerably across biogeoclimatic zones (Figure 3.3). Narrow marker years common in more than one biogeoclimatic zone included 1916 (RMNR and ICHwk1), and 1956 (CWHxm1 and CWHvm2) (Figure 3.3). Reoccurring wide marker years include 1927 (IDFdm2 and RMNR), 1942 (CWHxm2, CWHxm1, and IDFdm2), 1990 (CDFmm and CWHvm2), 1981 (CWHxm2, IDFdm2, and ICHwk1), 1984 (ICHwk1 and MSdm1), 1998 (ICHwk1 and MSdm1), and 2006 (MSdm1, IDFdm2, and CWHxm2) (Figure 3.3).

Table 3.2: Dendrochronological characteristics of standardized tree ring-width chronologies of Douglas-fir in the Sooke Watershed.

Biogeoclimatic Zone	Variety	Subzone / Subregion	# Plots	Chronology (years)	Trees (n)	IC	Mean Sensitivity	EPS
CWHxm1	Coastal	Very Dry Maritime	n=3	1445-2016 (572 yrs)	128	0.581	0.211	0.96
CWHxm2	Coastal	Very Dry Maritime	n=3	1281-2016 (736 yrs)	110	0.564	0.190	0.98

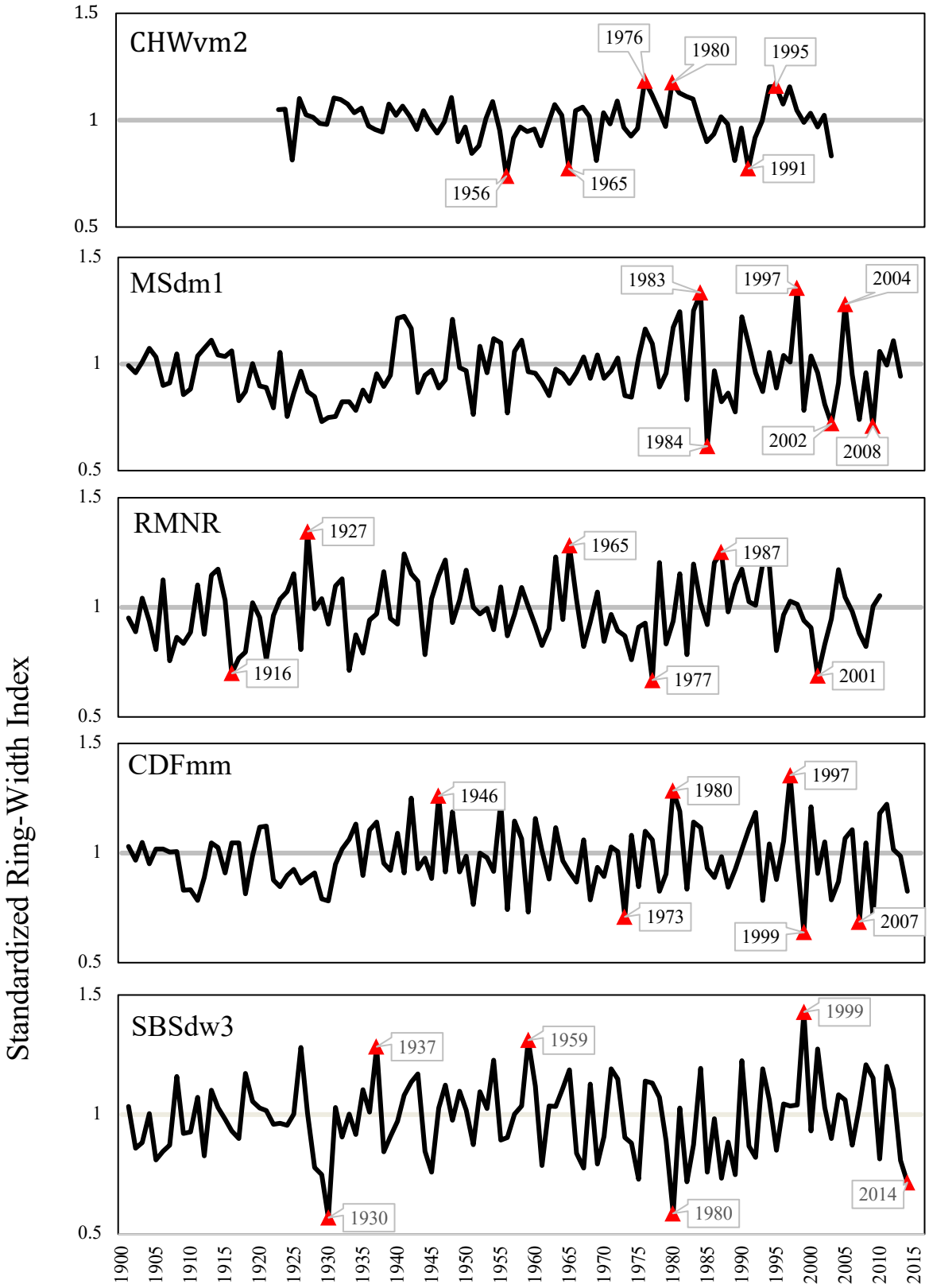
Standardized Ring-Width Index
CHWvm2
1976
1980
1995
1956
1965
1991
MSdm1
1983
1997
2004
1984
2002
2008
RMNR
1927
1965
1987
1916
1977
2001
CDFmm
1946
1980
1997
1973
1999
2007
SBSdw3
1999
1937
1959
1930
1980
2014
1.5
1
0.5
1900
1905
1910
1915
1920
1925
1930
1935
1940
1945
1950
1955
1960
1965
1970
1975
1980
1985
1990
1995
2000
2005
2010
2015

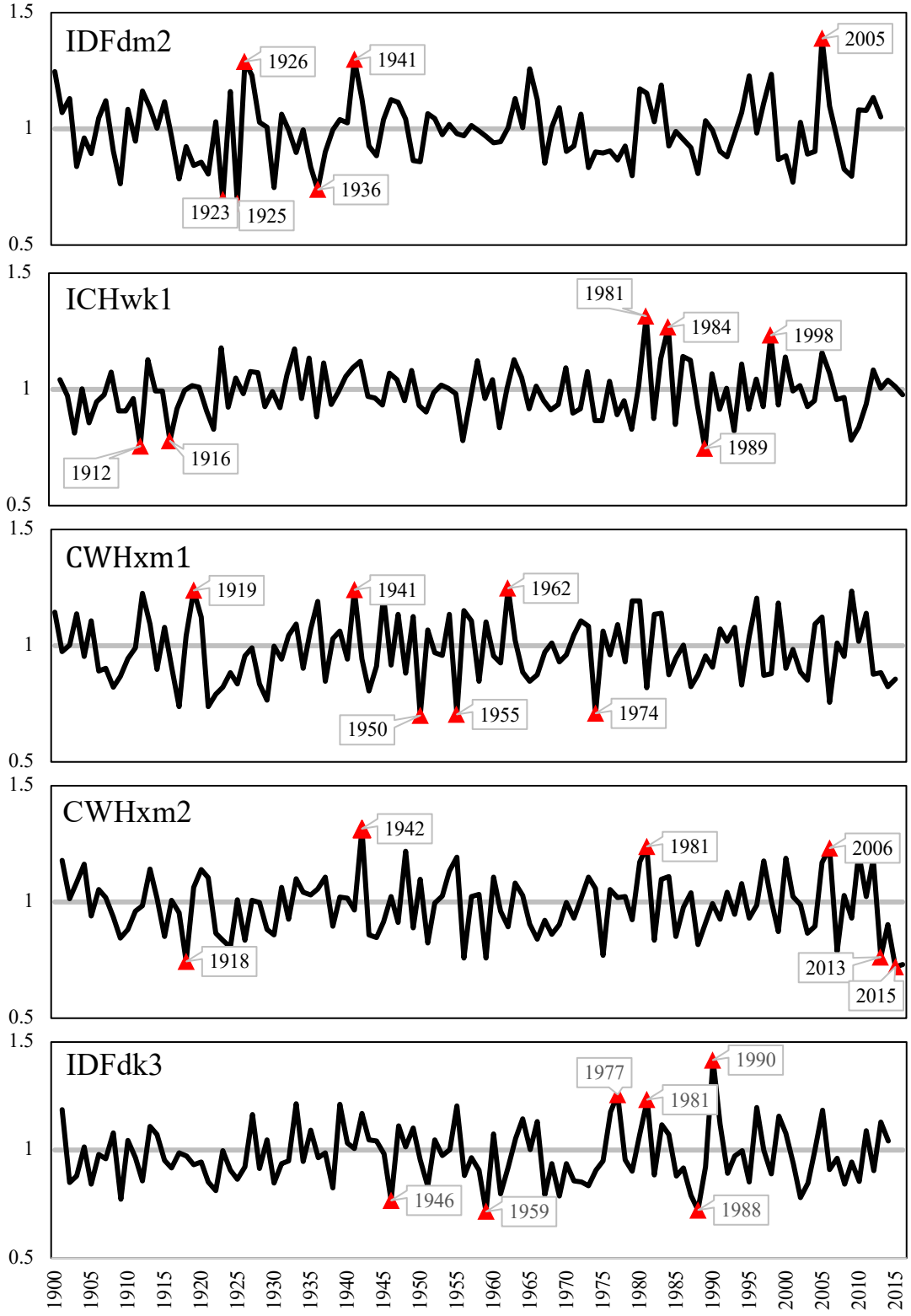

Figure 3.3: Master chronologies of tree ring-width index by biogeoclimatic zone. Red triangles indicate marker years (i.e. the top three widest and narrowest ring widths).

3.5.2 Climate-growth relationships in the Sooke Watershed

3.5.2.1 Long-term climate growth relationships

Temperature did not have a significant influence on Douglas-fir radial growth at the sites sampled in the Sooke Watershed (Table 3.3). In contrast, all the sites sampled within the Sooke Watershed had significant long-term climate-growth responses to precipitation. This finding was interpreted to indicate that the radial growth of Douglas-fir trees in the Sooke Watershed is moisture-limited.

Significant climate-growth relationships were associated with total June precipitation in the CWHxm1 (R=0.467) and CWHxm2 subzones (R =0.0419). Precipitation-growth relationships were significant from April through July in CWHxm1, and in May, June, October, and November in CWHxm2, indicating that precipitation has a larger effect on radial growth in the latter half of the seasonal growing season in CWHxm1, but not in CWHxm2 forests. Precipitation falling in both August and September was significantly related to radial growth in the following growing season in both CWHxm1 and CWHxm2 forests.

The most significant correlations between tree ring-width index and CMD occurred in June; radial growth was negatively associated with high CMD values in the CWHxm1 and CWHxm2(Table 3.3). July CMD had a significant negative effect on Douglas-fir radial growth in CWHxm1 but not in CWHxm2. Previous May and June CMD had a negative effect on growth in CWHxm2, while it did not in CWHxm1.

Table 3.3: Significant correlation coefficients between monthly climate variables and indices of Douglas-fir tree-ring widths analyzed over the period of 1901 to 2016 (long-term growth variation) in the Sooke Watershed.

Region	Month	Correlation Coefficients		
		Precipitation	CMD	Temperature
CWHxm1	April	0.213		
	May	0.246	-0.224	
	June	0.467	-0.469	
	July	0.214	-0.242	
	Previous August	0.199	-0.204	
	Previous September	0.210	-0.194	
CWHxm2	May	0.246	-0.282	
	June	0.419	-0.359	
	October	-0.228		
	November	0.210		
	Previous May		-0.219	
	Previous June		-0.207	
	Previous August	0.182		
	Previous September	0.244		

Note: All coefficients shown are significant at $P < 0.05$, based on bootstrapped confidence limits. CMD, Hargreaves Climate Moisture Deficit.

3.5.2.2 Short-term climate-growth relationships

The short-term moving correlation windows (MCFs) revealed that CWHxm1 and CWHxm2 generally reacted similarly in timing and significance to precipitation. While long-term April precipitation had a significant positive correlation with the ring-width indices in CWHxm1 (Table 3.3), growth-climate relationships analyzed over shorter time periods indicated that April precipitation only had significantly positive correlations with ring-width between the 1946 and 1970 intervals (Figure 3.4A). Similarly, May precipitation had intermittent periods of significant effects on ring-width throughout the time period for CWHxm1 and CWHxm2. A temporal shift in significant correlation coefficients for June to July precipitation occurred in both biogeoclimatic zones within

the Sooke Watershed. The relationship between ring-width and annual precipitation was significantly positive in June during the early portion of the twentieth century, gradually decreased after the 1956 period, became insignificant over the middle of the twentieth century, and then returned again starting in the 1981 period (Figure 3.4). Indexed tree ring-width became significantly positively correlated with mid-century July precipitation in the 1946 period, about the same time that there was a shift to a relationship to June precipitation. After the 1946 period, the relationship between ring-width and July precipitation was insignificant as a significant response to June precipitation emerged in the later half of the 20th century (Figure 3.4a). A significant positive relationship between ring-width and precipitation was observed in September in the 1937 period in CWHxm1, and in the 1939 period in CWHxm2 (Figure 3.4). This relationship changed in the 1956 MCF in CWHxm1 and CWHxm2; in the 1974 MCF in the CWHxm1 and in the 1981 MCF in CWHxm2, ring-width was significantly negatively related to September precipitation (Figure 3.4).

A) CWHxm1

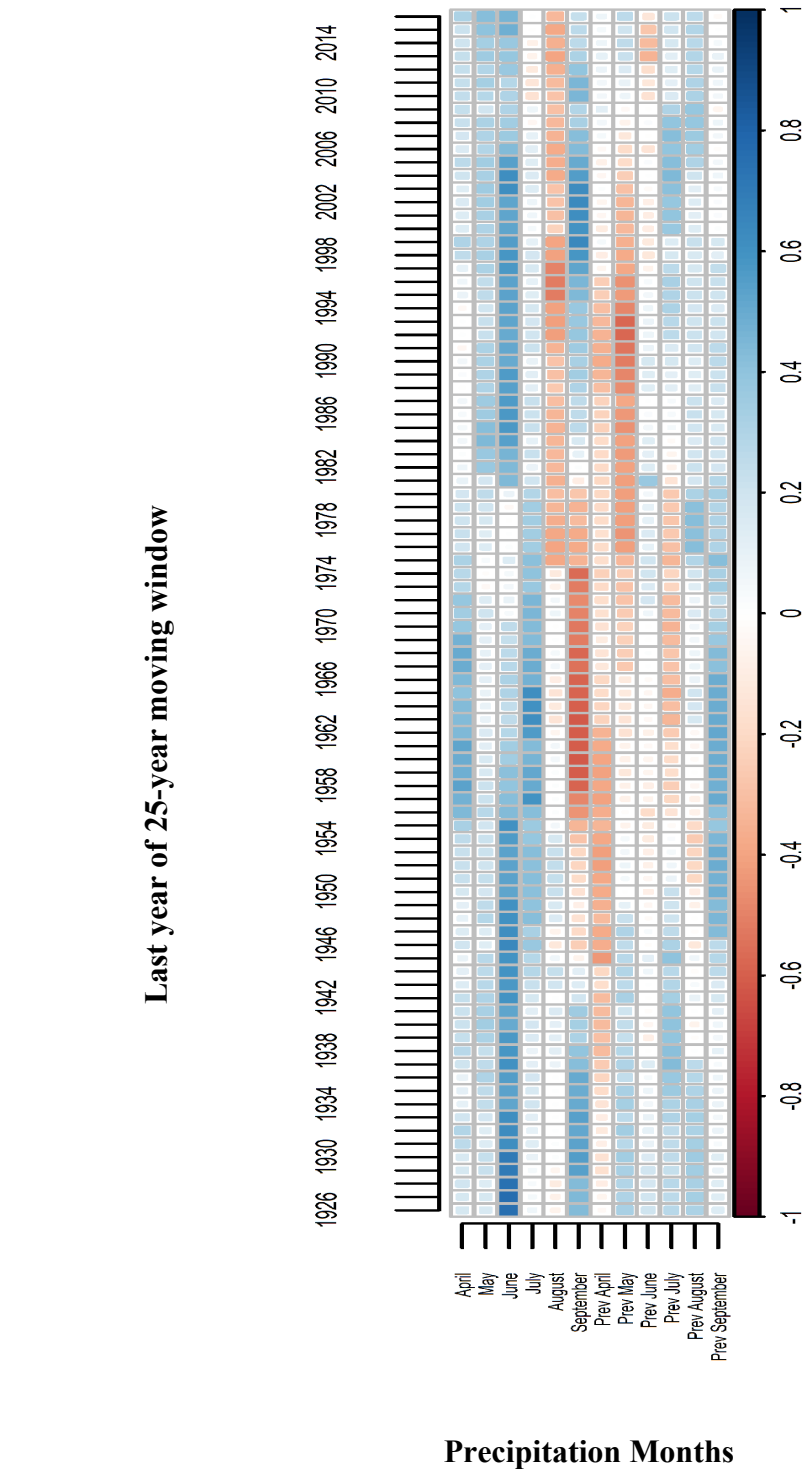
Last year of 25-year moving window
1926
1930
1934
1938
1942
1946
1950
1954
1958
1962
1966
1970
1974
1978
1982
1986
1990
1994
1998
2002
2006
2010
2014
April
May
June
July
August
September
Prev April
Prev May
Prev June
Prev July
Prev August
Prev September
Precipitation Months
Correlation Coefficient
-1
-0.8
-0.6
-0.4
-0.2
0
0.2
0.4
0.6
0.8
1

B) CWHxm2

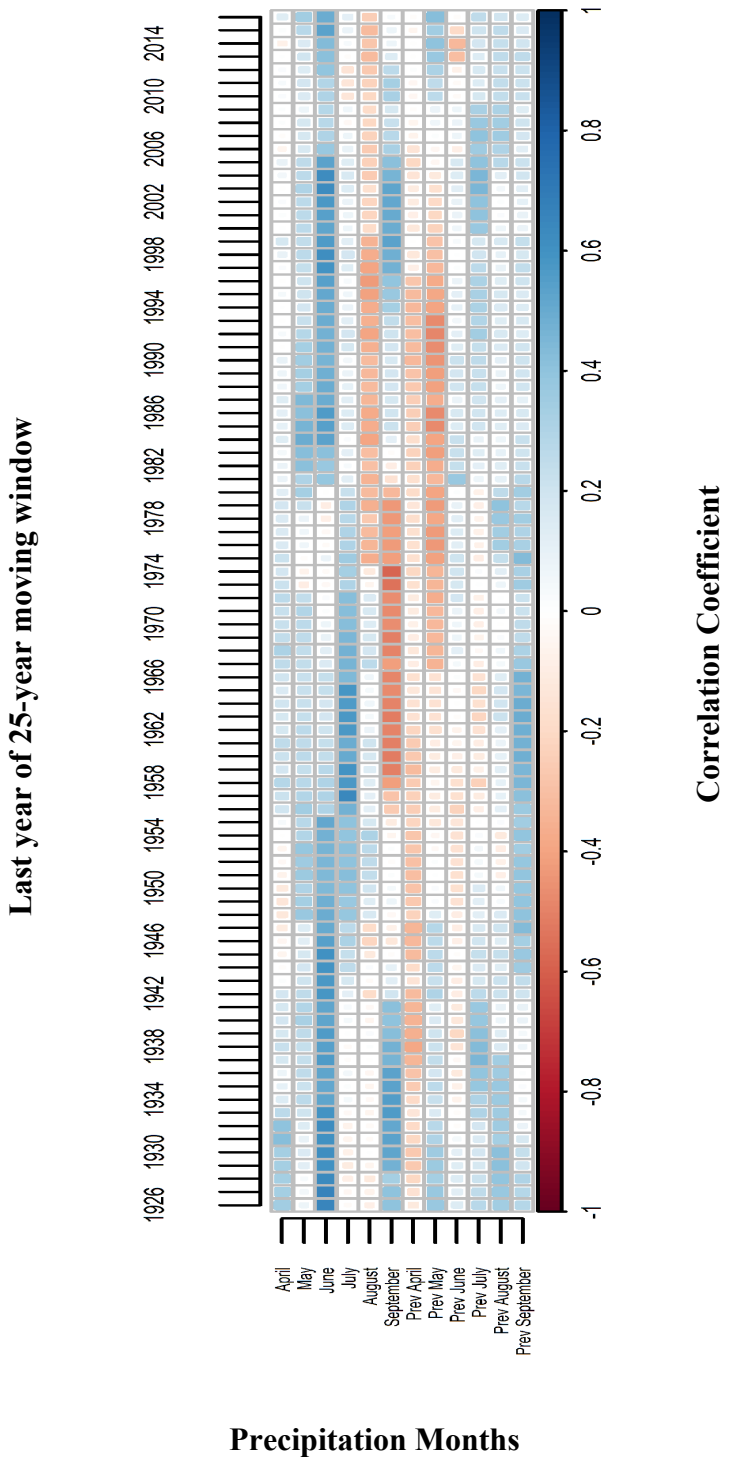
Last year of 25-year moving window
1926
1930
1934
1938
1942
1946
1950
1954
1958
1962
1966
1970
1974
1978
1982
1986
1990
1994
1998
2002
2006
2010
2014
April
May
June
July
August
September
Prev April
Prev May
Prev June
Prev July
Prev August
Prev September
Precipitation Months
-1
-0.8
-0.6
-0.4
-0.2
0
0.2
0.4
0.6
0.8
1
Correlation Coefficient

Figure 3.4: Correlation coefficients indicating relationships between standardized annual tree ring-width of Douglas-fir and monthly precipitation in the CWHxm1 (Figure 3.4A) and CWHxm2 (Figure 3.4B) biogeoclimatic zone of southern Vancouver Island. Correlation coefficients are calculated over 25-year moving windows, with the correlation coefficient being reported for the last year of the 25 year window. Detectable colour indicates significant correlation ($p < 0.05$). Darker colours indicate highest correlation coefficients (R).

The temporal shifts in ring-width sensitivity to CMD in the Sooke Watershed were similar to that of precipitation (Figure 3.5). Standardized ring-width of Douglas-fir was significantly negatively correlated with June CMD during the beginning of the 20th century until the 1956 interval and then again s from the 1981 period onward (Figure 3.5). July CMD was significantly correlated from the 1948 to 1968 period. The effect of September CMD on ring-width was similar to the effect of September precipitation, with a mid-century shift from negative to positive relationship with ring-width, and a returning negative response in the latter half of the time frame.

A) CWHxm1

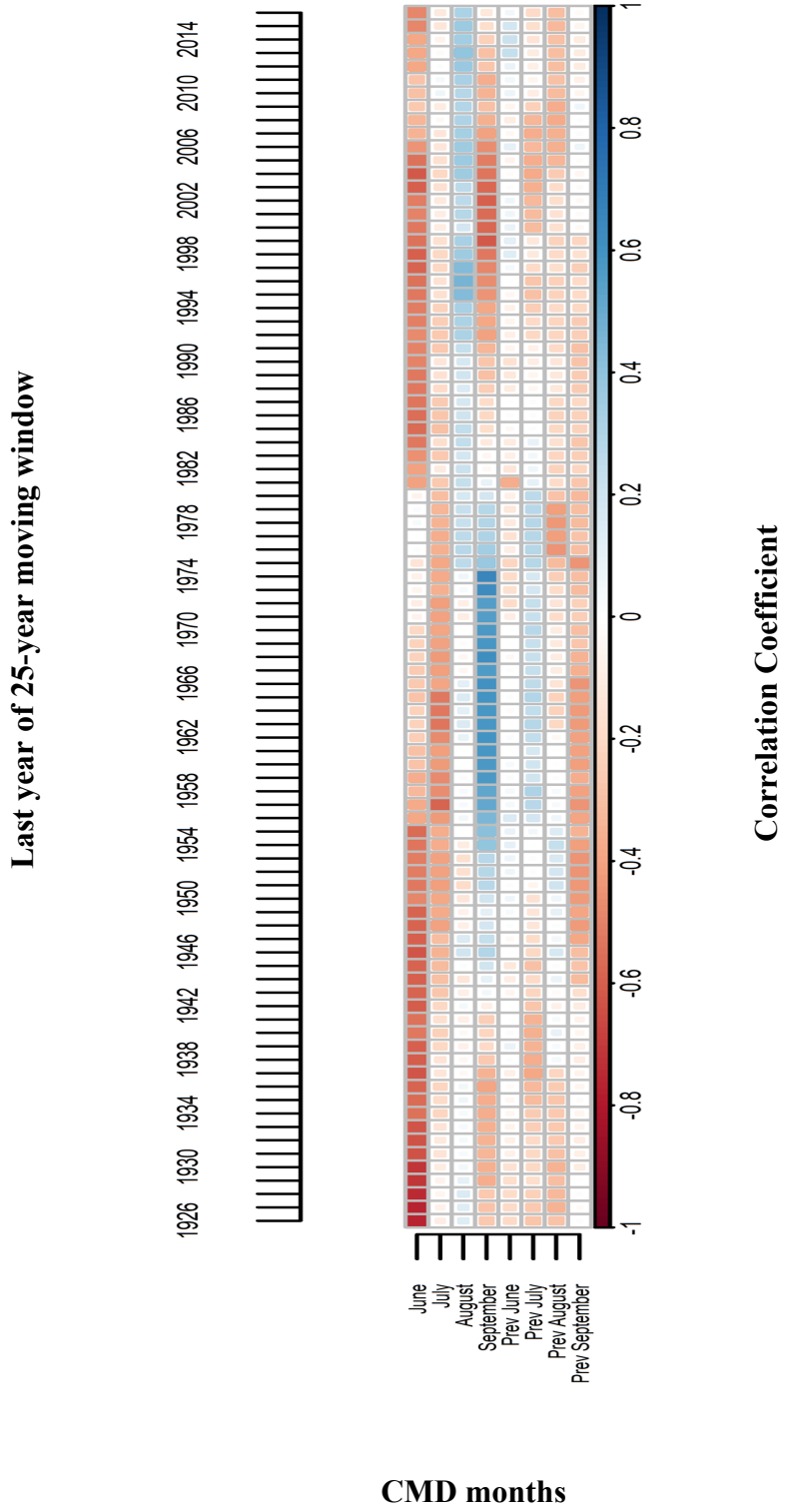
Last year of 25-year moving window
1926
1930
1934
1938
1942
1946
1950
1954
1958
1962
1966
1970
1974
1978
1982
1986
1990
1994
1998
2002
2006
2010
2014
June
July
August
September
Prev June
Prev July
Prev August
Prev September
CMD months
-1
-0.8
-0.6
-0.4
-0.2
0
0.2
0.4
0.6
0.8
1
Correlation Coefficient

B) CWHxm2

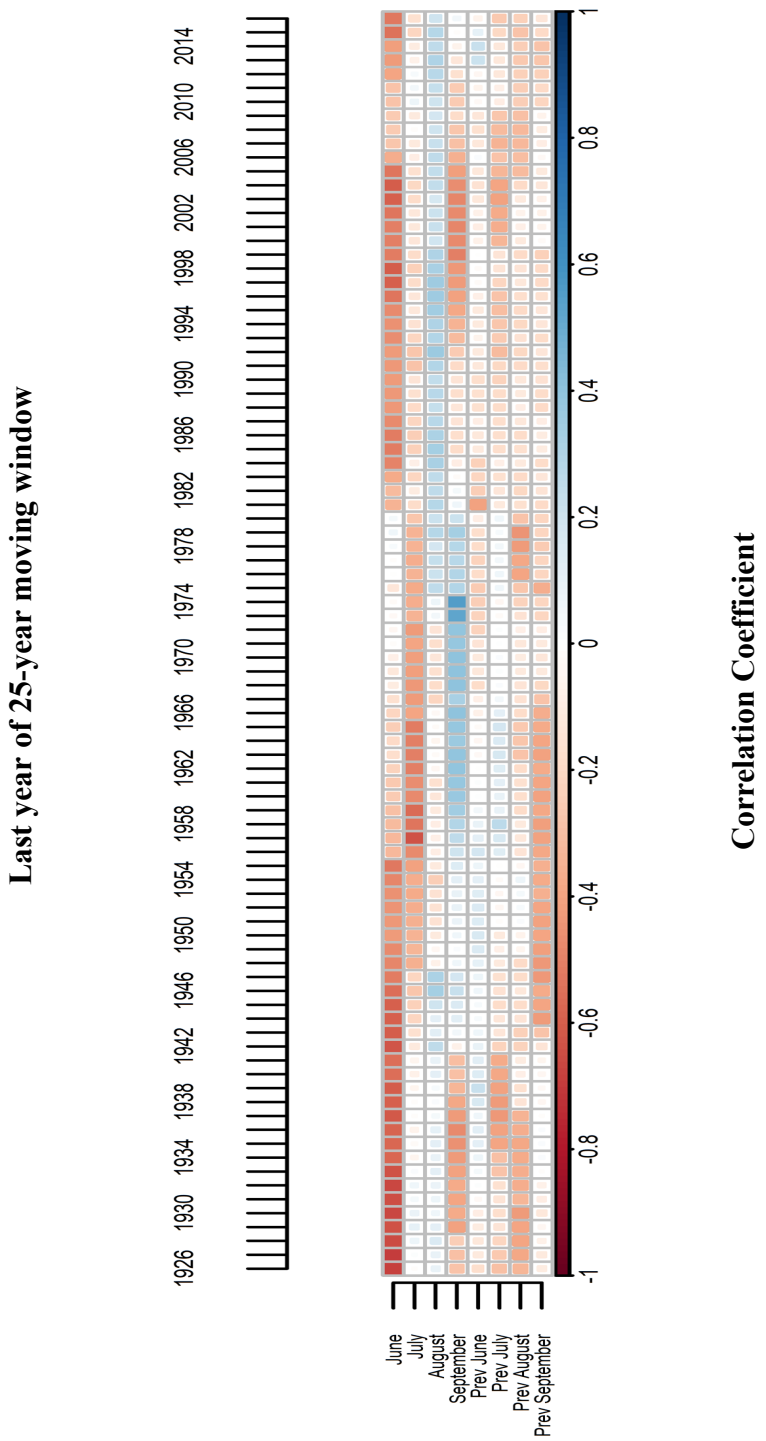
Last year of 25-year moving window
1926
1930
1934
1938
1942
1946
1950
1954
1958
1962
1966
1970
1974
1978
1982
1986
1990
1994
1998
2002
2006
2010
2014
June
July
August
September
Prev June
Prev July
Prev August
Prev September
CMD months
-1
-0.8
-0.6
-0.4
-0.2
0
0.2
0.4
0.6
0.8
1
Correlation Coefficient

Figure 3.5: Correlation coefficients indicating relationships between standardized annual tree ring-width of Douglas-fir and current and previous June to September CMD months in the CWHxm1 (Figure 3.5A) and CWHxm2 (Figure 3.5B) biogeoclimatic zone of southern Vancouver Island. Correlation coefficients are calculated over 25-year moving windows, with the correlation coefficient being reported for the last year of the 25 year window. Detectable colour indicates significant correlation ($p < 0.05$). Darker colours indicate highest correlation coefficients (R).

Temperature did not have a significant relationship with the Douglas-fir ring-width in the Sooke Watershed until end of century in June and July. A statistically significant negative relationship was observed in CWHxm1 in June in 2016 and in July in 2014 (Figure 3.6). This apparent increased sensitivity of ring-width to temperature concided with increasing average annual temperature at the end of the century in both the CWHxm1 and CWHxm2 (Table 3.4).

Table 3.4: Changes in climate variables between first and last 25-year window of the observation period (1901-2016).

	Temperature 1901-1926	Temperature 1991-2016	Precipitation 1901-1926	Precipitation 1991-1926	CMD 1901-1926	CMD 1991-1926
CWHxm1	8.2	9.3	1588	1548	300	298
CWHxm2	7.7	8.8	1815	1781	288	287

Note: Temperature: mean annual temperature (°C), Precipitation: mean annual precipitation (mm), CMD: Hargreaves climatic moisture deficit (mm).

Last year of 25-year moving window
1926
1930
1934
1938
1942
1946
1950
1954
1958
1962
1966
1970
1974
1978
1982
1986
1990
1994
1998
2002
2006
2010
2014
CWHxm2 June
CWHxm2 July
CWHxm1 June
CWHxm1 July
-1
-0.8
-0.6
-0.4
-0.2
0
0.2
0.4
0.6
0.8
1
Correlation Coefficient
June and July Temperature

Figure 3.6: Temporal stability of correlation between June and July temperature to Douglas-fir growth response within certain biogeoclimatic zones over 25-year moving windows. Correlation coefficients are calculated over 25-year moving windows, with the correlation coefficient being reported for the last year of the 25 year window. Detectable colour indicates significant correlation ($p<0.05$).Darker colour indicates higher R values.

3.5.3 Growth-climate relationships in other biogeoclimatic zones

To compare the climate-radial growth responses of Douglas-fir trees in the Sooke Watershed to Douglas-fir trees in other regions, eight mean ring-width chronologies were constructed from other biogeoclimatic zones in BC and Alberta (Table 3.5). Expressed population signal (EPS) exceeded 0.80 in all chronologies, indicating a sufficient signal for climate-growth analysis in all biogeoclimatic zones. Chronology mean sensitivity ranged from to 0.194 to 0.277 and interseries correlation ranged from 0.345 to 0.553 (Table 3.5).

Table 3.5: Biogeoclimatic zone and dendrochronological characteristics of Douglas-fir trees included in analyses.

Biogeoclimatic Zone	Variety	Subzone / Subregion	# Plots	Chronology (years)	Trees (n)	IC	Mean Sensitivity	EPS
CDFmm	Interior	Moist Maritime	n=9	1475-2014 (540 yrs)	92	0.469	0.277	0.867
CWHvm2	Interior	Very Wet Maritime	n=5	1918-2003 (86 yrs)	29	0.353	0.215	0.875
IDFdk3	Interior	Dry Cool	n=10	1683-2014 (332 yrs)	56	0.413	0.276	0.941
IDFdm2	Interior	Dry Mild	n=7	1880-2014 (135 yrs)	23	0.416	0.257	0.841
MSdm1	Interior	Dry Mild	n=8	1778-2013 (236 yrs)	28	0.345	0.263	0.895
SBSdw3	Interior	Dry Warm	n=2	1891-2014 (123 yrs)	9	0.553	0.236	0.850
RMNR	Interior	Alpine and Subalpine	n=3	1887-2010 (124 yrs)	20	0.455	0.246	0.871
ICHwk1	Interior	Wet Cool	n=7	1864-2017 (154 yrs)	45	0.475	0.194	0.914

Note: IC, interseries correlation; EPS, expressed site signal.

3.5.3.1 Frequency distribution of significant climate-growth relationships

Most Douglas-fir chronologies of tree ring-width had significant relationships with precipitation in the current and previous growing season. Tree ring-width chronologies in seven out of ten biogeoclimatic zones had significant correlations to June precipitation, and six out of ten in May, July, and previous August (Figure 3.7). Tree ring-width variability in dry biogeoclimatic zones (i.e., CWHxm1, CWHxm2, MSdm1, IDFdk3, SBSdw3) showed significant relationships to May precipitation. Seven out of ten Douglas-fir chronologies in each regional climate had significant correlations between ring-widths and June CMD – the highest amount of significant correlations among all tested CMD months. Six of ten had significant correlations with July CMD, five of ten with May CMD, and five of ten with previous August CMD (Figure 3.7). Wet or moist sites like CWHvm2, ICHwk1, and the Rocky Mountains Natural Region sites did not have a significant relationships to current June precipitation. Similarly, outlying biogeoclimatic zones to June CMD included those characterized as wet; CWHvm2 and ICHwk1, with the exception of SBSdw3, which is, characterized as dry warm. Trees growing in drier biogeoclimatic zones (including CWHxm2, IDFdm2, and SBSdw3) were also not significantly correlated with July precipitation. Precipitation had the highest number of significant correlations among all the climate variables.

The Douglas-fir chronologies examined in this study demonstrate a low overall climate-growth response to temperature (Figure 3.7). The month with the most significant correlation was previous June, where four out of ten regional chronologies had significant correlations (Figure 3.7). These included CDFmm, ICHwk1, RMNR, and SBSdw3. ICHWk1 was the regional climate with the most frequent response to

temperature; tree ring-width was significantly correlated with temperature in January, March, August, and November. Temperature-related climate variables such as minimum, maximum, and average temperature were tested there were no significant correlations with Douglas-fir tree ring-width (not shown).

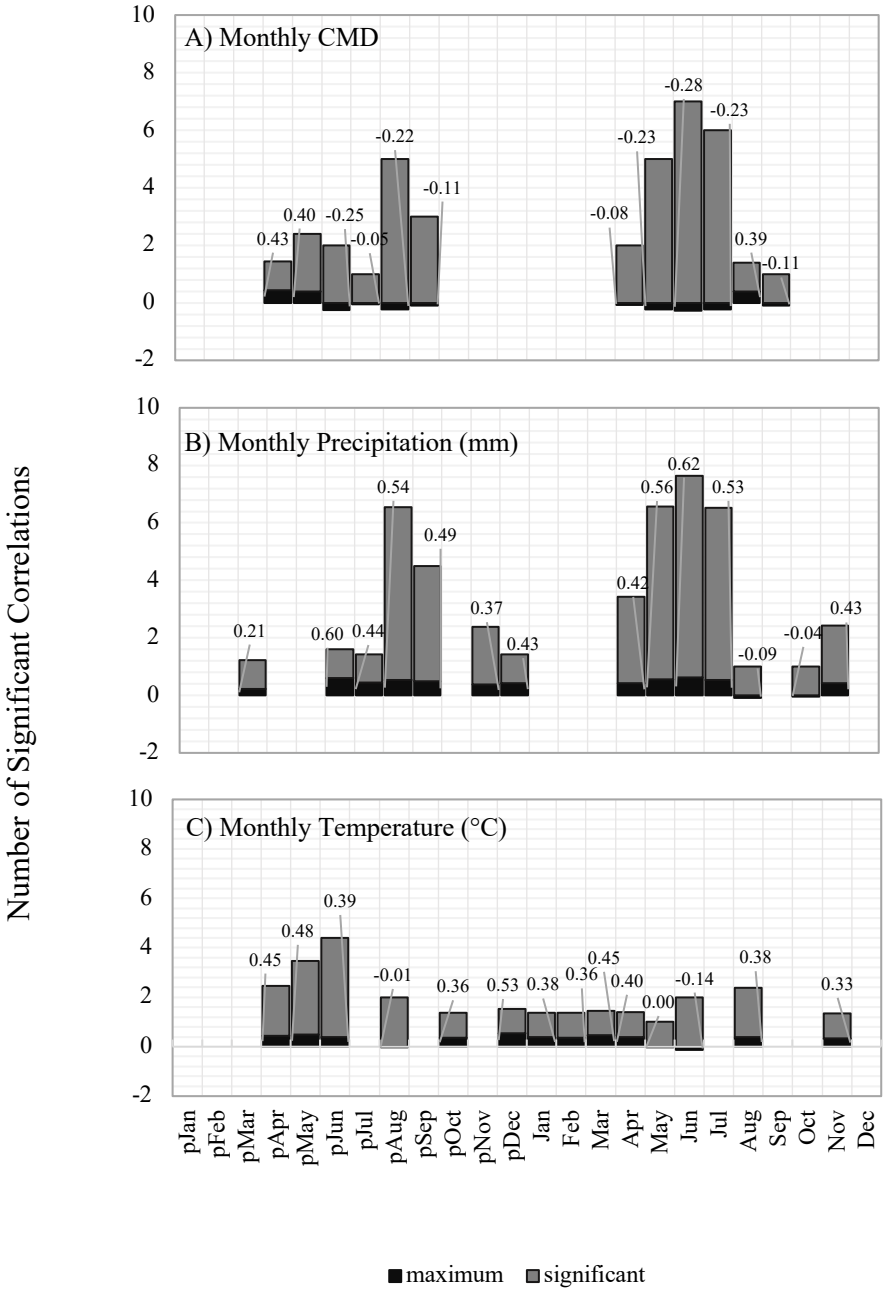

Figure 3.7: Number of significant correlations ($p < 0.05$) between the number of chronologies (of the 10 analyzed) that exhibit a significant correlation with a climate variable in that month. The maximum statistically significant correlation coefficient for each analysis is presented above each column.

3.5.3.2 Comparison of growth-climate relationships between Sooke Watershed and other climate regions

Similar to the Sooke Watershed biogeoclimatic zones, most Douglas-fir tree ring-widths in other biogeoclimatic zones were moisture-limited, indicated by the majority of responses to precipitation being significantly positive and stable. Lagged long-term effects of precipitation on Douglas-fir tree ring-width occurred in dry biogeoclimatic zones, including the CDFmm (previous August precipitation), IDFdk3 (previous August precipitation and CMD), and IDFdm2 zones (previous August and September precipitation, previous August and September CMD), and MSdm1 (previous August precipitation and CMD)(Table 3.6). Douglas-fir tree ring-width in the IDFdm2 and MSdm1 was most responsive to precipitation, with six significant correlations across current and previous months. While most other biogeoclimatic zones had positive relationships between Douglas-fir tree ring-width and precipitation, ICHwk1 had a negative correlation to current August precipitation.

The majority of responses to CMD were significantly negative and statistically stable (Table 3.6). Lagged long-term effects of CMD on Douglas-fir tree ring-widths occurred in dry variant biogeoclimatic zones, including the IDFdk3 (previous August CMD), and IDFdm2 zones (previous August and September CMD,), and MSdm1 (previous August CMD)(Table 3.6). Similar to precipitation responses, ICHwk1 demonstrated a negative correlation to current August CMD. Stable and significant positive correlation to the previous May CMD is observed in SBSdw3, which is one of the few observed instances of a positive relationship to CMD across all the biogeoclimatic zones.

The negative relationship between June and July temperature and Douglas-fir tree-ring width revealed in the Sooke Watershed is similar to that also observed in zones IDFdk3, MSdm1, and SBSdw3. The negative response started in a variety of years depending on the biogeoclimatic zone. The negative temperature response started in the 1968 window for IDFdk3 and in the 1980 window for SBSdw3 (results not displayed). In contrast, the negative effect of the rise in temperature on MSdm1 started in the 1992 window. SBSdw3 was an outlier in it's response to temperature; the chronology responded negatively to current May and June temperature and positively correlated to previous May and June temperature (Table 3.6), indicating that high temperatures in May and June seem to have a negative short-term effect on Douglas-fir growth, however, have a long-term positive effect on growth on the following year.

Table 3.6: Correlation coefficients between annual growth variation across Douglas-fir biogeoclimatic zones and monthly climate variables from 1901 to 2016.

Biogeoclimatic Zone	**Month**	**Correlation Coefficients**		
		Precipitation	CMD	Temperature
CDFmm	April	0.259	-0.256	
	June	0.348	-0.345	
	July	0.184	-0.228	
	Previous June			-0.191
	Previous August	0.179	-0.212	
CWHvm2	July	0.408	-0.403	
	September		-0.307	
	Previous April			0.261
	Previous December	0.242		0.322
IDFdk3	May	0.284	-0.282	
	June	0.337	-0.398	-0.294
	July	0.217	-0.237	
	Previous April		0.233	0.253
	Previous March	-0.153		
	Previous August	0.395	-0.381	
IDFdm2	May	0.250	-0.231	
	June	0.342	-0.370	
	August			0.201
	Previous June	0.452	-0.418	
	Previous August	0.161	-0.180	
	Previous September	0.306	-0.289	
	Previous October			0.184
	Previous November	0.205		
MSdm1	February			0.204
	April	0.249	-0.244	
	May	0.438	-0.395	
	June	0.370	-0.372	
	July	0.282	-0.306	
	Previous May			0.182
	Previous July	0.263	-0.254	
	Previous August	0.379	-0.388	-0.177

SBSdw3	May	0.196		-0.177
	June	0.360		-0.217
	Previous May		0.234	0.316
	Previous June			0.223
RMNR	April			0.246
	June		-0.204	
	July	0.245	-0.199	
	November	0.273		
	Previous June			0.226
	Previous August			-0.167
	Previous September	0.325	-0.282	
	Previous November	0.198		
ICHwk1	January			0.214
	March			0.298
	August	-0.243	0.261	0.219
	November			0.188
	Previous May			0.290
	Previous June			0.164

Note: All coefficients shown are significant at $P<0.05$, based on bootstrapped confidence limits.

3.6 Discussion

The radial growth of Douglas-fir was moisture- rather than temperature-limited in both the Sooke Watershed and across most of the other biogeoclimatic zones examined. This finding agrees with those of prior studies conducted in western North America (e.g., Zhang 2000; Watson and Luckman 2002; Spittlehouse 2003; Zhang and Hedba 2004; Case and Pederson 2005; Littell et al. 2008; Griesbauer et al. 2010; Beedlow et al. 2013; Coulthard 2015; Griesbauer et al. 2019). Water availability during the summer months is the primary factor limiting growth of Douglas-fir due to transpiration stress from a lack of soil moisture (Brubaker 1980; Robertson et al. 1990; Spittlehouse 2003). This behavior likely explains my observation that ring-width was positive correlated with precipitation and negatively correlated with May to July temperature.

Douglas-fir ring-widths were more temperature- than precipitation- limited in some biogeclimatic zones, including the SBSdw3 zone in northern BC and the ICHwk1 zone. SBSdw3 was an anomaly among the zones in that high temperatures in May and June seem to have a negative short-term effect on Douglas-fir growth, however, have a long-term positive effect on growth on the following year. This zone also did not have reoccuring marker years in common with other zones of our study, suggesting that growth might limited by a different set of variables. Since it is the biogeoclimatic zone that receives the most snow, and has the lowest mean annual temperature, mean warmest month temperature, and mean coldest month temperature, I interpret this long-term positive relationship to mean that temperatures play an important role in allowing snow to melt and increasing the infiltration of moisture into the ground. Similar effects of snowmelt on tree ring-width has been found by Zhang et al. (2019) – positive growth

responses were found to increasing temperatures and early season water availability from snowmelt. In addition, ICHwk1 is not limited by moisture as it is characterized by high precipitation and low mean annual temperature. These results differ from Griesbauer et al. (2010) who found that, even at the northernmost distribution, Douglas-fir radial growth was limited by precipitation more than temperature. However, my results are similar to Chen et al. (2010) who found that the Douglas-fir in continental biogeoclimatic zones was less limited by precipitation and more limited by summer temperature.

Short-term temporal analyses of the radial growth sensitivity to climate of Douglas-fir trees in the Sooke Watershed suggests that temperature was becoming a limitation for growth by the end of the 20th century in CWHxm1 and CWHxm2 biogeoclimatic zones. Presumed to be a response to temperature-induced water stress, these results are consistent with other studies describing how warming temperatures are playing an increasingly important role in controlling growth of Douglas-fir (Zhang and Hebda 2004; Littell et al. 2008; Griesbauer et al. 2019). This response appears to be especially significant in coastal climates (Brubaker 1980; Meko et al. 1993; Little et al. 1995; Nakawatase and Peterson 2006; Littell et al. 2008). Given Lewis et al. (2001) found photosynthetic rates with sharp declines for Douglas-fir in western Oregon, USA when temperatures exceed 25°C, Douglas-fir might become maladapted to future changes in climate (O'Neill et al. 2008). The results of my study stand in contrast to the findings of others that predict an increase of Douglas-fir growth with warmer temperatures (e.g. Case and Peterson 2005; Coops et al. 2007), suggesting further research at a finer scale is warranted.

I found a significant negative relationship between Douglas-fir growth and June

and July temperature in recent decades. This negative relationship is observed in the Sooke Watershed sites (CWHxm1 and CWHxm2), and in IDFdk3, MSdm1, and especially SBSdw3. A common finding among these biogeoclimatic zones is the characterization of a dry zone description, suggesting that the recent rise in temperatures are exceeding Douglas-fir tolerance thresholds in dry regional climates. IDFdk3 is characterized by low annual and summer precipitation, indicating that higher temperatures might be exacerbating the lack of moisture present on this site. The high-elevation site of MSdm1 has one of the lowest mean annual temperatures among the zones, indicating that Douglas-fir in this zone has adapted to this lower regional temperature and is becoming more susceptible to rising temperatures. In contrast, Chen et al. (2010), found that summer temperatures only limited growth in interior climates, whereas winter temperature was limiting growth of the coastal climates. Similarly, Wiley et al. (2018) report that growth was never negatively correlated with temperature even under recent rising temperatures in the SBS zone of central BC. Rising temeprature are therefore likely to have different effects on growth in different region where Douglas-fir grows.

Lagged negative relationships between precipitation and CMD and annual tree-ring width were detected in Douglas-fir trees in CWHxm1, CWHxm2, and on Douglas-fir trees located in dry variant BEC zones, including CDFmm, IDFdk3, IDFdm2, and MSdm1. Below average August and September precipitation negatively affected growth in the following summer in these biogeoclimatic zones. This relationship suggests that Douglas-fir trees in these biogeoclimatic zones are very sensitive to precipitation variability, with decreasing August precipitation totals reducing the annual increment of

growth (Griesbauer and Green 2010). These results suggest that ring-width variation is regulated by precipitation and moisture near the end of the prior growing season, and by moisture availability in the spring of the current year of growth. These results are consistent with findings from Watson and Luckman (2002) who reported that Douglas-fir trees located in the southern Canadian Cordillera showed stronger correlations to seasonal precipitation for the prior year and early summer of the current year. The largest percentages of the chronologies were significantly correlated with prior June, July, and August precipitation, and with current May and June (Watson and Luckman 2002). Little et al. (1995) reported similar findings in Oregon; growth was positively correlated with a drought index and precipitation prior to the growth year.

3.7 Limitations

Factors such as chronology length, chronology sample size, and site differences limit the interpretation of my results. The differing duration of the master chronologies characterizing each biogeoclimatic zone limited my ability to gain a full understanding of the climate-growth relationships, especially in zone CWHvm2, where available tree-ring data only extended from 1918 to 2003. This limitation did not allow for the same scale of comparison that was available for other sites, especially when interpreting the effect of rising temperatures in recent decades. Additionally, chronologies in biogeoclimatic zones come from several different plot locations within that climatic region, meaning site differences might be generating biased and variable findings.

3.8 Conclusion

The results presented in this chapter describe both local and large-scale climate-growth relationships that provide forestry managers with insights into the link between

climate and radial tree growth in the Sooke Watershed. Successful forest management practices in the Watershed will require a good understanding of the ecological and climatic factors that influence tree limitations and sensitivities, especially under a changing climate. Key findings of this chapter indicate that Douglas-fir forests in the Sooke Watershed are susceptible to increasing mean annual temperature, and are moisture-limited. Therefore, the combined projected rise in temperature of 1.5°C and the expected summer precipitation decrease of 14% by 2050 (Pacific Climate Impacts Consortium 2012) will likely exacerbate the existing negative influence on radial growth in the coming decades. If this occurs, Watershed managers can look to dry biogeoclimatic zone from this study that have demonstrated a similar negative climate-growth relationship to June or July temperature in recent decades; IDFdk3, MSdm1, and SBSdw3, for example.

Sooke Watershed forest managers should expect changes to ecosystem functions resulting from high temperature and low water availability in the future. These changes might lead to slower rates of Douglas-fir tree growth, causing injury or death. Ecosystem changes also can affect Douglas-fir trees indirectly by increasing their susceptibility to wildfire, insect pests, and disease. Given the strong connection between forest and hydrological ecosystem health, a reduction in Douglas-fir growth might affect the loss of water back to the atmosphere, snowmelt regulation, surface runoff, infiltration into soil, soil water storage, and movement through the soil. These might lead to a change in the the quantity, quality, and regimen of water moving out of the terrestrial and into aquatic ecosystems.

Chapter 4 : Dendrohydrological Reconstruction of Precipitation in the Sooke Watershed

4.1. Introduction

Human-induced greenhouse gas emissions have changed the world's climate since its pre-industrial state and are predicted to lead to additional global temperatures increases of 1.5°C by 2030 to 2052 (IPCC 2018), with climate models suggesting distinct regional consequences are likely (Barnett et al. 2005; Huntington 2006). These regional climate outcomes include significant hydrological shifts that range from an increased number of extreme precipitation events, to the probability that some regions will begin to experience drought and precipitation deficits (Allen et al. 2010; IPCC 2018). In some regions, climate projections suggest that recent droughts will resemble average conditions in the future (Van Loon and Laaha 2015), and that future droughts will extend over greater areas and be characterized by longer intervals of warm temperatures (Crausbay et al. 2017).

Meteorological drought, hereafter referred to as drought, occurs when dry weather patterns dominate an area (Wilhite and Glantz 1985). It can occur in high as well as low rainfall areas, as it is a condition relative to a long-term relationship between rainfall and evapotranspiration in a specific area (Wilhite and Glantz 1985). Anthropogenic climate change has, however, increased the likelihood of drought events similar to what western Canada experienced in 2015 (Szeto et al. 2016). This event is recognized as one of the most extreme droughts on record in terms of severity, extent, and impacts (Herring et al. 2016). The water-rich province of British Columbia (BC) is, therefore, not expected to be immune to water scarcity in the future (Bonsal et al. 2001). Although average annual

rainfall in BC is expected to increase from 2 to 12% by 2050, summers are expected to be drier, leading to more frequent and severe droughts (BC Ministry of Environment and Climate Change Strategy 2019). As an indication of these ongoing changes, droughts on Vancouver Island are no longer unusual and have become commonplace in recent years (Coulthard 2015; Simms and Brandes 2016). In June 2016, southern Vancouver Island experienced a Stage 4 drought -the earliest date that this designation had ever been applied - for the second year in a row (Simms and Brandes 2016).

The Sooke Lake Reservoir and Watershed located on southern Vancouver Island, hereafter referred to as the Sooke Watershed, provides the majority of the drinking water required by communities in the Greater Victoria area (Capital Region District 2007). The Watershed depends on winter rainfall to refill its reservoir following what are typically warm, dry, summers in the region (Capital Regional District Water District 2001). Despite being characterized by wet winter conditions (Kolisnek 2005), four historical droughts since 1914 (1928-1930, 1940-1942, 1991-1995, 2001-2003) were severe enough to warrant implementation of a drought management action plan (Capital Regional District 2001; Kolisnek 2005) and prompted expansion of the reservoir storage by 70% in 2002.

The sensitivity of watersheds to climate variation is a growing concern for water managers globally. Currently, hydrologists and climatologists estimate probabilities and magnitudes of extreme drought based on climatic and hydrometric data (Coulthard 2015), with the reliability of their estimates often dependent upon on the length of historic records. In western Canada, however, these instrumental records typically only extend back 100 years or so (Meko and Woodhouse 2011). Consequently, they may only reflect

a portion of the natural range in variability.To effectively assess past, present, and future water-reservoir supply systems for climate-related vulnerability and water management it is important to understand the full range of natural variability that can affect a system during extreme wet and dry conditions.

Dendrohydrology, a subfield of dendrochronology, is one of the few avenues available for developing long-term hydrological reconstructions with annual and/or seasonal resolution (Meko and Woodhouse 2011). The resulting proxy records of hydrological variability have been widely incorporated over the past 30 years into a variety of water conservation and hazard management schemes, and climate change adaptation and mitigation strategies (e.g., Earle 1993). A key principle in the field of dendrochronology is the principle of limiting factors on tree growth (Fritts 1976; Speer 2010), which states that the annual radial growth of a tree is controlled by the most limiting environmental variable, and that this factor is likely to be recorded in a given tree-ring chronology. Therefore, in order for dendrohydrological reconstructions to effectively model a certain variable, the growth of the trees sampled needs to be limited by the variable in question.

Douglas-fir trees found growing in maritime climate regions are generally regarded as having complacent radial growth trends when compared to, for example, Douglas-fir trees growing in more arid climates (Speer 2010). Despite its maritime location, the Sooke Watershed is often characterized by precipitation and soil moisture deficits during the summer months (Capital Regional District Water Department 1999). These conditions were previously shown to impact the radial growth of Douglas-fir trees in the Watershed (Jarret 2008), and present an opportunity to employ dendrohydrological

methodologies to reconstruct hydrologic variables over the duration of the available tree-ring chronologies.

The purpose of the research presented in this chapter was to reconstruct past May-June-July (MJJ) precipitation regimes (i.e. pluvial and drought periods) in the Sooke Watershed in order to better understand summer precipitaiton variability. The results are intended to assist water managers in the Capital Regional District meet commitments articulated in the 2017 Regional Water Supply Strategic Plan - to provide an adequate, long-term, supply of drinking water (Capital Regional District 2017a). The novelty of the research stems from two aspects; the use of coastal Douglas-fir trees to reconstruct precipitation, and the application of Ensemble Empirical Mode Decomposition as the method for detrending. The research aims to equip the water managers responsible for the Sooke Watershed with a greater understanding of long-term summer water availability, essential information as they plan for predicted hydrologic changes.

4.2. Research Objectives

The main objectives of the research presented in this chapter were:

1. To determine whether tree ring records from the Sooke Watershed retain a signal of precipitation change and/or variability over the instrumental period.

2. To develop robust dendrohydrologic relationships that could be used to extend the instrumental record back over the duration of the tree-ring chronology, as justified by the climate-growth relationships presented in Chapter 3.

3. To examine the temporal patterns identified in the reconstructed precipitation records and test for links to major atmospheric and oceanic teleconnection indices.

4.3. Methods

4.3.1 Tree-ring processing and chronology development

Tree cores were collected within the Sooke Watershed in June 2017 to extend and deepen the tree-ring chronologies constructed by Jarrett (2008) and archived by the University of Victoria Tree-Ring Laboratory (UVTRL). Following standard dendrochronological protocols (Briffa and Jones 1990), two samples were collected from each tree and placed in plastic straws for transport. After air drying, the samples were glued to slotted mounting boards, allowed to dry, and were then sanded to a fine polish to distinguish the annual ring boundaries.

Digital images of the trees cores were then processed using a high-resolution scanner. A WinDendro^{TM} image processing measurement system was subsequently employed to measure the annual tree ring widths. A Velmex measuring system equipped with a high magnification microscope was used to visually examine the samples when ring boundaries were difficult to distinguish. Visual cross-dating of the 5 mm ring-width data was completed following standard cross-dating protocols (Stokes and Smiley 1996). COFECHA (Dendrochronology Program Library described in Holmes 1983) was used to quality check the cross-dating by examining correlations between 50-year segments with 25-year lags at a significance level of 0.01 (Grissino-Mayer 2001).

4.3.1.2 Detrending

Chronology development is one of the most critical procedures for determining the overall success of reconstructions. In this instance, an Ensemble Empirical Mode Decomposition (EEMD) was applied, as it leads to high-quality modeled reconstructions that best capture instrumental variability (Guan et al. 2018). Introduced by Guan et al. (2018), the EEMD approach has been applied in many fields, ranging from engineering

(Lei et al. 2009), to geology (Wang et al. 2012), and neuroscience (Guerrero-Mosquera et al. 2016). Employing the EEMD methodology to detrend tree ring data collected from regions outside Asia has, however, not previously been attempted.

EEMD was chosen for this analysis because of concerns associated with the traditional ARSTAN approach: the subjectivity of ARSTAN detrending functions; and, the lack of fidelity to data of chronology generation methods. In other words, a major advantage of using EEMD is that the user does not need to impose a subjectively selected function to remove intrinsic growth trends, and the original data are easily recoverable once the tree-cores have been detrended (Cook and Holmes 1986; Cook 1987). With trend removal being performed in an objective and *a posteriori* manner, the method retains all resolvable ring-width frequency variations present in the original data allowing for a better assessment of the relationships between ring-width and climate variability (Guan et al., 2018).

Empirical mode decomposition (EMD) was developed by Huang et al. (1998) to identify instantaneous frequencies embedded in a nonlinear and non-stationary series. EMD considers that at any time, complex signal series and oscillations known as intrinsic mode functions (IMFs) may be superimposed in a time series. EEMD was developed out of EMD to alleviate the problem of mode mixing in EMD (a consequence of signal intermittency), seeing as frequency modes may reside in more than one IMF and that an IMF may contain more than one mode (Huang and Wu 2008).

EEMD incorporates a Monte Carlo approach to the problem in which zero-mean Gaussian white noise is added to each EMD process to achieve better signal separation. An EEMD IMF is simply the ensemble mean of the corresponding EMD IMFs or trends

(Huang and Wu 2008; Wu and Huang 2009). The decomposition of time-series using EEMD does not assume an *a priori* structure about the trend; it is derived intrinsically and adaptively (Wu et al. 2007). The approach preserves all signals because summing the IMFs and residual will recover the original data. This allows the user to evaluate the physiological relationship between a ring characteristic and the abiotic factor of interest in a meaningful way.

4.3.1.3 Ensemble Empirical Mode Decomposition (EEMD) Detrending

Using the R Package Rlibeemd (Luukko et al. 2016), the ring-width series were compiled into site-specific master chronologies. EEMD decomposes signals into a small number of simple oscillatory intrinsic mode functions (IMFs). From a dendrochronology perspective, IMFs represent tree growth variability of different frequency modes. The residual after the extraction of IMFs will either be a constant, a monotonic function, or a function with at most one extremum.

In order to find the best combination of IMFs that provided a high R^2 while still capturing proper tree-ring signal, different combinations of IMFs (e.g. IMF1, IMF1 + IMF2, IMF12345, IMF45…) were paired with different combinations of monthly climatic and hydrologic variables such as Rithet Streamflow, Koksilah streamflow, temperature, SPEI, SSFI, and SPI. The best model for reconstruction was chosen based on the AIC in the stepwise model, as well as the exclusion of certain low-frequency IMFs that resulted in a trend-like behavior in the reconstruction.

EEMD first decomposes individual time series to remove trends. The IMFs are then summed and the detrended cores combined chronologically. EEMD is then applied again to extract the IMFs of the combined series to remove any residual trend component

(Guan et al. 2018). The standard deviation of the added Gaussian white noise for EEMD was 10% of the standard deviation of the input data, with an ensemble size of 5000 runs to minimize the influence of the introduced noise. After the development of the EEMD chronology, the spectral properties of the output were explored using a multi-taper method (Mann and Lees 1996).

In order to attain an Expressed Population Signal (EPS) and the mean sensitivity of the chronologies, standard and residual chronologies were developed using the ARSTAN program in the dplR package (Cook and Holmes 1986; Cook 1987) and the same tree-ring data. Mean sensitivity provides a measure of interannual growth variation (Cook and Kairuikstis 2013), while EPS estimates the strength of the climate signal within the growth where a minimum EPS value of 0.80 is suggested (Wigley et al. 1984).

4.3.2 Weather and Climate Data

Climatic variables commonly known to limit the radial growth of Douglas-fir trees and that demonstrated significant climate-growth relationships to the CWHxm1 and CWHxm2 zones discussed in Chapter 3 were examined. Relationships between tree-ring chronologies and individual months and/or groupings of months (e.g. the combination of May, June, and July, or July, August, and September…) were established by correlation. Radial growth relationships to climate in the previous year were also evaluated, to determine if they influence current-year growth.

4.3.2.1 Precipitation

Precipitation data from the Sooke Dam meteorological station (48°31'04", 123°42'00", 183 m asl) was obtained from Dr. Tobi Gardner (*personal communication,* Capital Regional District). Recording of daily precipitation at the station began when the

caretaker's house was constructed in 1914. This recording continued until about 1970 when the operation of the water supply changed jurisdiction. From 1970 to the early 1980s, the precipitation data was collected at a provincially operated site at the north end of the reservoir, after which precipitation data was once again recorded at the dam site. Hourly total precipitation data has been collected at the Sooke Dam since November, 1995.

A preliminary examination of the precipitation data (*not shown*) revealed that it was not normally distributed. In order to achieve normality, the precipitation records were transformed to square roots to stabilize variance inherent to the data. As this procedure provided a measure of precipitation in centimetres, the precipitation data was then back transformed to provide water managers with meaningful and useful precipitation data.

4.3.2.2 Atmospheric and Oceanic Oscillations

Temporal patterns were tested for links to major atmospheric and oceanic teleconnection indices. Atmospheric and oceanic oscillation indices were downloaded from the National Oceanic and Atmospheric Administration (NOAA) website in 2019. The Multivariate ENSO Index (MEI), Pacific Decadal Oscillation (PDO), and the Pacific North-American (PNA) were teleconnections of focus because they are known to influence weather patterns in the study area (Capital Regional District 2017, Coulthard et al. 2016; Mood 2019). MEI (https://www.esrl.noaa.gov/psd/enso/mei/) is a bi-monthly time series index and is the combination of five different variables; sea level pressure (SLP), sea surface temperature (SST), zonal and meridional components of the surface wind, and outgoing longwave radiation (PLR) over the tropical Pacific basin. The PDO

index is based on NOAA's reconstruction of SST and was downloaded from NOAA's teleconnection website (https://www.ncdc.noaa.gov/teleconnections/pdo/). The PNA index is calculated by projecting the PNA pattern to the daily anomaly 500 millibar height field over 0-90°N (https://www.ncdc.noaa.gov/teleconnections/pna/).

4.3.3 Reconstruction

To develop robust reconstruction models, a forward and backward stepwise regression model selection process was used based on the Akaike's Information Criterion (Kutner et al. 2004). The IMFs and the residual extracted from the combined series, as well as their sequential sums (*e.g.*, IMF1 + IMF2, IMF1+IMF2+IMF3, *etc.*), were used as predictors. Different combinations of monthly or seasonal precipitation sums served as the response variable.

After selecting the predictors and the response variable with the most significant correlations, a series of statistical tests widely used to assess the suitability for reconstruction was invoked. These tests include the coefficient of determination (R^2) and adjusted R^2, which are statistics demonstrating the explanatory power of the model accounting for lost degrees of freedom. Validation statistics were used to compare the instrumental data with the estimated values of the predictand. Such statistics included the reduction of error (RE)(Fritts et al. 1990) that provided a measure of model skill, with a positive RE value indicating that the reconstruction had some skill of prediction. The root mean square error of cross-validation ($RMSE_V$) was further tested and gave a measure of the uncertainty of the predicted values over the verification period.

Model reliability was examined by performing a split-period calibration-verification test commonly used in dendroclimatology (Fritts 1976). In this test, the

reconstructed variable established by regression from one half of the climate data set (calibration period) was tested against the actual precipitation of the remaining data (verification period) withheld from regression. I split the precipitation data into two datasets of the same length (50 years in each half; 1915 to 1965 and 1966 to 2016) in order to perform this step. This test was repeated by switching the calibration and verification periods, ensuring that each split-period passed the validation statistics such as the RE and coefficient of efficiency (CE). The CE statistic (Cook et al. 1994) is used to assess temporal stability of the calibrated relationship. CE is a measure of shared variance between the actual and modeled series and any value over zero indicates robust reconstructed values when compared to independent climate data not used in the calibration period (Wilson et al. 2013).

4.3.4 Analysis of the reconstruction

Statistical properties were compared between the reconstructed precipitation record in the pre-instrumental (1591 to 1915) and instrumental precipitation (1915 to 2016) period. This allowed for an observation of differences between the instrumental and pre-instrumental periods, and for an assessment of the model capacity to approximate characteristics of precipitation.

Drier and wetter than average years were defined as reconstructed precipitation totals below or above thresholds corresponding to percentiles of the instrumental precipitation for the based period (1915 to 2016). Episodes of extreme drought and pluvial events were identified as those falling into the bottom 5^{th} and top 95^{th} percentiles respectively, while episodes of drought and pluvial events were identified as those situated within the bottom 15^{th} and top 85^{th} percentiles, respectively. The bottom 5^{th} and

15th, and top 95th and 85th percentiles were also taken for the instrumental precipitation record in order to compare instrumental extremes to the modeled extremes.

Once categorized into drought and pluvial events, each year was ranked in order of severity and the sum per century tabulated. This procedure allowed for an observation of long-term conditions, and was used to identify the temporal spacing of extreme drought and pluvial events. To investigate multi-year dry and wet periods, a runs analysis procedure was undertaken (Sadeghipour and Dracup 1985; Touchan and Hughes 1999; Gray et al. 2011; Bekker et al. 2014). This procedure involved counting consecutive years falling below or above a certain threshold (example; years falling below or equal to the 5th percentile). In order to understand the severity of these single- and multi-year drought and pluvial events, departures from the mean precipitation over the instrumental period in the reconstruction (1915 to 2016) were calculated, following procedures taken in Weber and Stewart (2004) and Bekker et al. (2014). The duration, magnitude (cumulative departure over the consecutive years), and intensity (magnitude divided by departure) of consecutive years were determined and were ranked in order of severity.

The reconstructed and instrumental precipitation records were compared with ENSO, PDO, and PNA records to investigate the influence of large-scale climate modes on drought and pluvial episodes. Four different time scales were tested for each teleconnection index; annual, winter (October to March), summer (April to September), and May-June-July (MJJ). The average of each teleconnection index was identified within intervals, and a difference-of-correlations test conducted on the instrumental and reconstructed precipitation over the instrumental period. This procedure allowed for an observation of positive and negative phases on the selected climate oscillations.

4.4 Results

4.4.1 Tree-ring data

Tree-ring chronologies were established from increment cores collected at six sites in the Sooke Watershed in 2006 and 2017, at locations that ranged in elevation from 239 to 525 m asl. Approximately 20 representative Douglas-fir trees were sampled per site. The chronologies span different intervals of time and have interseries correlation values ranging from 0.491 to 0.630 (Table 4.1). Four out of the six chronologies (those with the most significant correlation to the precipitation data) were used to construct a master chronology. Consisting of 199 tree ring series, the master chronology spans the interval from 1445 to 2016. Following the 0.80 EPS cutoff recommendation (Wigley et al. 1981), the master chronology was subsequently limited to the 1591 to 2016 interval (Figure 4.1). Detrending of the tree-ring series resulted in eight IMFs and a residual trend (Figure 4.2), where each IMF represents tree growth variability of different frequency modes and the residual was an almost-constant function. The mid- to low-frequency terms, ranging from IMF 4 to the residual term, had trend-like behavior.

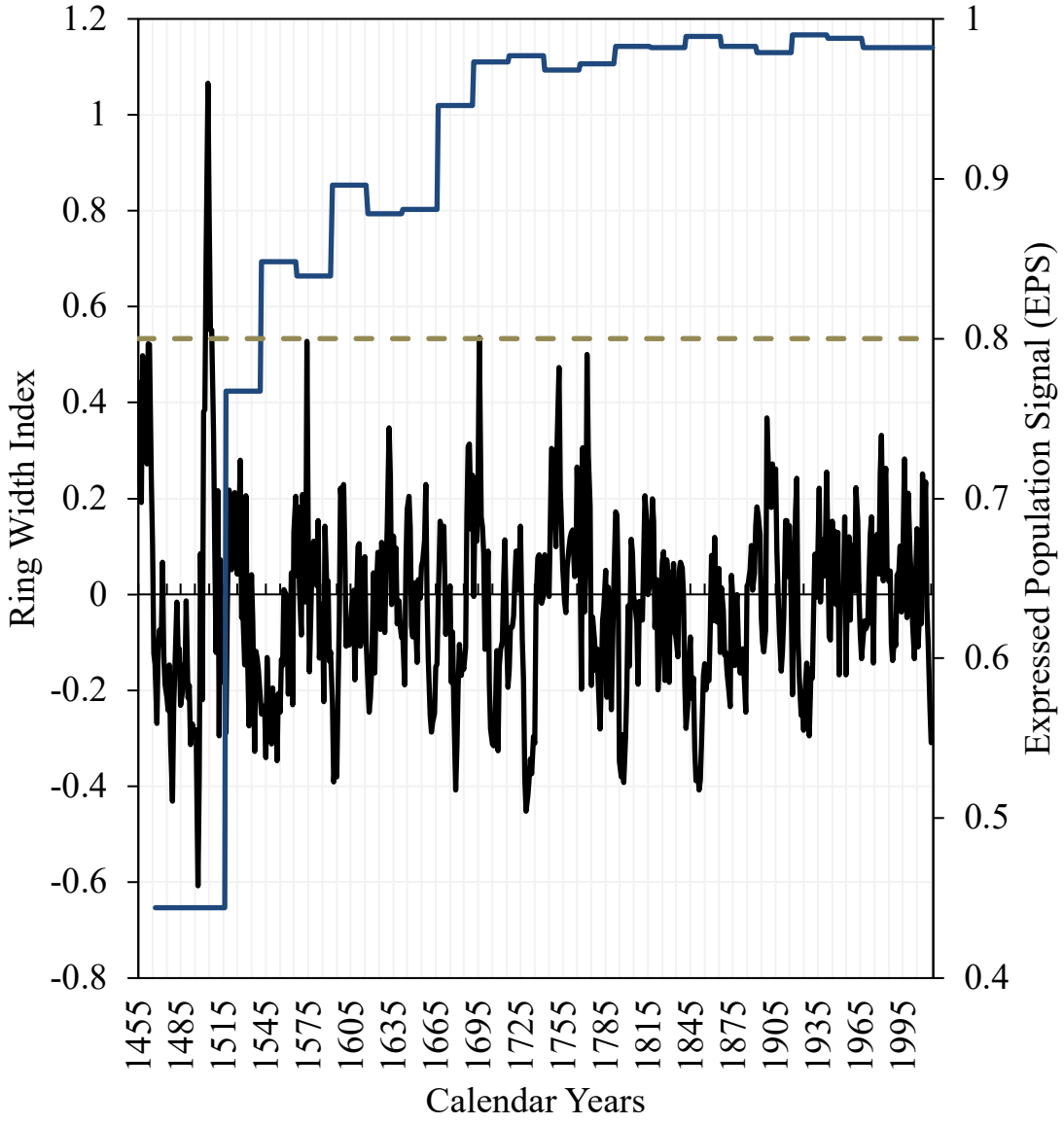

Figure 4.1: Douglas-fir master chronology for the Sooke Watershed (black line) and the Expressed Population Signal (EPS) (hatched line). The blue line represents the tree sample size.

Table 4.1: Location and tree-ring characteristics of Sooke Watershed chronologies. The bolded chronologies are those used in the precipitation reconstruction.

Site	Coordinates (Lat/Long)	Elevation m asl	Year Sampled	# of Trees	Average Tree Basal Area (m)	Years AD (Duration)	Interseries Correlation
Rithet	**N: 48° 35'10.44" W: 123° 43'56.94"**	**513**	**2016**	**34**	**2.23**	**1735- 2016 (281 yrs)**	**0.630**
	N: 48° 36' 6" W: 123° 43' 24"	**415**	**2006**	**37**	**NA**	**1695-2006 (311 yrs)**	**0.599**
	N: 48° 35' 13" W: 123° 44' 38"	415	2006	37	NA	1281-2006 (725 yrs)	0.563
Saddle Dam	**N: 48° 31' 46" W: 123° 42' 19"**	**239**	**2016**	**44**	**2.93**	**1561-2016 (455 yrs)**	**0.599**
			2006	**44**	**NA**	**1574- 2006 (432 yrs)**	**0.609**
Magee Main	N: 48°35' 38.16" W: 123°41'39"	446	2016	30	3.58	1821- 2016 (195 yrs)	0.491
Butchard Lake	**N: 48° 33' 3.3" W: 123° 39'32.04"**	**525**	**2016**	**40**	**2.93**	**1445-2016 (571 yrs)**	**0.597**

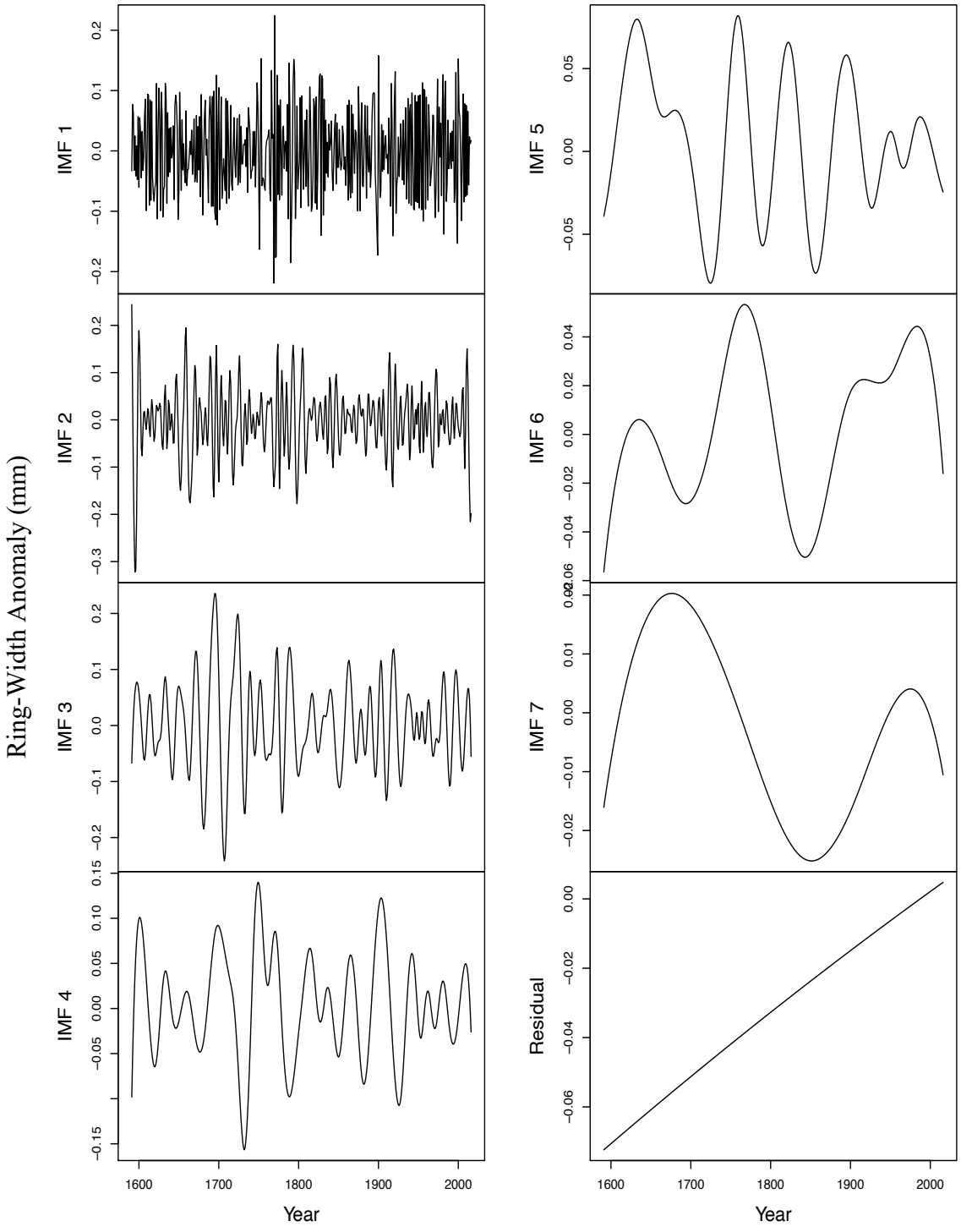

Figure 4.2: EEMD decomposition results of the Douglas-fir tree-ring width following the EPS cutoff. IMF; Intrinsic Mode Function.

4.4.2 Model Estimation and Reconstruction

The best regression model identified was with MJJ precipitation as a response variable, and with the first three IMFs (IMF1 + IMF2 + IMF3) from the combined four tree-ring chronologies used as predictors (see Figure 4.2). The reconstructed MJJ precipitation record extended from 1591 to 2016 after the EPS cutoff, extending the instrumental precipitation record by 324 years.

The MJJ precipitation model explained 28% of the overall variance in the precipitation instrumental data (1915 to 2016). As Table 4.2 indicates, the test of the correlation between actual and reconstructed precipitation was shown to be statistically significant ($p < 0.05$). The results of a regression line homogeneity test showed that the calibration functions of the two-split periods were not statistically different, and neither function significantly violated the usual regression assumptions. Verification tests, such as RE (Fritts 1976) and the coefficient of efficiency (CE)(Cook et al. 1999), resulted in positive values (Table 4.2), indicating a degree of model fidelity and adequate support of the regression model validity (Bekker et al. 2014). Autocorrelation function plots indicated that neither the instrumental or reconstructed MJJ precipitation data are significantly autocorrelated at lags <15 years.

Table 4.2: Calibration and verification statistics for the period of 1915-2016.

Calibration Period	**r**	**R^2**	**Verification Period**	**RE**	**CE**
Full (1915-2016)	0.31	0.28	-	-	-
Early Half (1915-1965)	0.22	0.21	1966-2016	0.22	0.42
Late Half (1966-2016)	0.42	0.41	1916-1965	0.37	0.16

4.4.3 Analysis of reconstruction

The modeled MJJ precipitation record captured annual trends in the instrumental MJJ record (Figure 4.3). While the precipitation extremes appear to be underestimated by the model, the modeled data generally corresponds to the trend deviations.

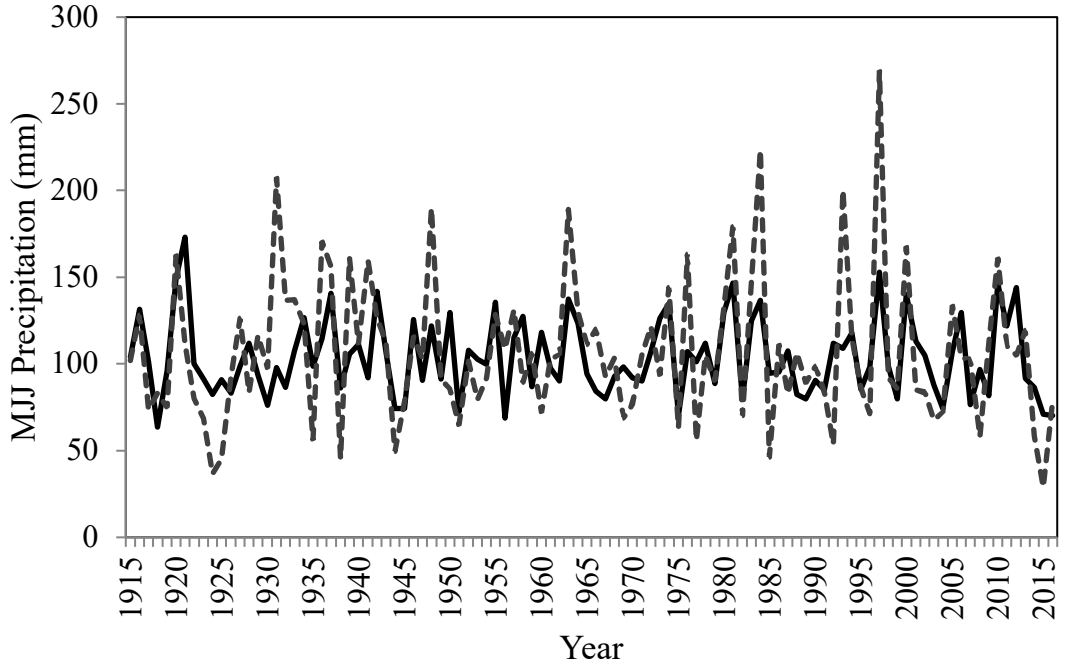

Figure 4.3: Time plot of the reconstructed (solid line) and instrumental (hatched line) May-June-July (MJJ) precipitation data. The reconstructed data has been back transformed to original units over the model calibration period. The data extends to 2016.

The reconstructed and instrumental precipitation data are summarized in Table 4.3. While the mean instrumental and reconstructed values of MJJ precipitation are similar in both cases, the standard deviation is significantly higher in the instrumental data. The variation in the minimum and maximum values are also a representation of this difference, and demonstrate the model's general underestimation of extreme values and magnitudes in the instrumental data.

Table 4.3: Recorded MJJ precipitation and reconstructed MJJ precipitation statistics.

Precipitation Data	Time Frame	Min	Mean	Max	Standard Deviation
Instrumental	1915- 2016	23.9	106.9	269.1	42.0
Reconstructed	1915-2016	63.6	103.8	173.1	22.5

A visual comparison of MJJ reconstructed precipitation, observed precipitation, and averaged Rithet Creek streamflow demonstrates the link between precipitation and runoff in the Watershed (Figure 4.4) since 1995; when the start of the streamflow measurements began. Trends among all three hydrological variables are similar, including peak years 1997 and 2010. The modeled precipitation captures the trend of the 2015 low precipitation record, however, the magnitude is not captured (Figure 4.4).

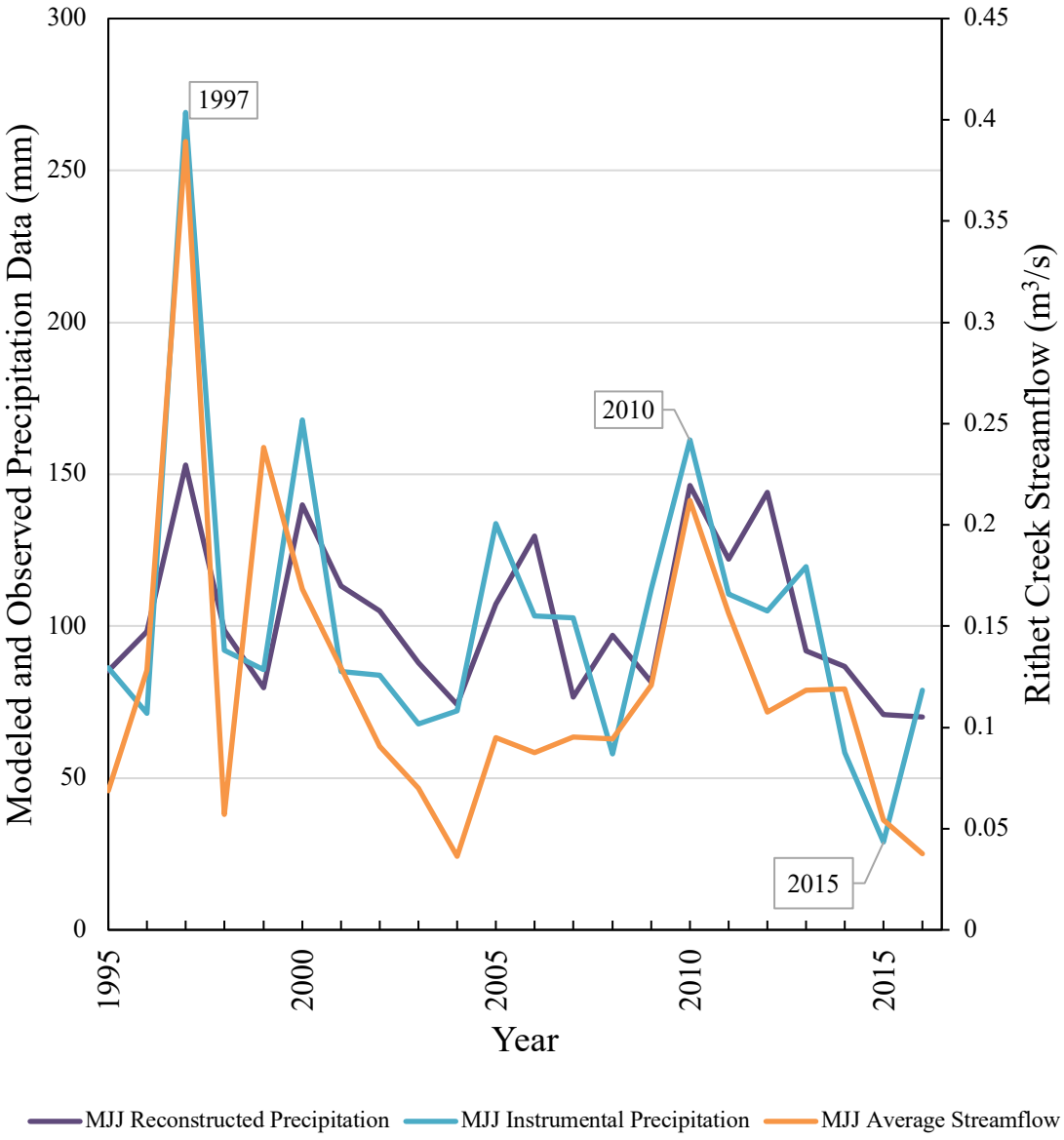

Figure 4.4: A visual relationship of averaged May-June-July (MJJ) Rithet Creek Streamflow, Modeled MJJ Precipitation, and Instrumental MJJ Precipitation.

4.4.4 Drought and Extreme Drought MJJ Periods

The MJJ precipitation reconstruction exhibits strong variability over the past five centuries (Figure 4.1). Extreme (5th percentile) individual MJJ droughts are evident in the reconstruction (Table 4.4) and, although some of these events occurred during the

instrumental period (1918, 1965, and 2016), a count of extreme droughts per century demonstrates that the highest number of MJJ droughts occurred in the 1700s (Table 4.6).

The reconstructed record successfully models some of the precipitation variability inherent to the instrumental record. When comparing the individual MJJ drought periods in the instrumental and reconstructed precipitation records (Table 4.4 and Table 4.5), the most severe instrumental MJJ drought periods (1914 and 2015) are captured in the 15th percentile of the modeled values. On the other hand, the reconstructed extreme MJJ droughts of 1918, 1965, and 2016 were not identified as droughts in the instrumental record.

The runs analysis of 5th and 15th percentile MJJ droughts provided a clearer understanding of the magnitude and intensity over the reconstructed timeframe. The runs analysis of 5th percentiles indicated four periods of extreme MJJ drought of at least two periods occurring since 1591, none of which occurred over the instrumental period. The longest extreme MJJ drought period occurred from 1662 to 1665 (Table 4.5; Figure 4.5). The runs analysis of 15th percentiles captures two three-year MJJ droughts, and another four-year MJJ drought from 1705-1708. The analysis of 15th percentile MJJ droughts also indicates two drought episodes occurring within the instrumental period (1944-1945, and 2015-2016). Therefore, 15th percentile MJJ droughts more efficiently captured the instrumental drought.

Table 4.7 allowed for an observation of magnitude and intensity of drought/extreme MJJ drought episodes. While 1662-1665 and 1705-1708 were, respectively, the longest episodes of consecutive MJJ drought, the most intense interval of drought occurred from 1594 to 1596. The drought episode from 1705 to 1710 was

broken by wetter conditions in 1709. Taken together, however, this episode is likely a more severe and persistent drought experienced within the watershed over the record period.

4.4.5 Pluvial and Extreme Pluvial MJJ Periods

Five extreme MJJ pluvial events were recorded over the instrumental period (Table 4.4; 5th percentile in 1921, 1997, 1920, 2010, and 2012). The reconstruction captured the extreme MJJ pluvial event of 1997, as well as those in 1920, 1981, and 2010 at the 15th percentile.

While single MJJ extreme pluvial events were more common in the 1600s than in any other century (Table 4.6), the runs analysis revealed no extreme pluvial events longer than 2 MJJ periods (Table 4.7). The runs analysis for the 85th percentile MJJ droughts captured three two-year pluvial episodes occurring throughout the reconstruction, the most intense – 1920 to 1921 - occurring within the instrumental period (Table 4.7; Figure 4.5). The runs analysis for the 85th percentile MJJ pluvial episodes also captured three three-year pluvial episodes, the most intense consecutive MJJ episode running from1793 to 1795.

Table 4.4: Ranking of the 22 (5th/95th percentile) extreme MJJ drought and pluvial periods in the instrumental record and reconstruction. Bold indicates years in the instrumental record. Precipitation units are in mm.

Rank	Extreme Drought Year	MJJ Precipitation Value	Extreme Pluvial Year	MJJ Precipitation Value
1	1769	43.8	1697	196.9
2	1680	58.5	1773	179.1
3	1596	58.7	**1921**	**173.1**
4	1799	60.2	1794	172.1
5	1776	62.3	1793	169.9
6	1771	62.4	1689	162.7
7	1594	62.5	1726	161.5
8	1797	63.0	1753	159.7
9	1898	63.1	1690	156.8
10	**1918**	**63.6**	1599	156.4
11	1663	64.3	1659	155.3
12	1899	64.8	1633	153.2
13	1796	65.8	**1997**	**153.0**
14	1595	66.9	1900	151.9
15	1710	67.4	1601	149.7
16	1662	67.9	**1920**	**149.1**
17	1664	68.3	**1981**	**146.7**
18	**1956**	**68.6**	**2010**	**146.2**
19	1809	69.4	1647	145.5
20	1910	69.6	1804	144.2
21	1665	69.8	**2012**	**144.1**
22	**2016**	**70.0**	1646	142.5

Table 4.5: Ranking of the (5th/95th percentile) extreme drought and pluvial years, and (15th/85th percentile) MJJ drought and pluvial episodes in the instrumental record. Bold years indicate those that are also present in the MJJ precipitation reconstruction. The 5th and 95th MJJ precipitation units are in mm.

Rank	Year	5th	Year	95th
1	2015	28.9	**1997**	**269.1**
2	1924	36.5	1984	223.3
3	1925	45	1931	207.6
4	1938	45.4	1993	200.3
5	1985	46.2	1948	189.9
6	1944	49.5	1963	189.1
Rank		15th		85th
7	1992	53.5	**1981**	**179.1**
8	1977	56	1936	170.6
9	1935	56.1	2000	167.8
10	2008	58	1976	163.4
11	2014	58.3	**1920**	**162.7**
12	1975	63.1	**2010**	**161.2**
13	1951	64.7	1939	160.9
14	2003	67.8	1941	159.4
15	1923	68.3	1937	156.4
16	1969	68.7	1983	147.2

Table 4.6: Number of 5th (drought) and 95th (pluvial) MJJ percentiles periods in the reconstruction per century. The first year of the reconstruction is 1591 and the last is 2016.

Century	Extreme Drought Years	Extreme Pluvial Years
2000s	1	2
1900s	3	5
1800s	3	1
1700s	7	5
1600s	5	8
1500s	3	1

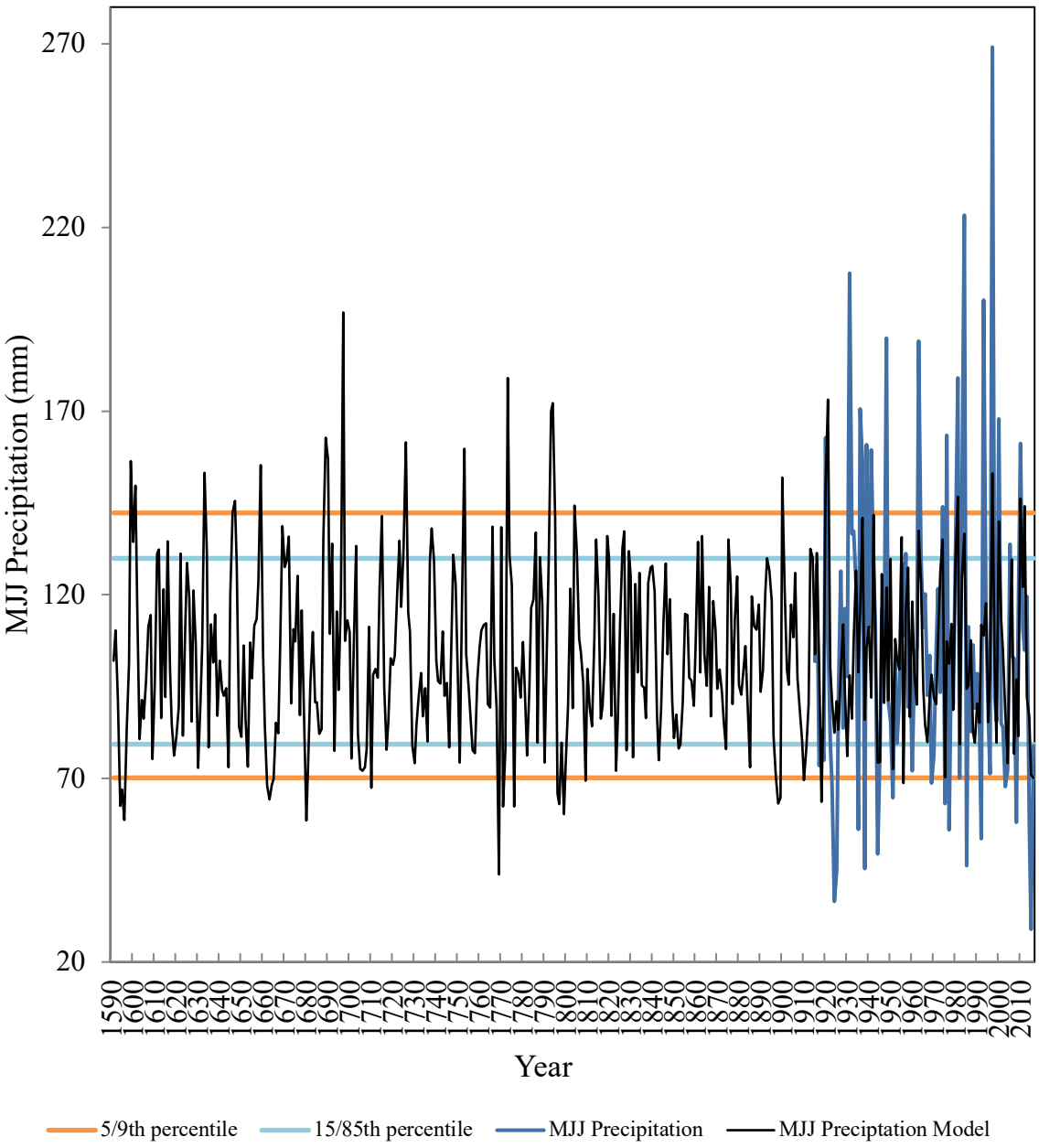

Figure 4.5: The modeled and instrumental precipitation. The red lines indicate the 5/95th percentile threshold, whereas the blue lines indicate the 15/85th percentiles.

Table 4.7: Periods in the bottom 5th and 15th , and top 95th and 85th percentile with consecutive MJJ periods (2 or more) of extreme drought or extreme pluvial, presented in order of intensity (magnitude/duration), and including magnitude (cumulative precipitation). Bold indicates those in the instrumental period. Precipitation units are in mm.

Period	Duration (years)	Magnitude (mm)	Intensity (mm/year)
Extreme Drought			
1594-1596	3	-132.9	-44.3
1898-1899	2	-86.1	-43.0
1796-1797	2	-85.2	-42.6
1662-1665	4	-157.7	-39.4
Extreme Pluvial			
1793-1794	2	128.0	64.0
1920-1921	**2**	**108.3**	**54.1**
1689-1690	2	105.6	52.8
1646-1647	2	74.0	37.0
Drought			
1594-1596	3	-132.9	-44.3
1796-1797	2	-85.2	-42.6
1897-1899	3	-122.4	-40.8
1680-1681	2	-81.4	-40.7
1799-1800	2	-79.7	-39.8
1662-1665	4	-157.7	-39.4
1771-1772	2	-73.6	-36.8
2015-2016	**2**	**-73.0**	**-36.5**
1910-1911	2	-66.4	-33.2
1705-1708	4	-132.4	-33.1
1944-1945	**2**	**-65.3**	**-32.6**
1729-1730	2	-60.9	-30.5
1757-1758	2	-59.4	-29.7
1852-1853	2	-56.6	-28.3
Pluvial			
1920-1921	**2**	**108.3**	**54.1**
1793-1795	3	161.7	53.9
1773-1774	2	95.9	48.0
1688-1690	3	133.7	44.6
1725-1726	2	79.8	39.9

1599-1601	3	119.6	39.9
1646-1647	2	74.0	37.0
1633-1634	2	70.7	35.4
1804-1805	2	62.1	31.0
1826-1827	2	56.0	28.0
1819-1820	2	52.0	26.0
1611-1612	2	49.5	24.8
1913-1914	2	48.6	24.3

4.4.6 Teleconnection Relationships

The measured and reconstructed MJJ precipitation were tested against the PDO, PNA, and ENSO teleconnection indices. The difference-of-correlations test revealed no significant interactions with ENSO or PNA, and some associations to PDO. The reconstructed precipitation had one interaction with the negative summer PDO (April to September), while the instrumental precipitation had associations with positive annual, MJJ, and summer PDO (Table 4.8). Less significant relationships of $p<0.1$were evident between the negative phase of MJJ PNA in both the reconstructed and instrumental record (Table 4.8).

Table 4.8: Difference-of-correlations tests for measured ENSO, PDO, PNA values against instrumental and reconstructed annual, MJJ, summer, and winter precipitation. Bold indicate $p<0.05$. An asterisk indicates $p<0.1$.

		Reconstructed			Instrumental		
	Teleconnection Phase						
Season	*Sample Size*	ENSO	PDO	PNA	ENSO	PDO	PNA
Annual	Positive	-0.06	0.05	0.15	-0.01	**0.38**	0.10
	n	47	36	37	47	36	37
	Negative	-0.05	-0.17	0.21	-0.03	0.02	0.30
	n	55	66	30	55	66	30
MJJ	Positive	0.03	0.14	0.16	0.09	**0.32**	0.05
	n	44	39	33	44	39	33
	Negative	-0.01	-0.19	*-0.30	0.01	-0.06	*-0.32
	n	58	63	34	58	63	34
Summer	Positive	0.02	0.15	0.11	0.05	**0.38**	0.06
	n	47	29	32	47	29	32
	Negative	0.01	**-0.27**	-0.23	-0.01	-0.03	-0.25
	n	55	73	35	55	73	35
Winter	Positive	-0.11	0.06	0.07	-0.08	0.18	0.13
	n	50	41	38	50	41	29
	Negative	-0.10	-0.08	-0.05	-0.11	-0.04	0.05
	n	52	61	38	52	61	29

4.5 Discussion

4.5.1 The Reconstructed Record

The precipitation reconstruction provides natural resource managers of the Sooke Watershed with a better understanding of the duration, magnitude, and intensity of MJJ drought and pluvial episodes over the last 425 years (1591 to 2016). However, the precipitation model does not capture the full range of instrumental precipitation variability, meaning the actual magnitude of pre-instrumental precipitation events may be more or less extreme than modeled. Furthermore, a dry or wet MJJ period does not necessarily imply a change in the year's water supply, seeing as the derived total distribution of MJJ precipitation in the instrumental record only makes up 6% of the annual precipitation. The precipitation model should therefore be interpreted conservatively.

My analysis suggests that the instrumental record may underestimate the length of dry and wet events compared to the reconstructed record. Up to four MJJ drought periods are possible in the natural range of variability (1662-1665, 1705-1708), while up to three pluvial episodes are possible (1599-1601, 1688-1690, 1793-1795). In contrast, MJJ drought and pluvial episodes present within the instrumental record do not last longer than two consecutive years. This is a common theme among dendrohydrological reconstruction (e.g., Bekker et al. 2014; Coulthard et al. 2016). Similar to hydrologic reconstructions from surrounding areas (e.g., Coulthard et al. 2016), this study suggests that severe summer droughts and consecutive dry periods were common pre-instrumental occurrences, and are often well outside the range of the instrumental record.

The results of my research suggest that MJJ droughts characteristically last longer than pluvial episodes in the Sooke Watershed. As noted above, the longest extreme MJJ drought intervals over the past 425 years occurred from 1662 to 1665 and from 1705 to 1708. The runs analysis of 15th percentiles recorded two three-year MJJ droughts. In contrast, while the runs analysis revealed no extreme pluvial events longer than 2 consecutive MJJ years over the duration of the reconstructions, an examination of the 85th percentile shows there were three three-year pluvial episodes. However, dendrohydrological reconstructions characteristically are more skilled at predicting dry years than wet years. This behaviour occurs during extremely wet years, tree growth is normally limited by some other factor such as soil nutrients, and additional moisture no longer benefits growth (Bekker et al. 2014).

4.5.2 Links to Teleconnections

No significant (p<0.05) relationships to ENSO were detected in either the reconstructed or instrumental precipitation records, despite the fact that El Niño events are known to bring warmer temperatures and reduced precipitation to the GVWSA in the spring (Shabbar et al. 1997; Werner 2007). The results between precipitation reconstructions and ENSO vary within the geographic area. Coulthard et al. (2016) reported no significant correlation between El Nino/La Nina years and the regionalized or reconstructed streamflows. Further, Jarrett (2008), who also tested the significance of atmospheric teleconnections on precipitation in the Sooke Watershed, suggests that radial growth and ENSO are not related. On the other hand, Mood (2019) detected relationships of significance with annual, winter (December to February), and spring (March to May) ENSO to both measured and modelled streamflow over the reconstruction period in the

nearby BC Coast Mountains. Lastly, Rodenhuis et al. (2009) reported that annual snowpack exceeds more than 30% above normal between warm and cool phases of ENSO.

Relationships of $p<0.1$were evident between the negative phase of MJJ PNA in both the reconstructed and instrumental record, indicating that the reconstruction captures the climatic teleconnection that drives patterns in the instrumental data. Similarly, Mood (2019) recorded a significant relationship to negative June, July, and August (JJA) PNA in his reconstructed and instrumental streamflow records from the Great Vancouver Regional District. Starheim et al. (2013) further found that episodes of increased July-August discharge are typically associated with negative PNA conditions in west central BC. Negative PNA anomalies are associated with a weaker Aleutian Low pressure center, leading to cooler winter temperatures and an increase in winter precipitation (Bonsal et al 2001; Stahl et al. 2006). This relationship emphasizes that PNA is important in influencing winter precipitation, and possibly snowpack storage, in the Sooke Watershed. This enhanced moisture availability is indirectly integral to enhanced ring growth in the spring.

Significant relationships are evident between PDO and the reconstructed and measured precipitation. However, these relationships are significant at different time scales. While the measured precipitation is significantly related to positive annual, MJJ, and summer PDO, the reconstructed precipitation is significantly correlated to negative summer PDO. These results indicate that PDO had a greater effect on the instrumental record, which the reconstruction did not capture, likely resulting from the underestimation of magnitudes of the reconstruction. In contrast, Jarrett (2008) found that

ring-widths are independent of PDO phasing as the reconstruction did not have a relationship of significance to PDO. Coulthard et al.'s (2016) reconstructed instrumental streamflow were significantly negatively correlated with values of the PDO index during winter (October to March), and Mood's (2019) reconstructed and measured streamflow demonstrated significant relationships at annual and seasonal timeframes.

Overall, the reconstructed precipitation record demonstrated a lack of correlation to climate indices, especially to ENSO. This finding suggests that the annual radial growth of Douglas-fir trees in the Sooke Watershed is not dependent on the climate impacts exerted by large-scale atmospheric and oceanic teleconnections. This growth response may result from the timeframe of the reconstruction versus the general timing of effects from the teleconnections of focus; ENSO, PDO, and PNA events largely affect winter weather in BC, which the radial growth in the spring could not capture. As described in Chapter 2, ENSO and the PDO primarily modifies weather in the Pacific North America during the late fall and winter (Steinman et al. 2014). Lastly, the limitation of the model's ability to capture the full range of instrumental variability might explain why the relationship between PDO and instrumental record is not captured between PDO and the reconstructed record.

4.5.3 Relationship to other dendrohydrologic reconstructions

The precipitation reconstruction resulting from this research supports similar dry and pluvial summer records developed in surrounding areas. A Tsable River, Vancouver Island, streamflow reconstruction identified extreme summer droughts in 1651, 1660, and 1665, with a cluster of seven summer droughts occurring between 1647 and 1667, and only one drought episode persisting for three or more years (1665 to 1667)(Coulthard et al. 2016). Similarly, the Sooke Watershed precipitation reconstruction identified the 1662 to 1665 MJJ interval as associated with the longest extreme drought event on record. If a drought period had initially been defined as falling under the 23rd percentile, this period of summer drought would have been extended from 1661 to 1667. Coulthard et al. (2016) also reported the most extreme summer drought year over the instrumental period occurred in year 1992. Although 1992 was not identified as an extreme MJJ drought in the Sooke Watershed precipitation reconstruction, it did rank as the 7th most extreme drought in the instrumental record.

This research was intended to build upon the MJJ precipitation reconstruction presented by Jarrett (2008). The two studies span different intervals of time (Jarrett (2008): 1390 to 2006; this study: 1591 to 2016), employed different detrending methods, and were developed from different chronology sets. A comparison of the two models indicates that my updated model more accurately captures the explained variance in MJJ rainfall over the duration of the instrumental record; Jarrett (2008)'s model explained 20% of the variance, while the one developed in this thesis describes 28% of the variance. Comparable research focused on reconstructing spring precipitation from tree ring data in the surrounding region area was successful in explaining from 15% (Laroque

2002) to 57% (Zhang 2000) of the variance in rainfall over the period of the instrumental record. Similar results are evident between Jarrett (2008) and this updated reconstruction.

Key findings from Jarrett's (2008) research included identification of: the driest MJJ period in 1466, the MJJ wettest in 1599, and several instances of consecutive dry periods including 1727-1728, 1513-1517, 1608-1610, 1704-1706, 1727-1731, and 1922-1924. Overlapping MJJ drought episodes between Jarrett (2008) and my updated reconstruction include 1796, 1710, 1776, 1918, 1594, 1956, and pluvial episodes including 1599, 1773, 1697, 1633, 1689, 1900, and 1793. Similar time frames of consecutive dry MJJ episodes were also reported, however, they were shifted by a few years; 1705-1708 (updated) versus 1704-1706 (Jarrett 2008), and 1729-1731 (updated) versus 1727-1731 (Jarrett 2008). The model developed by this research did not account for the other extreme episodes noted by Jarrett (2008).

4.5.4 Historical Accounts

The reconstructed MJJ precipitation confirms some of the dry and pluvial periods in historical accounts. Recorded drought years occurring in the Victoria area include 1928-1930, 1940-1942, 1991-1995 and 2001-2003 (Capital Regional District Water District 2001; Kolisnek 2005; Jarrett 2008). The summer drought in 2015 is characterized by extreme low precipitation and drought across the province of BC (Simms and Brandes 2016). Within the context of the long-term reconstruction, the MJJ model does not include these drought episodes as being part of the bottom 5^{th} or 15^{th} percentile droughts. However, consecutive droughts from 1944-1945 are included in the bottom 15^{th} percentile drought, and the drought of 2016 is counted as an individual summer drought episode in the model. This suggests the presence of a multi-year biological lag in the

tree's response to summer drought. Recorded pluvial events are not as well documented in the Sooke Watershed, but a comparison of MJJ pluvial events in the modeled versus instrumental timeframe demonstrates pluvial summers of 1997, 1920, 1981, and 2010 are well-captured.

4.5.5 Limitations

The discrepancies between modeled and instrumental MJJ drought and pluvial episodes may be a representation of site-specific disturbance, stand dynamics, or geographic location on a slope. Furthermore, the use of coastal Douglas-fir for reconstruction is problematic as coastal Douglas-fir growing in a maritime climate regions are generally regarded as having complacent radial growth trends when compared to, for example, Douglas-fir growing in arid environments where the rainfall is limited each year (Speer 2010). Lastly, as mentioned above, the precipitation model only captures the variability of the MJJ timeframe, which makes up 6% of the annual precipitation received in the Watershed. This means the consecutive dry and pluvial MJJ years does not translate to an annual characterization of drought and therefore results should be interpreted conservatively.

Chapter 5 : Conclusion

5.1 Conclusion

The intent of the research presented in this thesis was to analyze the biotic and abiotic processes that drive forest growth, and to analyze MJJ drought and pluvial episodes within the Sooke Watershed. The thesis identifies the climate-related factors that play a role in Douglas-fir growth variability, and describe the history of precipitation in the Sooke Reservoir from 1591 to 2016. The climate-growth variability (Chapter 3) and record of MJJ precipitation (Chapter 4) are of immediate use to resource managers because of their direct application to present and future management strategies and policies.

The objectives of the thesis were outlined in Chapter 1. By updating and expanding upon the Sooke Watershed tree-ring chronologies collected by Jarrett (2008), I was able to develop a more comprehensive understanding of the climate-radial growth relationships within the Sooke Watershed and compare those to relationships elsewhere in BC (Objectives 1 and 2). This climate-growth relationship justified and contextualized the development of a pre-instrumental proxy record of precipitation in the Sooke Watershed (Objective 3), and its link to major atmospheric and oceanic climatic teleconnections (Objective 4).

An understanding of the climate-radial growth relationships was gained in Chapter 3, as tree-ring chronologies were examined with respect to various climate variability such as temperature, precipitation and the Hargreaves Climate Moisture Deficit (CMD). Correlations with current and previous year climatic values were tested, and the influence of climate variables on growth were tested at short- and long-term

timescales. These methods were conducted on Douglas-fir sites located across southern Alberta and BC, and the results were then compared and contrasted to those from sites in the Sooke Watershed, which allowed for objective 3 to be accomplished.

The robust development of climate-growth relationships in Objective 3 justified the development of a precipitation reconstruction in MJJ for the Sooke Watershed. This reconstruction captured 28% of precipitation variance. Temporal patterns of pluvial and drought episodes were then analyzed, and indicated that the natural drought and pluvial episodes in the instrumental period do not represent the actual length of natural events possible in the Sooke Watershed. Objective 5 was accomplished by analyzing the influence of PDO, PNA, and ENSO on the MJJ precipitation reconstruction.

5.2 Applications to Environmental Management

5.2.1 Applications to Forest Management

Successful forest management practices in the Sooke Watershed requires a sound understanding of the ecological and climatic factors that influence tree growth limitations and sensitivities, especially under a changing climate. As noted, the increase in mean annual June and July temperature over the last century had a significant negative effect on the radial growth of Douglas-fir in the Sooke Watershed (CWHxm1 and CWHxm2). Given the projected temperature rise of 1.5°C by 2050 (Pacific Climate Impacts Consortium 2012), the negative influence of temperature on radial growth will likely be exacerbated. Sooke Watershed forest managers can likely expect change in forest functions resulting from high temperature exceeding growth thresholds in the future; increasing June and July temperature will likely result in further climatic moisture deficits and a reduction in soil moisture, which are essential for Douglas-fir growth.

The radial growth of Douglas-fir trees within the Sooke Watershed proved to be moisture-limited. Growth in CWHxm1 and CWHxm2 sites demonstrated strong long-term positive correlations to precipitation and negative correlation to CMD in months of the growing season. Seeing as summer precipitation is expected to decrease 14% by 2050 (Pacific Climate Impacts Consortium 2012), sites within the Sooke Watershed might undergo further moisture-related stress. Moisture-related stress can affect Douglas-fir directly by slowing growth, and causing injury or death. It also can affect them indirectly by increasing their susceptibility to wildfire, insect pests, and disease. There is a strong connection between forest and hydrological ecosystem health (Jones et al. 2009; Lee et al. 2009), therefore, a reduction in Douglas-fir growth might affect the loss of water back to the atmosphere, snowmelt regulation, surface runoff, infiltration into soil, water storage in and movement through the soil, and the quantity, quality, and regimen of water moving out of the terrestrial ecosystem into aquatic ecosystems (Kimmins 1987).

Chapter 3 provides a heightened understanding of climate-growth relationships for Douglas-fir across spatial and temporal scales. The results from Chapter 3 can help the CRD achieve the goals outlined in the 2017 Regional Water Supply Strategic Plan (Capital Regional District 2017a). Among those goals is the need to manage and protect the GVWSA by controlling adjacent catchment lands such as forests, which act as a buffer and a natural draining structure (Capital Regional District 2017a). Active management related to forest protection, health, and resilience, is also highlighted in the CRD's Regional Water Supply Strategic Plan. Moreover, the CRD's website defines Stewardship of the GVWSA as "caring, thoughtful, and cautious management of the

ecosystems and watersheds that sustain source water quality, and other important ecosystem goods and services".

Results from Chapter 3 are significant to Sooke Watershed management because of the strong connection between the heath of terrestrial ecosystems, such as forests, and the hydrological cycle; trees regulate the loss of water back to the atmosphere, and regulate snowmelt, surface runoff, infiltration into soil, water storage in and movement through the soil, and the quantity, quality, and regimen of water moving out of the terrestrial ecosystem into aquatic ecosystems. Understanding climate-mediated physiological processes, especially their underlying mechanisms, is a key step to better prediction of climate-change impacts in forest ecosystems. As a result, it is important that we improve our understanding of how trees are currently responding to climate and how they have responded to climate over time.

5.2.2 Applications to Water Management

Water managers can use the results from Chapter 4 to consider that the May-June-July instrumental period does not represent the actual length of the natural summer droughts possible in the Watershed. The most severe continuous summer drought during the instrumental record occurred between 2015 and 2016, but it was exceeded in intensity by 7 events and in duration by 5 events over the period of the reconstruction. The longest drought during the reconstructed record occurred between 1662 and 1665, and 1705 to 1708, while the most intense occurred from 1594 to 1596. These results indicate that there have been consecutive MJJ drought events in the Sooke Watershed that would be categorized as a worst-case scenario event in the future.

Protecting water resources is highlighted as an overlying theme in the CRD's water management policies and strategies. The CRD's 2018 Climate Action Annual Report (Capital Regional District 2018) highlights taking action on climate change and protecting valuable resources like water to create a more resilient future. The reconstructed precipitation model contributes towards the accomplishment of this task by providing water managers with a more complete understanding of the natural variability of MJJ drought and pluvial events in the Sooke Watershed. Results from Chapter 4 suggest that incorporating tree-ring data into existing water system models, in combination with historic extreme events of the instrumental record, can broaden the understanding of the Watershed's natural behavior.

Results from Chapter 4 are applicable to goals outlined by the Resource Planning Section of Watershed Protection (Capital Regional District 2018). These include: 1. conducting a review of how the latest climate change projections for the CRD relate to the records of climate for the water supply area over the past 100 years; and, 2. Identifying needs for additional information to better understand the effects of climate change on the GVWSA. Results from this dendrohydrologic reconstruction add depth to the first mentioned task, as it expands the understanding of the instrumental MJJ precipitation records of the GVWSA to 1591. It also expands upon information of the natural climatic variability within the GVWSA by placing summer drought and pluvial events within the instrumental record in a longer-term context. Although future changes in climate, population growth, and land-use changes cannot be incorporated into the past, the reconstruction alone can be used in water management as a basis for the assessment

of drought and pluvial events, or included to forecast models or in water depletion scenarios for water management.

5.3 Future Research

This thesis presents many opportunities for future research, such as strengthening the reconstruction using other tree-ring indices. This research could include analyses of isotopes, early/latewood, and density. These indices would allow for analysis at a more refined scale, and offer insight into relationships between climate variability and wood growth for different periods in the growing season. Relationships between the density parameters themselves (e.g. minimum earlywood density and maximum latewood density) can also be analyzed. In studies where correlations between wood density parameters and instrumental climate records were compared with correlations between ring-width and the same climatic data, correlations with wood density were consistently stronger (Polge 1970; Conkey 1986). The temporally refined nature of density data has afforded more detailed information about climate-tree growth relationships, sometimes detecting these relationships through correlations present only between density and climate data, and missing from the ring-width values.

Incorporating other tree-ring master chronologies could have proved useful in the context of Chapter 3 and Chapter 4. Further Douglas-fir tree-ring chronologies and study sites could benefit results from Chapter 3 by widening the scope of the study sites and increasing the strength of the results. Different species could also have been analyzed and compared to the Douglas-fir climate-growth relationships. The results from the climate-growth response to drought indices could also be used to corroborate a soil-moisture analysis based drought prediction tool in the future.

Chapter 4 could have benefitted from more selective sample collection; choosing based on sites already known to be most limited by moisture within the Watershed. Future dendrochronological reconstructions of streamflow, fire, or insect outbreak within the Watershed could also strengthen results from Chapter 4. Results from the dendrohydrological reconstruction of precipitation could potentially be incorporated into a climate projection model, or a water budget model, that would predict future changes in the natural cycle of the Watershed. With this prediction, scenarios including climate change, land-use changes, and population growth could be incorporated and could allowed management of the Sooke Watershed with a more reliable idea of what the future holds for the resources within the Watershed.

References Cited

Aber, J., Neilson, R.P., McNulty, S., Lenihan, J.M., Bachelet, D. and Drapek, R.J. 2001. Forest processes and global environmental change: predicting the effects of individual and multiple stressors: we review the effects of several rapidly changing environmental drivers on ecosystem function, discuss interactions among them, and summarize predicted changes in productivity, carbon storage, and water balance. BioScience 51: 735-751.

Allen, C.D., Macalady, A.K., Chenchouni, H., Bachelet, D., McDowell, N., Vennetier, M., Kitzberger, T., Rigling, A., Breshears, D.D., Hogg, E.T. and Gonzalez, P. 2010. A global overview of drought and heat-induced tree mortality reveals emerging climate change risks for forests. Forest Ecology and Management 259: 660-684.

Alley, N. and Chatwin, S. 1975. Late Pleistocene history and geomorphology, southwestern Vancouver Island, British Columbia. Canadian Journal of Earth Sciences 16: 1645-1657.

B.C. Ministry of Environment and Climate Change Strategy. 2019. Impacts of climate change. Retrieved from: https://www2.gov.bc.ca/gov/content/environment/climate-change/adaptation/impacts

Barnett, T.P., Adam, J.C. and Lettenmaier, D.P. 2005. Potential impacts of a warming climate on water availability in snow-dominated regions. Nature 438(7066): 303.

Beedlow, P.A., Lee, E.H., Tingey, D., Waschmann, R.S. and Burdick, C.A. 2013. The importance of seasonal temperature and moisture patterns on growth of Douglas-fir in western Oregon, USA. Agricultural and Forest Meteorology 169: 174-185.

Biondi, F. 2000. Are climate–tree growth relationships changing in north-central Idaho, U.S.A. Arctic Antarctic and Alpine Research 32: 111–116.

Biondi, F. and Waikul, K. 2004. DENDROCLIM2002: A C++ program for statistical calibration of climate signals in tree-ring chronologies. Computers & Geosciences 30: 303-311.

Bonsal, B.R., Shabbar, A. and Higuchi, K. 2001. Impacts of low frequency variability modes on Canadian winter temperature. International Journal of Climatology 21: 95-108.

Briffa, K. and Jones, P.D. 1990. Basic chronology statistics and assessment. In: Methods of dendrochronology: Applications in the environmental sciences. Edited by: Cook, E. R. and Kairiukstis, L. A. Kluwer Academic Publishers. 137–152.

Briffa, K.R., Jones, P.D. and Schweingruber, F.H. 1992. Tree-ring density reconstructions of summer temperature patterns across western North America since 1600. Journal of Climate 5: 735-754.

Brubaker, L.B. 1980. Spatial patterns of tree growth anomalies in the Pacific Northwest. Ecology 61: 798-807.

Bryson, R.A. and Hare, F.K. 1974. Climates of North America: Volume 11 of World Survey of Climatology. Elsevier Scientific Publishing Company, Amsterdam, London, New York. 417 pp.

Bunn, A.G. 2008. A dendrochronology program library in R (dplR). Dendrochronologia 26:115-124.

Capital Regional District Water Department. 1999. Strategic Plan for Watershed Management. Chapter 2: Guiding Principles. Capital Regional District, Victoria, B.C.

Capital Regional District Water Department. 1999a. Strategic Plan for Watershed Management. Chapter 3B: Terrestrial Resources: Capital Regional District, Victoria, B.C.

Capital Regional District Water District. 2001. Regional water supply commission staff report: drought management action plan - frequency of two-year droughts, Capital Regional District, Victoria, BC. Capital Regional District, Victoria, B.C

Capital Regional District. 2004. Review of the Strategic Plan For Water Management. Capital Regional District, Victoria, B.C.

Capital Regional District. 2015. Greater Victoria Water Supply Area: Facts and Figures. Capital Regional District, Victoria, B.C. Retrieved from: https://www.crd.bc.ca/docs/default-source/Partnerships-PDF/gvdwsa-school-tours/factsandfigures2015.pdf?sfvrsn=3cc579ca_2

Capital Regional District. 2017. Climate Projections for the Capital Region. Capital Regional District, Victoria, BC. Capital Regional District, Victoria, B.C. Retrieved from: https://www.crd.bc.ca/docs/default-source/climate-action-pdf/reports/2017-07-17_climateprojectionsforthecapitalregion_final.pdf

Capital Regional District. 2017a. Regional Water Supply: 2017 Strategic Plan. Capital Regional District, Victoria, B.C.

Capital Regional District. 2018. Climate Action Annual Report. Capital Regional District, Victoria, B.C. Retrieved from: https://crd.bc.ca/docs/default-source/crd-document-library/plans-reports/climate/2018-reports/crd-climate-action-2018-annual-report.pdf?sfvrsn=4e20dbca_4

Capital Regional District. 2018a. Regional Growth Strategy: January 2018. Capital Regional District, Victoria, B.C. Retrieved from https://www.crd.bc.ca/docs/default-source/crd-document-library/bylaws/regionalgrowthstrategy/4017--capital-regional-district-regional-growth-strategy-bylaw-no-1-2016.pdf?sfvrsn=ecb611ca_4

Carrer, M. and Urbinati, C. 2006. Long-term change in the sensitivity of tree-ring growth to climate forcing in *Larix decidua*. New Phytologist 170: 861–872.

Case, M.J. and Peterson, D.L. 2005. Fine-scale variability in growth climate relationships of Douglas-fir, North Cascade Range, Washington. Canadian Journal of Forest Research 35: 2743-2755.

Cayan, D.R., Redmond, K.T. and Riddle, L.G. 1999. ENSO and hydrologic extremes in the western United States. Journal of Climate 12: 2881-2893.

Chen, P.Y., Welsh, C. and Hamann, A. 2010. Geographic variation in growth response of Douglas-fir to interannual climate variability and projected climate change. Global Change Biology 16: 3374-3385.

Conkey, L.E. 1986. Red spruce tree-ring widths and densities in eastern North America as indicators of past climate. Quaternary Research 26:232-243.

Cook, E R. and Kairiukstis, L.A. (Eds.). 2013. Methods of Dendrochronology: Applications in the Environmental Sciences. Kluwer Academic Publishers, Netherlands. 97-162.

Cook, E R. and Krusic, P.J. 2005. Program ARSTAN: a tree-ring standardization program based on detrending and autoregressive time series modeling, with interactive graphics. Lamont-Doherty Earth Observatory, Columbia University, Palisades, NY.

Cook, E.R. 1987. The decomposition of tree-ring series for environmental studies. Tree-Ring Bulletin 47: 37–59.

Cook, E.R. and Holmes, R.L. 1986. Users manual for program ARSTAN. Laboratory of Tree- Ring Research, University of Arizona, Tucson, USA.

Coops, N.C., Hember, R.A. and Waring, R.H. 2010. Assessing the impact of current and projected climates on Douglas-Fir productivity in British Columbia, Canada, using a process-based model (3-PG). Canadian Journal of Forest Research 40: 511-524.

Coops, N.C., Hilker, T., Wulder, M.A., St-Onge, B., Newnham, G., Siggins, A. and Trofymow, J.T. 2007. Estimating canopy structure of Douglas-fir forest stands from discrete-return LiDAR. Trees 21: 295-310.

Coulthard, B.L. 2015. Multi-century records of snow water equivalent and streamflow drought from energy-limited tree rings in south coastal British Columbia. Unpublished Ph.D. dissertation, University of Victoria, Victoria, B.C.

Coulthard, B., Smith, D. J. and Meko, D. M. 2016. Is worst-case scenario streamflow drought underestimated in British Columbia? A multi-century perspective for the south coast, derived from tree-rings. Journal of Hydrology 534: 205-218.

Crausbay, S.D. and Ramirez, A.R. 2017. Defining ecological drought for the twenty-first century. Bulletin of the American Meteorological Society 98: 2543-2550.

Daly, C., Halbleib, M., Smith, J.I., Gibson, W.P., Doggett, M.K., Taylor, G.H. and Curtis, J. 2008. Physiographically sensitive mapping of temperature and precipitation across the conterminous United States. International Journal of Climatology 28: 2031–2064.

Dettinger, M.D., Cayan, D.R.; Diaz, H.F. and Meko, D.M. 1998. North-south precipitation patterns in western North America on interannual- to-decadal timescales. Journal of Climate 11: 3095–3111.

Earle, C.J. 1993. Asynchronous droughts in California streamflow as reconstructed from tree rings. Quaternary Research 39: 290-299.

Fairburn, D. 2001. The spatial distribution of precipitation in the Sooke Lake Reservoir catchment area, southern Vancouver Island, British Columbia. Unpublished Honours Thesis. University of Victoria. Victoria, B.C.

Fleming, S.W., Whitfield, P.H., Moore, R.D. and Quilty, E.J. 2007. Regime-dependent streamflow sensitivities to Pacific climate modes cross the Georgia–Puget transboundary ecoregion. Hydrological Processes 24: 3264-3287.

Fritts, H.C., Guiot, J., Gordon, G.A. 1990. Verification. In methods of dendrochronology: Applications in the environmental sciences, Cook ER, Kairiūkštis L (eds). Kluwer Academic Publishers: Netherlands. 178–184.

Fritts, H. C. 1976. Tree Rings and Climate. Academic Press, San Diego, California. 567 pp.

González-Elizondo, M., Jurado, E., Návar, J., González-Elizondo, M. S., Villanueva, J., Aguirre, O., and Jiménez, J. 2005. Tree-rings and climate relationships for Douglas-fir chronologies from the Sierra Madre Occidental, Mexico: a 1681–2001 rain reconstruction. Forest Ecology and Management 213: 39-53.

Greater Victoria Water District. 1994. An environmental impact assessment of the proposed expansion of the Sooke Lake Reservoir. Prepared by: Axys Environmental Consulting Ltd. Victoria, B.C.

Griesbauer, H.P. and Green, D.S. 2010. Assessing the climatic sensitivity of Douglas-fir at its northern range margins in British Columbia, Canada. Trees 24:375-389.

Griesbauer, H.P., Green, D.S. and O'Neill, G.A. 2011. Using a spatiotemporal climate model to assess population-level Douglas-fir growth sensitivity to climate change across large climatic gradients in British Columbia, Canada. Forest Ecology and Management 261:589-600.

Griesbauer, H.P., Klassen, H., Saunders, S.C. and Spittlehouse, D.L. 2019. Variation in climate-growth relationships for Douglas-fir growth across spatial and temporal scales on

southern Vancouver Island, British Columbia. Forest Ecology and Management 444: 30-41.

Grissino-Mayer, H. D. 2001. Evaluating crossdating accuracy: a manual and tutorial for the computer program Cofecha. Tree-Ring Research 57: 205-221.

Guan, B.T., Wright, W.E. and Cook, E.R. 2018. Ensemble empirical mode decomposition as an alternative for tree-ring chronology development. Tree-Ring Research 74:28–38.

Guerrero-Mosquera, C., Borragán, G. and Peigneux, P. 2016. Automatic detection of noisy channels in fNIRS signal based on correlation analysis. Journal of Neuroscience Methods 271:128–138.

Hamann, A. and Wang, T. 2006. Potential effects of climate change on ecosystem and tree species distribution in British Columbia. Ecology 87:2773-2786.

Hermann, R. K. and Lavender, D. P. 1990. Douglas-fir. Silvics of North America, 1: 527-540.

Herring, S.C., Hoell, A., Hoerling, M.P., Kossin, J.P., Schreck III, C.J. and Stott, P.A. 2016. Explaining extreme events of 2015 from a climate perspective. Bulletin of the American Meteorological Society 97: S1-S145.

Hijmans, R.J., Cameron, S., Parra, J., Jones, P., Jarvis, A. and Richardson, K. 2005. Very high resolution interpolated climate surfaces for global land areas. International Journal of Climatology: A Journal of the Royal Meteorological Society 25: 1965-1978.

Holmes, R. L. 1983. Computer-assisted quality control in tree-ring dating and measurement. Tree-Ring Bulletin 43: 69-75.

Howes, D.E. and Kenk, E. 1988. Terrain classification system for British Columbia (Revised edition). Recreational Fisheries Branch, Ministry of Environment, and Surveys and Resources Mapping Branch, Ministry of Crown Lands, Victoria, British Columbia. Ministry of Environment Manual 10. 90 pp.

Huang, N.E. and Wu, Z.H. 2008. A review on hilbert-huang transform: Method and its applications to geophysical studies. Reviews of Geophysics 46: 200-206.

Huang, N.E., Shen, Z., Long, S.R., Wu, M.C., Shih, H.H., Zheng, Q., Yen, N-C., Tung, C.C., and Liu, H.H. 1998. The empirical mode decomposition and the hilbert spectrum for nonlinear and non-stationary time series analysis. Proceedings of the Royal Society of London. Series A: Mathematical, Physical and Engineering Sciences 454(1971): 903-995.

Huntington, T.G. 2006. Evidence for intensification of the global water cycle: review and synthesis. Journal of Hydrology 319: 83-95.

IPCC. 2018: Summary for Policymakers. In: Global warming of 1.5°C. An IPCC special report on the impacts of global warming of 1.5°C above pre-industrial levels and related global greenhouse gas emission pathways, in the context of strengthening the global response to the threat of climate change, sustainable development, and efforts to eradicate poverty [V. Masson-Delmotte, P. Zhai, H. O. Pörtner, D. Roberts, J. Skea, P.R. Shukla, A. Pirani, W. Moufouma-Okia, C. Péan, R. Pidcock, S. Connors, J. B. R. Matthews, Y. Chen, X. Zhou, M. I. Gomis, E. Lonnoy, T. Maycock, M. Tignor, T. Waterfield (eds.)].

Jarrett, P. 2008. A dendroclimatic investigation of moisture variability and drought in the Greater Victoria Water Supply Area, Vancouver Island, British Columbia. Unpublished MSc thesis. University of Victoria, Victoria, B.C.

Jones, J.A., Achterman, G.L., Augustine, L.A., Creed, I.F., Folliott, P.F., MacDonald, L. and Wemple, B.C. 2009. Hydrologic effects of a changing forested landscape – challenges for the hydrological sciences. Hydrological Process 23: 2699-2704.

Jungen, J.R. 1985. Soils of southern Vancouver Island. B.C. Soil Survey Report 44. MOE Technical Report 17. B.C. Ministry of Environment, Victoria, B.C.

Kimmins, J.P. 1987. Forest Ecology, 2nd Edition. Upper Saddle River, Prentice-Hall, Englewood Cliffs, NJ, 596 pp.

Klinka, K., Nuszdorfer, F.C. and Skoda, L. 1979. Biogeoclimatic units of central and southern Vancouver Island. B.C. Ministry of Forests, Victoria, B.C.

Kolisnek, P.K. 2005. Assessing the vulnerability of Greater Victoria's drinking water system to climate-induced water shortages. Unpublished MSc thesis. University of Guelph, Guelph, Ont.

Kutner, M.H., Nachtsheim, C.J., Neter, J. and Li, W. 2005. Applied Linear Statistical Models (Vol. 5). McGraw-Hill, Irwin, CA.

Lassoie, J.P. 1982. Physiological activity in Douglas-fir. Hutchinson Ross, Stroudsberg, Pennsylvania, USA. 14: 126-185.

Latif, M. and Barnett, T P. 1994. Causes of decadal climate variability over the North Pacific and North America. Science 266(5185): 634-637.

Lee, S.W., Hwang, S.J., Lee, S.B., Hwang, H S. and Sung, H.C. 2009. Landscape ecological approach to the relationships of land use patterns in watersheds to water quality characteristics. Landscape and Urban Planning 92: 80-89.

Lee, E.H., Beedlow, P.A., Waschmann, R.S., Tingey, D.T., Wickham, C., Cline, S., and Carlile, C. 2016. Douglas-fir displays a range of growth responses to temperature, water, and Swiss needle cast in western Oregon, USA. Agricultural and Forest Meteorology 221: 176-188.

Lei, Y., He, Z. and Zi, T. 2009. Application of the EEMD method to rotor fault diagnosis of rotating machinery. Mechanical Systems and Signal Processing 23: 1327–1338.

Lewis, J.D., Lucash, M., Olszyk, D. and Tingey, D. T. 2001. Seasonal patterns of photosynthesis in Douglas fir seedlings during the third and fourth year of exposure to elevated CO_2 and temperature. Plant, Cell & Environment 24: 539-548.

Littell, J.S., Peterson, D.L. and Tjoelker, M. 2008. Douglas-fir growth in mountain ecosystems: water limits tree growth from stand to region. Ecological Monographs 78: 349-368.

Littke, K.M., Zabowski, D., Turnblom, E. and Harrison, R.B. 2018. Estimating shallow soil available water supply for Douglas-fir forests of the coastal Pacific Northwest: climate change impacts. Canadian Journal of Forest Research 48: 421-430.

Little, R.L., Peterson, D.L., Silsbee, D.G., Shainsky, L.J. and Bednar, L.F. 1995. Radial growth patterns and the effects of climate on second-growth Douglas-fir (*Pseudotsuga menziesii*) in the Siskiyou Mountains, Oregon. Canadian Journal of Forest Research 25: 724-735.

Littell, J. S. and Peterson, D. L. 2005. A method for estimating vulnerability of Douglas-fir growth to climate change in the northwestern US. The Forestry Chronicle 81: 369-374.

Luukko, P.J.J., Helske, J. and E. Räsänen, 2016. Introducing libeemd: A program package for performing the ensemble empirical mode decomposition. Computational Statistics 31: 545-557.

Mann, M.E. and Lees, J.M. 1996. Robust estimation of background noise and signal detection in climatic time series. Climate Change 33: 409–445.

Mantua, N.J., Hare, S.R., Zhang, Y., Wallace, J.M. and Francis, R.C. 1997. A Pacific interdecadal climate oscillation with impacts on salmon production. Bulletin of the American Meteorological Society 78: 1069-1079.

McCreary, D. D., Lavender, D. P. and Hermann, R. K. 1990. Predicted global warming and Douglas-fir chilling requirements. Annales des sciences forestières 47: 325-330.

McKenney, D.W., Pedlar, J.H., Lawrence, K., Campbell, K. and Hutchinson, M.F. 2007. Potential impacts of climate change on the distribution of North American trees. Bioscience 57: 939–948.

Meidinger, D. and Pojar, J. 1991. Ecosystems of British Columbia. Research Branch, B.C. Ministry of Forests 95. Victoria, B.C.

Meko, D., Cook, E.R., Stahle, D.W., Stockton, C.W. and Hughes, M. 1993. Spatial patterns of tree-growth anomalies in the United States and southeastern Canada. Journal of Climate 6: 1773-1786.

Meko, D., and C. A. Woodhouse. 2011. Application of streamflow reconstruction to water resources management. Dendroclimatology, Developments in Paleoenvironmental Research, M. K. Hughes, T. W. Swetnam, and H. F. Diaz, Eds., Springer Netherlands 11: 231–261.

Mood, B.J. 2019. Dendrohydrological reconstruction and hydroclimatic variability in southwestern British Columbia, Canada. Unpublished PhD dissertation. University of Victoria, Victoria, B.C.

Nakawatase, J.M. and Peterson, D.L. 2006. Spatial variability in forest growth–climate relationships in the Olympic Mountains, Washington. Canadian Journal of Forest Research 36: 77-91.

O'Neill, G.A., Hamann, A. and Wang, T. 2008. Accounting for population variation improves estimates of the impact of climate change on species' growth and distribution. Journal of Applied Ecology 45: 1040-1049.

Oliver, C.D., Hanley, D.P. and Johnson, J.A. (Eds.). 1986. Douglas-fir: Stand management for the future. College of Forest Resources, University of Washington. Seattle, Washington.

Pacific Climate Impacts Consortium. 2012. Plan2Adapt: Summary of climate change for Vancouver Island in the 2050s. Victoria, BC. Retrieved from: http://www.plan2adapt.ca/tools/planners.

Parmesan, C. 2006. Ecological and evolutionary responses to recent climate change. Annual Review of Ecology, Evolution, and Systematics 37: 637-669.

Pike, R.G., Redding, T.E., Moore, R.D., Winkler, R.D. and Bladon, K.D. 2010. Compendium of forest hydrology and geomorphology in British Columbia. Land Management Handbook-Ministry of Forests and Range, B.C. 66.

Pojar, J., Klinka, K. and Meidinger, D.V. 1987. Biogeoclimatic ecosystem classification in British Columbia. Forest Ecology and Management 22: 119-154.

Pojar, J., Klinka, K. and Demarchi, D.A. 1991. Coastal western hemlock zone. In Meidinger D, Pojar J (eds) Ecosystems of British Columbia. BC Special Report Series No 6 Victoria: BC Ministry of Forests. 95–111.

Polge, H. 1970. The use of x-ray densitometric methods in dendrochronology. Tree-Ring Bulletin 30: 1-10.

Radić, V., Cannon, A.J., Menounos, B. and Gi, N. 2015. Future changes in autumn atmospheric river events in British Columbia, Canada, as projected by CMIP5 global climate models. Journal of Geophysical Research: Atmospheres 20: 9279-9302.

Rehfeldt, G. E., Crookston, N. L., Warwell, M. V. and Evans, J. S. 2006. Empirical analyses of plant-climate relationships for the western United States. International Journal of Plant Sciences 167: 1123-1150.

Robertson, E.O., Jozsa, L.A. and Spittlehouse, D.L. 1990. Estimating Douglas-fir wood production from soil and climate data. Canadian Journal of Forest Research 20: 357-364.

Shabbar, A. and Khandekar, M. 1996. The impact of El Niño southern oscillation on the temperature field over Canada: Research note. Atmosphere-Ocean 34: 401-416.

Shabbar, A., Bonsal, B. and Khandekar, M. 1997. Canadian precipitation patterns associated with the southern oscillation. Journal of Climate 10: 3016-3026.

Simms, R. and Brandes, O.M. 2016. Top 5 water challenges that will define British Columbia's future. POLIS Project on Ecological Governance, University of Victoria, Victoria, B.C.

Starheim, C.C.A., Smith, D.J., and Prowse, T.D. 2013. Dendrohydroclimate reconstructions of July-August runoff for two nival-regime rivers in western central British Columbia. Hydrological Processes 27: 405-420.

Smiley, B.P., Trofymow, J.A. and Niemann, K.O. 2016. Spatially-explicit reconstruction of 100 years of forest land use and disturbance on a coastal British Columbia Douglas-fir-dominated landscape: Implications for future watershed-scale carbon stock recovery. Applied Geography 74: 109-122.

Speer. 2010. Fundamentals of Tree-Ring Research. University of Arizona Press, Tucson, Arizona. 333 pp.

Spittlehouse, D.L. 2003. Water availability, climate change and the growth of Douglas-fir in the Georgia Basin. Canadian Water Resource Journal 28: 673–688.

Stahl, K., Moore, R.D. and McKendry, I.G., 2006. The role of synoptic-scale circulation in the linkage between large-scale ocean-atmosphere indices and winter surface climate in British Columbia, Canada. International Journal of Climatology 26: 541-560.

Steinman, B.A., Abbott, M.B., Mann, M.E., Ortiz, J.D., Feng, S., Pompeani, D.P., Stansell, N.D., Anderson, L., Finney, B.P. and Bird, B.W. 2014. Ocean-atmosphere forcing of centennial hydroclimate variability in the Pacific Northwest. Geophysical Research Letters 41: 2553-2560.

Steinschneider, S., Ho, M., Williams, A.P., Cook, E.R. and Lall, U. 2018. A 500-year tree ring-based reconstruction of extreme cold-season precipitation and number of atmospheric river landfalls across the southwestern United States. Geophysical Research Letters 45: 5672-5680.

Stokes, M.A. and Smiley, T.L. 1996. An Introduction to Tree-Ring Dating. University of Arizona Press, Tucson. 73 pp.

Szeto, K., Zhang, X., White, R. E. and Brimelow, J. 2016. The 2015 extreme drought in Western Canada. Bulletin of the American Meteorological Society 97: 42-46.

Touchan, R. and Hughes, M.K. 1999. Dendrochronology in Jordan. Journal of Arid Environments 42: 291-303.

Trenberth, K.E. 1997. The definition of El Niño. Bulletin of the American Meteorological Society 78: 2771-2777.

Tuller, S.E. 1979. Chapter 4. Climate. In: Vancouver Island, Land of Contrasts. Forward. C.N. (Ed.). University of Victoria, Victoria. 71-91.

Van Loon, A.F., and Laaha, G. 2015. Hydrological drought severity explained by climate and catchment characteristics. Journal of Hydrology 526: 3-14.

Wang, T., Hamann, A., Spittlehouse, D.L. and Murdock, T.Q. 2012. ClimateWNA—high-resolution spatial climate data for western North America. Journal of Applied Meteorology and Climatology 51:16-29.

Wang, T., Hamann, A., Spittlehouse, D.L. and Carroll, C. 2016. Locally downscaled and spatially customizable climate data for historical and future periods for North America. PLoS ONE 11: e0156720. doi:10.1371/journal.pone.0156720

Wang, T., Zhang, M., Yu, Q. and Zhang, H. 2012a. Comparing the applications of EMD and EEMD on time-frequency analysis of seismic signal. Journal of Applied Geophysics 83: 29–34.

Watson, E. and Luckman, B.H. 2002. The dendroclimatic signal in Douglas-fir and Ponderosa pine tree-ring chronologies from the southern Canadian Cordillera. Canadian Journal of Forest Research 32: 1858-1874.

Weiskittel, A.R., Crookston, N.L. and Rehfeldt, G. E. 2012. Projected future suitable habitat and productivity of Douglas-fir in western North America. Schweizerische Zeitschrift für Forstwesen 163: 70-78.

Werner, A.T. 2007. Seasonality of the water balance of the Sooke Reservoir, BC, Canada. Unpublished MSc thesis. University of Victoria, Victoria, B.C.

Wigley, T.M.L., Briffa, K.R. and Jones, P.D. 1984. On the average value of correlated time series, with applications in dendroclimatology and hydrometeorology. Journal of the American Meteorological Society 23: 201-213.

Wilhite, D.A. and Glantz, M.H. 1985. Understanding: the drought phenomenon: the role of definitions. Water international 10: 111-120.

Wilson, R., Miles, D., Loader, N.J., Melvin, T., Cunningham, L., Cooper, R. and Briffa, K. 2013. A millennial long March–July precipitation reconstruction for southern-central England. Climate Dynamics 40: 997-1017.

Wise, E.K., Wrzesien, M.L., Dannenberg, M.P. and McGinnis, D.L. 2015. Cool-season precipitation patterns associated with teleconnection interactions in the United States. Journal of Applied Meteorology and Climatology 54: 494-505.

Wu, Z.H., Huang, N.E., Long, S.R. and Peng, C.K. 2007. On the trend, detrending, and variability of nonlinear and non-stationary time series. Proceedings of the National Academy of Sciences of the United States of America 104: 14889–14894.

Wu, Z.H. and Huang, N.E. 2009. A study of the characteristics of white noise using the empirical mode decomposition methods. Proceedings of the Royal Society: A Mathematical Physical and Engineering Sciences 460: 1597-1611.

Yu, B. and Zwiers, F.W. 2007. The impact of combined ENSO and PDO on the PNA climate: a 1,000-year climate modeling study. Climate Dynamics 29: 837-851.

Zang, C. and Biondi, F. 2015. Treeclim: an R package for the numerical calibration of proxy-climate relationships. Ecography 38: 431-436.

Zhang, Q.-B. 2000. Modern and late Holocene climate-tree-ring growth relationships and growth patterns in Douglas-fir, coastal British Columbia, Canada. Unpublished PhD dissertation. University of Victoria, Victoria, B.C.

Zhang, Q.-B. and Hebda, R.J., 2004. Variation in radial growth patterns of *Pseudotsuga menziesii* on the central coast of British Columbia, Canada. Canadian Journal of Forest Research 34: 1946-1954.

Zhang, X., Manzanedo, R. D., D'Orangeville, L., Rademacher, T. T., Li, J., Bai, X. and Pederson, N. 2019. Snowmelt and early to mid-growing season water availability augment tree growth during rapid warming in southern Asian boreal forests. Global Change Biology 25: 3462-3471.

Zhu, J. and Mazumder, A. 2008. Estimating nitrogen exports in response to forest vegetation, age and soil types in two coastal-forested watersheds in British Columbia. Forest Ecology and Management 255: 1945-1959.

Appendix A: Full MJJ Reconstruction Values

Year	MJJ	Year	MJJ	Year	MJJ	Year	MJJ	Year	MJJ
1591	102	1676	125	1761	110	1846	128	1931	98
1592	110	1677	87	1762	112	1847	104	1932	86
1593	91	1678	116	1763	112	1848	119	1933	108
1594	62	1679	87	1764	90	1849	91	1934	127
1595	67	1680	59	1765	89	1850	81	1935	99
1596	59	1681	74	1766	139	1851	87	1936	115
1597	83	1682	97	1767	103	1852	78	1937	141
1598	101	1683	110	1768	89	1853	79	1938	86
1599	156	1684	91	1769	44	1854	91	1939	106
1600	134	1685	91	1770	138	1855	115	1940	111
1601	150	1686	82	1771	62	1856	114	1941	92
1602	117	1687	83	1772	78	1857	97	1942	142
1603	81	1688	135	1773	179	1858	97	1943	107
1604	91	1689	163	1774	131	1859	90	1944	74
1605	86	1690	157	1775	123	1860	106	1945	74
1606	96	1691	109	1776	62	1861	134	1946	126
1607	111	1692	134	1777	100	1862	99	1947	90
1608	114	1693	78	1778	98	1863	136	1948	122
1609	75	1694	115	1779	92	1864	104	1949	91
1610	96	1695	94	1780	107	1865	95	1950	130
1611	131	1696	120	1781	95	1866	122	1951	73
1612	132	1697	197	1782	76	1867	87	1952	108
1613	86	1698	107	1783	95	1868	118	1953	103
1614	122	1699	113	1784	116	1869	110	1954	100
1615	92	1700	110	1785	119	1870	94	1955	136
1616	135	1701	75	1786	137	1871	100	1956	69
1617	100	1702	106	1787	80	1872	93	1957	115
1618	85	1703	133	1788	130	1873	86	1958	127
1619	76	1704	82	1789	118	1874	78	1959	87
1620	81	1705	73	1790	74	1875	135	1960	118
1621	89	1706	72	1791	99	1876	122	1961	98
1622	131	1707	73	1792	129	1877	90	1962	90
1623	82	1708	78	1793	170	1878	113	1963	137
1624	111	1709	111	1794	172	1879	125	1964	123
1625	129	1710	67	1795	141	1880	95	1965	94
1626	119	1711	98	1796	66	1881	93	1966	84
1627	85	1712	100	1797	63	1882	100	1967	80

1628	121	1713	97	1798	80	1883	106	1968	93
1629	107	1714	121	1799	60	1884	89	1969	98
1630	73	1715	141	1800	74	1885	73	1970	92
1631	90	1716	95	1801	90	1886	120	1971	90
1632	106	1717	78	1802	122	1887	111	1972	107
1633	153	1718	85	1803	89	1888	111	1973	126
1634	132	1719	103	1804	144	1889	117	1974	135
1635	78	1720	101	1805	132	1890	94	1975	70
1636	112	1721	104	1806	108	1891	99	1976	107
1637	102	1722	120	1807	104	1892	121	1977	101
1638	115	1723	135	1808	96	1893	130	1978	112
1639	87	1724	117	1809	69	1894	127	1979	89
1640	102	1725	132	1810	100	1895	118	1980	130
1641	94	1726	162	1811	89	1896	82	1981	147
1642	92	1727	115	1812	84	1897	71	1982	79
1643	95	1728	110	1813	108	1898	63	1983	125
1644	73	1729	79	1814	135	1899	65	1984	137
1645	120	1730	74	1815	120	1900	152	1985	94
1646	142	1731	84	1816	86	1901	122	1986	95
1647	146	1732	93	1817	90	1902	100	1987	108
1648	128	1733	99	1818	104	1903	95	1988	82
1649	84	1734	87	1819	136	1904	117	1989	80
1650	81	1735	95	1820	130	1905	108	1990	90
1651	106	1736	80	1821	87	1906	126	1991	85
1652	86	1737	129	1822	115	1907	97	1992	112
1653	73	1738	138	1823	72	1908	89	1993	109
1654	107	1739	129	1824	86	1909	80	1994	118
1655	97	1740	102	1825	113	1910	70	1995	85
1656	112	1741	97	1826	133	1911	78	1996	98
1657	113	1742	96	1827	137	1912	90	1997	153
1658	123	1743	110	1828	78	1913	132	1998	99
1659	155	1744	92	1829	132	1914	130	1999	80
1660	104	1745	96	1830	125	1915	104	2000	140
1661	84	1746	78	1831	76	1916	131	2001	113
1662	68	1747	102	1832	123	1917	101	2002	105
1663	64	1748	131	1833	99	1918	64	2003	88
1664	68	1749	123	1834	126	1919	96	2004	74
1665	70	1750	96	1835	95	1920	149	2005	107
1666	85	1751	74	1836	95	1921	173	2006	130
1667	82	1752	119	1837	86	1922	100	2007	77
1668	104	1753	160	1838	123	1923	91	2008	97

1669	139	1754	104	1839	127	1924	82	2009	82
1670	128	1755	95	1840	128	1925	91	2010	146
1671	129	1756	85	1841	121	1926	83	2011	122
1672	136	1757	78	1842	87	1927	99	2012	144
1673	90	1758	77	1843	75	1928	112	2013	92
1674	111	1759	97	1844	89	1929	93	2014	87
1675	107	1760	106	1845	112	1930	76	2015	71
								2016	70

Appendix B: Summary of Study Site Characteristics.

Biogeoclimatic zone	Site	Site Name	Year Cored	N	Latitude N	Longitude W	Elevation m asl
CWHxm1	this study	Sooke Watershed Saddle Dam	2017	44	48.52944	-123.705	239
CWHxm1	this study	Sooke Watershed Butchart Lake	2017	40	48.55092	-123.659	525
CWHxm1	Jarrett	Sooke Watershed Saddle Dam	2006	44	48.52944	-123.705	239
CWHxm2	this study	Sooke Watershed Rithet	2017	34	48.58623	-123.732	513
CWHxm2	Jarrett	Sooke Watershed Rithet West	2006	37	48.58694	-123.705	415
CWHxm2	Jarrett	Sooke Watershed Rithet East	2006	37	48.60167	-123.723	415
CDFmm	FLNRO_PSP	Fd01001	2008	4	48.48791	-123.347	92
CDFmm	PFC	Gabriola Island	2011	7	49.17917	-123.834	0
CDFmm	PFC	Wildwood	2014	15	49.06361	-123.804	59
CDFmm	PFC	Maple Bay	2011	9	48.82361	-123.599	1
CDFmm	PFC	Heal Lake	1992	15	48.53333	-123.47	239
CDFmm	PFC	Thetis Lake	2013	11	48.46639	-123.465	104
CDFmm	PFC	Costco	2014	15	48.46056	-123.503	102
CDFmm	PFC	Royal Roads	2014	7	48.43167	-123.485	33
CDFmm	PFC	Rocky Point	1995	9	48.32139	-123.545	1
CWHvm2	FLNRO_PSP	Fd11015	2003	1	49.10033	-121.713	984
CWHvm2	FLNRO_PSP	Fd11016	2003	6	49.09692	-121.704	737
CWHvm2	FLNRO_PSP	Fd11022	2003	9	49.0943	-121.712	702
CWHvm2	FLNRO_PSP	Fd11031	2003	7	49.09426	-121.715	778
CWHvm2	FLNRO_PSP	Fd11038	2003	6	49.09395	-121.717	844
IDFdk3	FLNRO_PSP	Fd48010	2012	2	52.27144	-122.512	936
IDFdk3	FLNRO_PSP	Fd48012	2012	1	52.27144	-122.512	936
IDFdk3	FLNRO_PSP	Fd48013	2012	1	52.08295	-122.349	921
IDFdk3	FLNRO_PSP	Fd48014	2012	6	52.15993	-122.351	900
IDFdk3	FLNRO_PSP	Fd48020	2012	5	52.08295	-122.349	921
IDFdk3	FLNRO_PSP	Fd47001	2012	5	51.98292	-121.759	930
IDFdk3	FLNRO_PSP	Fd47006	2012	4	52.08769	-122.154	877
IDFdk3	FLNRO_PSP	Fd47090	2014	3	51.22233	-121.302	996
IDFdk3	PFC	Bull Mountain	2002	20	52.1967	-122.158	946
IDFdk3	PFC	Veasy Lake	2011	9	51.06667	-121.367	1060
IDFdm2	FLNRO_PSP	Fd18001	2014	3	49.34742	-115.388	818
IDFdm2	FLNRO_PSP	Fd19007	2014	4	49.33302	-115.175	926
IDFdm2	FLNRO_PSP	Fd19011	2014	5	49.27687	-115.153	868
IDFdm2	FLNRO_PSP	Fd19016	2014	2	49.27948	-115.152	875
IDFdm2	FLNRO_PSP	Fd19018	2014	1	49.33007	-115.206	868

IDFdm2	FLNRO_PSP	Fd19019	2014	1	49.33101	-115.209	839
IDFdm2	PFC	Whiteswan PP	2001	12	50.12556	-115.618	1184
MSdm1	FLNRO_PSP	Fd24031	2008	5	49.38174	-119.061	1220
MSdm1	FLNRO_PSP	Fd24036	2008	1	49.4531	-119.132	1270
MSdm1	FLNRO_PSP	Fd24037	2008	1	49.45535	-119.133	1274
MSdm1	FLNRO_PSP	Fd24038	2008	4	49.46651	-119.126	1387
MSdm1	FLNRO_PSP	Fd24042	2008	3	49.42051	-119.073	1247
MSdm1	FLNRO_PSP	Fd24045	2008	3	49.41934	-119.07	1246
MSdm1	FLNRO_PSP	Fd24048	2008	3	49.41177	-119.065	1266
MSdm1	FLNRO_PSP	Fd24001	2013	8	49.54564	-119.044	1195
SBSdw3	FLNRO_PSP	Fd66001	2014	6	54.11169	-124.645	879
SBSdw3	FLNRO_PSP	Fd66005	2014	3	54.11149	-124.641	852
Rocky Mountain	PFC	Waterton:WB1	2005	9	49.02681	-113.869	1623
Rocky Mountain	PFC	Waterton Park 1	2010	7	49.067	-113.789	1630
Rocky Mountain	PFC	Waterton Park 5	2002	6	49.00871	-113.669	1532
ICHwk1	FLNRO_PSP	Fd44001	2017	5	51.0171	-119.382	1025
ICHwk1	FLNRO_PSP	Fd44004	2017	5	51.01869	-119.383	999
ICHwk1	FLNRO_PSP	Fd44013	2017	6	51.00609	-119.362	1175
ICHwk1	FLNRO_PSP	Fd44019	2017	8	51.04553	-119.364	1068
ICHwk1	FLNRO_PSP	Fd44027	2017	7	51.04184	-119.371	1067
ICHwk1	PFC	Revelstoke	2003	14	51.0792	-118.843	1268

Appendix C: Master Chronology Values. TR; tree-ring chronology value.

Year	TR	Year	TR	Year	TR	Year	TR	Year	TR
1456	0.233	1568	0.039	1680	-0.408	1792	0.021	1904	0.272
1457	0.442	1569	0.183	1681	-0.317	1793	0.172	1905	0.216
1458	0.191	1570	0.014	1682	-0.187	1794	0.166	1906	0.262
1459	0.498	1571	-0.085	1683	-0.104	1795	0.026	1907	0.090
1460	0.420	1572	0.208	1684	-0.169	1796	-0.348	1908	0.003
1461	0.371	1573	0.145	1685	-0.144	1797	-0.381	1909	-0.078
1462	0.273	1574	-0.016	1686	-0.156	1798	-0.292	1910	-0.160
1463	0.522	1575	0.528	1687	-0.111	1799	-0.392	1911	-0.120
1464	0.521	1576	0.141	1688	0.165	1800	-0.296	1912	-0.050
1465	0.241	1577	-0.161	1689	0.308	1801	-0.193	1913	0.154
1466	0.105	1578	-0.001	1690	0.313	1802	-0.024	1914	0.154
1467	-0.123	1579	0.100	1691	0.136	1803	-0.150	1915	0.037
1468	-0.146	1580	0.111	1692	0.249	1804	0.115	1916	0.143
1469	-0.269	1581	0.073	1693	-0.004	1805	0.087	1917	-0.003
1470	-0.117	1582	0.019	1694	0.188	1806	-0.004	1918	-0.209
1471	-0.074	1583	0.153	1695	0.111	1807	-0.021	1919	-0.043
1472	-0.094	1584	-0.133	1696	0.246	1808	-0.059	1920	0.174
1473	0.067	1585	-0.057	1697	0.535	1809	-0.187	1921	0.243
1474	-0.129	1586	-0.020	1698	0.161	1810	-0.014	1922	-0.088
1475	-0.187	1587	-0.224	1699	0.141	1811	-0.046	1923	-0.173
1476	-0.215	1588	0.143	1700	0.085	1812	-0.053	1924	-0.252
1477	-0.242	1589	0.011	1701	-0.114	1813	0.078	1925	-0.233
1478	-0.147	1590	0.028	1702	0.009	1814	0.205	1926	-0.283
1479	-0.310	1591	-0.139	1703	0.090	1815	0.150	1927	-0.208
1480	-0.431	1592	-0.120	1704	-0.186	1816	0.000	1928	-0.143
1481	-0.233	1593	-0.226	1705	-0.281	1817	0.015	1929	-0.221
1482	-0.150	1594	-0.391	1706	-0.312	1818	0.075	1930	-0.294
1483	-0.016	1595	-0.359	1707	-0.316	1819	0.200	1931	-0.154
1484	-0.114	1596	-0.381	1708	-0.286	1820	0.153	1932	-0.174
1485	-0.113	1597	-0.202	1709	-0.117	1821	-0.069	1933	-0.034
1486	-0.232	1598	-0.057	1710	-0.327	1822	0.031	1934	0.084
1487	-0.203	1599	0.222	1711	-0.151	1823	-0.200	1935	-0.005
1488	-0.147	1600	0.165	1712	-0.116	1824	-0.141	1936	0.095
1489	-0.177	1601	0.229	1713	-0.098	1825	-0.017	1937	0.222
1490	-0.014	1602	0.084	1714	0.028	1826	0.069	1938	-0.016
1491	-0.216	1603	-0.108	1715	0.114	1827	0.089	1939	0.082
1492	-0.189	1604	-0.070	1716	-0.097	1828	-0.181	1940	0.115
1493	-0.314	1605	-0.105	1717	-0.193	1829	0.072	1941	0.038

1494	-0.270	1606	-0.065	1718	-0.158	1830	0.046	1942	0.255
1495	-0.297	1607	-0.003	1719	-0.069	1831	-0.184	1943	0.091
1496	-0.282	1608	0.009	1720	-0.067	1832	0.045	1944	-0.089
1497	-0.283	1609	-0.178	1721	-0.046	1833	-0.056	1945	-0.095
1498	-0.608	1610	-0.066	1722	0.029	1834	0.064	1946	0.153
1499	-0.380	1611	0.099	1723	0.090	1835	-0.080	1947	-0.002
1500	0.085	1612	0.105	1724	0.008	1836	-0.091	1948	0.132
1501	-0.220	1613	-0.108	1725	0.059	1837	-0.130	1949	-0.022
1502	0.381	1614	0.043	1726	0.142	1838	0.047	1950	0.129
1503	0.385	1615	-0.098	1727	-0.094	1839	0.067	1951	-0.167
1504	0.705	1616	0.078	1728	-0.179	1840	0.056	1952	0.004
1505	1.066	1617	-0.092	1729	-0.384	1841	-0.001	1953	0.002
1506	0.784	1618	-0.188	1730	-0.452	1842	-0.186	1954	0.009
1507	0.551	1619	-0.245	1731	-0.420	1843	-0.279	1955	0.161
1508	0.551	1620	-0.215	1732	-0.384	1844	-0.229	1956	-0.167
1509	0.335	1621	-0.160	1733	-0.343	1845	-0.138	1957	0.062
1510	0.083	1622	0.045	1734	-0.374	1846	-0.088	1958	0.121
1511	-0.121	1623	-0.164	1735	-0.296	1847	-0.217	1959	-0.054
1512	0.216	1624	-0.008	1736	-0.311	1848	-0.174	1960	0.104
1513	-0.294	1625	0.088	1737	-0.019	1849	-0.322	1961	0.028
1514	0.073	1626	0.065	1738	0.077	1850	-0.389	1962	0.007
1515	-0.178	1627	-0.073	1739	0.082	1851	-0.363	1963	0.222
1516	-0.184	1628	0.108	1740	-0.012	1852	-0.407	1964	0.152
1517	-0.121	1629	0.065	1741	-0.019	1853	-0.387	1965	-0.006
1518	-0.288	1630	-0.079	1742	-0.003	1854	-0.307	1966	-0.085
1519	-0.042	1631	0.041	1743	0.082	1855	-0.168	1967	-0.133
1520	0.217	1632	0.142	1744	0.019	1856	-0.145	1968	-0.083
1521	0.067	1633	0.348	1745	0.056	1857	-0.199	1969	-0.055
1522	0.051	1634	0.248	1746	-0.004	1858	-0.178	1970	-0.071
1523	0.130	1635	-0.021	1747	0.146	1859	-0.180	1971	-0.062
1524	0.212	1636	0.122	1748	0.305	1860	-0.068	1972	0.033
1525	0.084	1637	0.062	1749	0.299	1861	0.081	1973	0.126
1526	0.043	1638	0.097	1750	0.196	1862	-0.054	1974	0.162
1527	0.162	1639	-0.062	1751	0.099	1863	0.119	1975	-0.142
1528	0.281	1640	-0.013	1752	0.321	1864	-0.013	1976	0.056
1529	-0.048	1641	-0.067	1753	0.473	1865	-0.057	1977	0.054
1530	-0.034	1642	-0.090	1754	0.219	1866	0.053	1978	0.125
1531	-0.148	1643	-0.086	1755	0.143	1867	-0.121	1979	0.042
1532	0.206	1644	-0.188	1756	0.054	1868	0.014	1980	0.251
1533	-0.089	1645	0.060	1757	-0.015	1869	-0.034	1981	0.332
1534	-0.274	1646	0.177	1758	-0.039	1870	-0.126	1982	0.029

1535	-0.031	1647	0.205	1759	0.055	1871	-0.121	1983	0.230
1536	0.042	1648	0.139	1760	0.097	1872	-0.164	1984	0.263
1537	-0.055	1649	-0.067	1761	0.119	1873	-0.203	1985	0.055
1538	-0.327	1650	-0.088	1762	0.129	1874	-0.234	1986	0.027
1539	-0.118	1651	0.025	1763	0.134	1875	0.040	1987	0.049
1540	-0.133	1652	-0.075	1764	0.037	1876	-0.003	1988	-0.104
1541	-0.156	1653	-0.142	1765	0.039	1877	-0.148	1989	-0.138
1542	-0.214	1654	0.031	1766	0.265	1878	-0.044	1990	-0.090
1543	-0.250	1655	-0.009	1767	0.116	1879	-0.001	1991	-0.108
1544	-0.237	1656	0.059	1768	0.053	1880	-0.141	1992	0.040
1545	-0.232	1657	0.070	1769	-0.198	1881	-0.164	1993	0.048
1546	-0.341	1658	0.113	1770	0.305	1882	-0.138	1994	0.100
1547	-0.131	1659	0.229	1771	-0.037	1883	-0.113	1995	-0.037
1548	-0.214	1660	-0.010	1772	0.067	1884	-0.184	1996	0.041
1549	-0.273	1661	-0.138	1773	0.500	1885	-0.245	1997	0.283
1550	-0.313	1662	-0.252	1774	0.291	1886	0.018	1998	0.054
1551	-0.194	1663	-0.287	1775	0.184	1887	0.023	1999	-0.048
1552	-0.281	1664	-0.266	1776	-0.190	1888	0.051	2000	0.211
1553	-0.244	1665	-0.249	1777	-0.047	1889	0.102	2001	0.085
1554	-0.347	1666	-0.151	1778	-0.095	1890	0.009	2002	0.033
1555	-0.206	1667	-0.146	1779	-0.159	1891	0.044	2003	-0.060
1556	-0.246	1668	-0.016	1780	-0.113	1892	0.143	2004	-0.134
1557	-0.136	1669	0.153	1781	-0.185	1893	0.182	2005	0.035
1558	-0.148	1670	0.123	1782	-0.281	1894	0.164	2006	0.137
1559	0.010	1671	0.130	1783	-0.173	1895	0.124	2007	-0.109
1560	0.000	1672	0.142	1784	-0.053	1896	-0.048	2008	-0.004
1561	-0.050	1673	-0.083	1785	-0.026	1897	-0.100	2009	-0.061
1562	-0.208	1674	-0.005	1786	0.050	1898	-0.120	2010	0.251
1563	-0.102	1675	-0.035	1787	-0.215	1899	-0.074	2011	0.160
1564	0.044	1676	0.018	1788	0.016	1900	0.368	2012	0.234
1565	-0.230	1677	-0.184	1789	-0.036	1901	0.279	2013	-0.027
1566	0.129	1678	-0.078	1790	-0.240	1902	0.197	2014	-0.099
1567	0.204	1679	-0.236	1791	-0.112	1903	0.181	2015	-0.239
								2016	-0.309